Università degli Studi di Padova

Dipartimento di Scienze Biomediche

CORSO DI DOTTORATO DI RICERCA IN SCIENZE BIOMEDICHE
31° CICLO

CHARACTERIZATION OF A NOVEL FOXO-DEPENDENT ATROGENE

Coordinatore: Ch.mo Prof. Paolo Bernardi
Supervisore: Ch.mo Prof. Marco Sandri
Co-Supervisore: Ch.mo Dott.ssa. Vanina Romanello

Dottorando: Anaïs Franco Romero

INDEX

1. RIASSUNTO

Il muscolo scheletrico è l'organo più grande del nostro corpo e rappresenta il 40-50% del peso corporeo. L'omeostasi muscolare è essenziale sia per la funzionalità che per l'integrità del nostro corpo; infatti un'eccessiva perdita di muscolatura (atrofia) porta ad un peggioramento delle malattie, aumentando la morbilità e la mortalità.

La massa muscolare è il risultato di un bilanciamento tra sintesi e degradazione proteica. Si è visto che la perdita di massa muscolare è strettamente collegata ad un'eccessiva degradazione delle proteine; ne sono alcuni esempi l'invecchiamento (sarcopenia), la cachessia, l'AIDS, la denervazione, la sepsi, l'infarto e il diabete. Nelle cellule eucariote esistono due principali sistemi proteolitici, coinvolti nel controllo del regolare ricambio delle proteine: il sistema ubiquitina-proteasoma e il sistema autofagia-lisosoma. Nel muscolo scheletrico sono presenti entrambi i processi, i quali hanno la funzione di degradare proteine e organelli che hanno bisogno di essere riciclati. In particolare, durante l'autofagia si ha la formazione di una struttura a doppia membrana, che ha la funzione di espandersi per catturare proteine citoplasmatiche e organelli, prima di richiudersi a formare l'autofagosoma. L'autofagosoma si fonde successivamente con il lisosoma, portando alla degradazione del materiale interno e al rilascio nel citosol di prodotti, quali amminoacidi, lipidi e glucosio.

I membri della famiglia di proteine *Forkhead box class O* (FoxO) sono fattori trascrizionali altamente conservati, che sono negativamente regolati dalla chinasi *AKT* e giocano un ruolo fondamentale nell'omeostasi cellulare. Negli esseri umani ci sono quattro isoforme (FoxO1, FoxO3, FoxO4 e FoxO6), tutte espresse nel muscolo scheletrico. Questi fattori sono implicati nella regolazione del ciclo cellulare, nell'apoptosi, nella rigenerazione muscolare, nell'adattamento all'esercizio fisico e promuovono l'espressione di diversi "atrogeni". Infatti, il profilo di espressione genica eseguito a digiuno in topi *wild-type* (WT) e in topi FoxO1/3/4 *knockout* (KO) muscolo-specifici ha mostrato che FoxO è necessario per l'induzione

di più del 50% degli atrogeni conosciuti. Tra questi sono inclusi le ubiquitine ligasi muscolo-specifiche (Atrogin1 e MuRF1), diverse subunità proteasomiche (Psme4/PA200, Psma1) e alcuni geni implicati nell'autofagia (LC3, GABARAPL, Bnip3, p62).

Di conseguenza, l'eliminazione di FoxO nel muscolo previene la riduzione della massa muscolare e la perdita di forza in topi sottoposti a digiuno e denervazione. I membri della famiglia FoxO sono stati, quindi, identificati come i regolatori principali dell'omeostasi proteica in diverse condizioni cataboliche. Tuttavia, l'attivazione degli atrogeni identificati fino ad ora non è sufficiente a spiegare i livelli di proteolisi osservati. Per questa ragione, la scoperta di nuovi *players* coinvolti nella degradazione proteica è ad oggi un campo di enorme interesse.

Lo scopo di questo lavoro è quello di scoprire nuovi atrogeni FoxO-dependenti; in particolare, ci si è focalizzati su geni fino ad oggi non caratterizzati, ma precedentemente sequenziati dal consorzio RIKEN e non aventi ancora funzioni note. Capire il ruolo e le funzioni di questi geni può essere utile per lo sviluppo di nuovi approcci terapeutici che prevengano o limitino la degenerazione muscolare.

Tra i diversi geni FoxO-dipendenti identificati, denominati RIKENs, ci siamo focalizzati principalmente su un gene, chiamato RIKEN1, in quanto è risultato essere chiaramente over-espresso in condizioni di digiuno e inibito nei topi FoxO1/3/4 KO. Questo gene presenta caratteristiche tipiche degli atrogeni; infatti, è indotto in differenti condizioni cataboliche come il digiuno (24 e 48 ore) e la denervazione (3 e 7 giorni). Inoltre si sono osservate alte concentrazioni di RIKEN1 sia in topi con cachessia che in biopsie umane di pazienti cachettici affetti da cancro colon-rettale (rispetto a pazienti non cachettici). Da queste prime osservazioni, RIKEN1 sembra essere un gene dipendente dallo stato di nutrizione, dall'attività e dal metabolismo.

Inoltre, dall'analisi di biopsie umane di individui giovani ed anziani (più di 65 anni), con e senza fratture all'anca, abbiamo riscontrato un considerevole aumento di RIKEN1 nei campioni di individui con frattura, suggerendo che l'aggiunta di condizioni cataboliche (oltre alla sarcopenia), quali ad esempio l'immobilità, può

contribuire all'espressione di geni responsabili di un ulteriore diminuzione del tessuto muscolare. È inoltre interessante che questo gene sia altamente conservato dal lievito alla specie umana e che sia espresso in molti organi, soprattutto nel fegato e nei polmoni. Nell'uomo RIKEN1 ha due isoforme che codificano per una proteina di circa 48kDa.

RIKEN1 è stato clonato in tre diversi vettori: RIKEN1 fusa con *flag* (vettore p3Xflag-Myc-CMV), RIKEN1 fusa con GFP (vettore pEGFP-N3) e RIKEN1-*flag* clonato in un vettore contenente YFP in un altro *multiple cloning site* (MCS) (vettore PBI-CMV1 p3XflagRIKEN1- YFP). In seguito, i loro pesi molecolari sono stati validati a 49kDa. E' stato dimostrato che la proteina RIKEN1 mostra una distribuzione puntiforme nel citoplasma delle cellule sia *in vitro* che *in vivo*. Per capire se RIKEN1 fosse sufficiente e necessario per indurre atrofia muscolare, è stato disegnato uno specifico shRNA con la funzione di inibire la sua espressione *in vivo*, il quale è stato poi trasfettato in muscoli Tibiali (TA) attraverso elettroporazione. Analizzando l'area delle fibre trasfettate è stato osservato che il silenziamento di RIKEN1 protegge dall'atrofia causata da condizioni di digiuno. Al contrario, un'overespressione di RIKEN1 nei muscoli tibiali ha portato ad una significativa perdita di massa muscolare. Si è quindi dedotto che RIKEN1 è necessario e sufficiente per indurre atrofia *in vivo*.

Il passo successivo è stato capire dove RIKEN1 fosse localizzato all'interno della cellula. Dal momento che la colorazione per RIKEN1 aveva mostrato una distribuzione puntiforme, generalmente indicativa della presenza di vescicole, ci siamo chiesti se potesse essere contenuto nella struttura membranosa di qualche organello. È stato, quindi, eseguito un protocollo di frazionamento in modo da separare le proteine solubili da quelle legate alle membrane ed è stato scoperto che RIKEN1 è presente in entrambi i compartimenti.

Inoltre, data la sua distribuzione, abbiamo deciso di investigare sulla possibile co-localizzazione di RIKEN1 con proteine del sistema autofagico-lisosomiale come LC3II e LAMP2. Esperimenti eseguiti trasfettando RIKEN1 fuso a LC3b-cherry o LAMP2-cherry su muscoli FDB e TA hanno mostrato che RIKEN1 co-localizza con

LC3 in condizioni basali e di digiuno mentre RIKEN1 co-localizza con LAMP2 soprattutto in condizioni di digiuno.

Successivamente, per capire se RIKEN1 si trova nell'autofagosoma o nel lisosoma, abbiamo trattato topi trasfettati con RIKEN1-LC3b-cherry e RIKEN1-LAMP2-cherry con colchicina, la quale previene la fusione lisosoma-autofagosoma bloccando il flusso autofagico. I risultati ottenuti hanno mostrato che, dopo il trattamento, RIKEN1 continuava a co-localizzare con LC3; tuttavia la co-localizzazione con LAMP2 era significativamente ridotta, suggerendo che RIKEN1 potrebbe essere situato nell'autofagosoma piuttosto che nel lisosoma. Per confermare i risultati, sono stati utilizzati topi ATG7 KO nei quali la formazione dell'autofagosoma è inibita. Si è dimostrato che RIKEN1 nei topi KO era prevalentemente localizzata nel citosol e meno puntiforme rispetto alla sua distribuzione nei topi WT di riferimento. Inoltre, i topi ATG7 KO non mostravano più co-localizzazione tra RIKEN1 e LAMP2. Tutti questi risultati suggeriscono che RIKEN1 è normalmente presente nell'autofagosoma, ma che, dopo la fusione con il lisosoma, si muove nell'autofagolisosoma.

RIKEN1 ha 4 *LC3-interacting motifs* (LIR) predetti con analisi bioinformatiche. Abbiamo eseguito delle mutagenesi specifiche in due aminoacidi essenziali per l'interazione con LC3. Le mutazioni nei motivi LIR1 e 4 non cambiano la distribuzione di RIKEN1, che continua ad essere puntiforme. Al contrario, le mutazioni LIR2 e 3 cambiano la sua distribuzione, rendendolo citosolico. Quindi, si ipotizza che queste due mutazioni siano quelle necessarie per l'interazione di RIKEN1 con gli autofagosomi.

In seguito ci si è chiesti se RIKEN1 potesse regolare il sistema autofagico-lisosomiale; abbiamo, quindi, analizzato la quantità di autofagosomi nelle fibre FDB in condizioni di over-espressione o inibizione di RIKEN1. Una sovra-espressione di RIKEN1 ha mostrato un significativo aumento della colorazione per LC3 nei muscoli FDB. Per analizzare il flusso autofagico, si è over-espresso RIKEN1 nelle cellule HEK trattate con clorochina, un farmaco che previene l'acidificazione dei lisosomi. Si è confermato che, bloccando il flusso autofagico, LC3 si accumula in maniera

maggiore nelle cellule in cui RIKEN1 è stato over-espresso rispetto alle cellule di controllo. Questo risultato ha suggerito che il flusso sia maggiore nelle cellule over-esprimenti RIKEN1. Al contrario, una sua down-regolazione con shRNA ha mostrato una riduzione di LC3II. Dopo il trattamento con colchicina, la quantità di LC3II è risultata simile, sia in condizioni basali che in condizioni di digiuno, a quella osservata nei campioni non trattati, suggerendo un blocco dell'autofagia quando RIKEN1 è down-regolato.

Per capire ulteriormente il ruolo di RIKEN1 nell'autofagia, abbiamo generato una linea di cellule C2C12 KO per RIKEN1 utilizzando l'innovativa tecnica CRISPR-CAS9. Le cellule KO hanno mostrato una riduzione del flusso autofagico comparate con le cellule WT, confermando così i dati ottenuti con shRNA. La colorazione per il marcatore autofagico p62, ha evidenziato un accumulo di questo nelle cellule KO, suggerendo una minor degradazione proteica.

L'importanza di questa proteina nel meccanismo autofagico ci ha fatto ipotizzare che possa essere indotta in qualche miopatia causata da una disregolazione dell'autofagia, come la malattia di Pompe. Analisi sui dati di microarray (GDS4410) effettuati su biopsie di bicipiti di pazienti con la malattia di Pompe hanno mostrato una maggiore espressione del gene RIKEN1. In linea con i dati microarray, globuli bianchi di pazienti con la malattia di Pompe hanno mostrato un aumento della proteina RIKEN1 in confronto ai campioni di controllo.

Concludendo, i risultati ottenuti suggeriscono che RIKEN1 è un nuovo atrogene sotto controllo di FoxO, che è coinvolto nella regolazione del sistema autofagico e che potrebbe avere un ruolo importante nell'induzione dell'atrofia muscolare. L'ipotesi sviluppata è che un'aumentata attivazione di RIKEN1 da parte di FoxO in condizioni cataboliche porti ad un elevato flusso autofagico, responsabile di un'eccessiva degradazione di proteine ed organelli e, come conseguenza, della perdita di massa muscolare. I nostri dati suggerisco, quindi, che RIKEN1 possa essere un possibile target terapeutico per prevenire le diverse miopatie associate ad una riduzione del tessuto muscolare.

2. SUMMARY

Skeletal muscle is the largest organ in the body which represents 40–50 % of human body weight. Muscle homeostasis is essential to whole body integrity and maintenance explaining why excessive muscle loss (atrophy) ultimately aggravates diseases and increases morbidity and mortality.

Muscle mass depends on a balance between synthesis and degradation of proteins. An excessive and sustained degradation of proteins results in muscle loss. This occurs during aging-sarcopenia and also in conditions such as cancer-cachexia, AIDS, denervation, sepsis, heart failure, diabetes, etc. There are two main proteolytic systems in eukaryotic cells that control protein turnover: the ubiquitin-proteasome and the autophagy-lysosome system. In skeletal muscle, both systems are coordinated to degrade proteins and organelles that need to be recycled. In particular, autophagy involves the formation of double-membrane structures that expands to sequester cytoplasmic proteins and organelles before it closes to form the autophagosome where after fusion with lysosomes the cargo is degraded and the components (amino-acids, lipids, glucose) are released into the cytosol via specific channels. The biogenesis of the autophagosome is not fully understood but it is thought to start from different organelles including the Endoplasmic Reticulum (ER) in a region named omegasome.

Muscle atrophy is controlled by a transcriptional program that regulates a group of genes which are commonly up or downregulated during different catabolic conditions. These genes are called atrophy-related genes or atrogenes and encode genes with an important role in the autophagy-lysosome pathway, ubiquitin-proteasome pathway, unfolded protein response, mitochondrial function, etc.

In this context, the Forkhead box class O (FoxO) family proteins are highly conserved transcription factors, which are negatively regulated by AKT Kinase, and play an important role in cellular homeostasis. There are four members in humans (FoxO1, FoxO3, FoxO4, and FoxO6) and all of them are expressed in skeletal muscle. They have been implicated in the regulation of cell cycle, apoptosis, muscle

regeneration, adaptation to exercise and promote the expression of several atrogenes. In fact, gene expression profiling in fasted wild-type (WT) and muscle specific FoxO1/3/4 Knock-out (KO) mice showed that FoxOs are required for the induction of more than 50% of the known atrogenes. Among these atrogenes are included the muscle specific ubiquitin ligases (Atrogin1 and MuRF1), several proteasome subunits (Psme4/PA200, Psma1) as well as the autophagy-related genes (LC3, Gabarapl, Bnip3, p62). Consequently, muscle-specific FoxO deletion in mice prevents muscle loss and force decline in starved and denervated mice. Thus, we have identified FoxO family members as the master regulators of protein homeostasis in catabolic conditions. However, the activation of the atrogenes identified until now cannot sustain all the protein breakdown during atrophy by themselves. For this reason, the discovery of new unknown players involved in muscle protein degradation is now of potential interest.

The aim of this project is to discover new FoxO-dependent atrogenes. We have focused our attention on uncharacterized genes that were sequenced by the FANTOM RIKEN consortium and whose functions are still unrevealed. A better understanding of the precise functions of the genes that are under FoxO control can be helpful for the development of new therapeutic approaches to prevent or limit the muscle wasting.

We identified several new FoxOs-dependent genes, here called RIKENs. We focused on one gene, named RIKEN1 which has the characteristics to be an atrogene because is up-regulated in different catabolic condition such as fasting (24h and 48h) and denervation (3 and 7 days). We also observed higher induction of RIKEN1 in a mouse model with cancer cachexia and interestingly, human biopsies of colon cancer cachectic patients had a significant higher expression of RIKEN1 compared with non-cachectic patients. Thus, RIKEN1 seems to be nutrition-, activity- and metabolic-dependent gene.

Interestingly, the analysis of human muscle biopsies of young versus old individuals (more than 65 years old) with and without hip fracture showed an increase expression of RIKEN1 in the group of old hip-fractured subjects compared to the

other groups suggesting that adding an extra catabolic factor to aging sarcopenia, such as the immobilization, could promote the expression of genes that makes worsening the atrophic condition.

Our interest increased due to its high conservation from yeast to human and its ubiquitously expression in many organs. We cloned RIKEN1 in three different expression vectors: RIKEN1 tagged with flag (p3Xflag-Myc-CMV vector), RIKEN1 tagged with GFP (pEGFP-N3 vector) and RIKEN1 tagged with flag in a vector containing YFP in another *multiple cloning site* (MCS) (PBI-CMV1 p3XflagRIKEN1-YFP) and validate their molecular weight of 49kDa. We showed that RIKEN1 protein has punctiform distribution in the cytoplasm of the cell *in vitro* and *in vivo*.

We perform a fractionation protocol separating soluble and membrane-bound proteins and we found RIKEN1 in both compartments but mostly in the membrane fraction. Thus, because of its punctiform distribution and its membrane localization we thought RIKEN1 may have a role in the autophagy-lysosomal system. Double transfection experiments of RIKEN1-gfp together with LC3b-cherry or LAMP2-cherry on Flexur Digitorum Brevis (FDB) muscle and Tibialis Anterior (TA) showed that RIKEN1 colocalizes with LC3 in both basal and fasting condition while RIKEN1 colocalizes with LAMP2 mostly in fasting condition. To know whether RIKEN1 is located in the autophagosome or in the lysosome we injected colchicine into mice to block autophagy flux and to prevent the fusion of the vesicles. Our results showed that there is still colocalization with LC3 but a reduced colocalization with LAMP2 after the treatment suggesting that RIKEN1 may be located in the autophagosomes rather than lysosomes. ATG7 KO mice model in which autophagosome formation is impaired RIKEN1 changed its localization being more cytosolic and less punctiform compared with the control WT mice. Moreover, RIKEN1 in ATG7 KO mice did not colocalize with LAMP2 confirming our hypothesis that RIKEN1 is located in the autophagosome and after fusion with lysosomes RIKEN1 goes into the autophagolysosomes.

RIKEN1 has 4 predicted LC3-interacting motifs (LIR). We performed-site directed mutagenesis in the two critical aminoacids required for the interaction with LC3.

RIKEN1 mutation in LIR1 and LIR4 motifs did not change the RIKEN1 localization whether LIR2 and LIR3 mutation changed its localization and became cytosolic. Thus, these two motifs might be required for the interaction with autophagosomes. We next wondered if RIKEN1 may regulate autophagosome-lysosome system by analysing the amount of autophagosomes in FDB fibers when we overexpress or inhibit RIKEN1. Overexpression of RIKEN1 increases LC3 puncta significatively in FDB muscle. To analyse the autophagic flux we overexpressed RIKEN1 in HEK cells treated with chloroquine, a drug that prevents lysosomes acidification. We confirmed that when blocking autophagic flux, LC3II accumulates more in the overexpressing RIKEN1 cells compared with the control. This result suggests that the flux was increased in RIKEN1 overexpressing cells. On the other hand, downregulation of RIKEN1 with shRNA decreased LC3II puncta. Following colchicine treatment, LC3II puncta does not increase in basal and starved condition compared with saline control suggesting a block of autophagy when cells downregulate RIKEN1.

To confirm the role of RIKEN1 in autophagy we created a C2C12 cell line KO for RIKEN1 using the innovative CRISPR-CAS9 technique. We could verify that KO cells had a reduced autophagic flux compared with WT cell line confirming our shRNA data. We stained the cells with the autophagy marker p62 and we could appreciate that KO cells accumulate more p62 than the WT cells suggesting a reduced level of protein degradation.

More interestingly, we observed that the knockdown of RIKEN1 protects from starved-induced atrophy by analysing cross-sectional area (CSA) of the fibers transfected by electroporation. On the other hand, overexpression of RIKEN1 in tibialis anterior induced atrophy. Thus, RIKEN1 is required and sufficient to induce atrophy in *in vivo* muscles.

The importance of this protein in the autophagy pathway made us reasoned about the possibility of RIKEN1 being induced in some myopathic autophagy-related diseases. Microarray data on muscle biopsies from untreated patients with infantile-onset Pompe (GDS4410/223440_at) showed an increased expression of

RIKEN1 gene in patients with Pompe disease. Interestingly, in line with the microarray database we found that leukocytes from patients with Pompe disease had an increased RIKEN1 protein expression compared with control samples.

Taken together, our results suggest for the first time that RIKEN1 is a novel atrophy-related gene under FoxO control that is involved in the regulation of autophagic system and may have an important role in inducing muscle atrophy. Our hypothesis is that the increased RIKEN1 expression by FoxO in catabolic conditions leads to an elevated autophagic flux that degrades excessive amount of proteins and organelles leading to atrophy. Overall, our data strongly suggest that RIKEN1 is a novel therapeutic target for preventing muscle diseases.

3. INTRODUCTION

3.1 SKELETAL MUSCLE

Skeletal muscle is the largest organ in the body which represents 40–50 % of human body weight. It is a highly organized tissue designed to produce force for movement, postural control or even breathing. Because of its predominant protein component, is considered the major protein reservoir of the organism[1]. Moreover, more recently it has been demonstrated its important role in the control of metabolic homeostasis and blood glycemia [2,3]. Thus, this organ started to be considered not only for its contractile properties but also for its pivotal role in controlling whole body metabolism.

3.1.1. STRUCTURE AND FUNCTION

Skeletal muscle tissue is formed by a collection of muscle fibers wrapped in connective tissue sheaths named by their location.

The endomysium surrounds individual muscle fibers and acts as a site of metabolic exchange between the muscle fiber and small-diameter nerve or capillaries. The exchange of sodium, potassium and calcium is essential for the excitation and the subsequent contraction of a muscle fiber.

The perimysium is a thicker layer of connective tissue that consist mainly of type I and III collagen and surrounds a group of fibers. This fiber group is called fascicle and are the functional units of skeletal muscle tissue. The perimysium contains thicker nerves and vessels than those travelling through endomysium.

Finally, the epimysium is a dense connective tissue formed mainly by type I collagen. It surrounds the entire collection of fascicles making up an individual muscle. The epimysium contains the neurovascular supply to the muscle.

Blood vessels are essential to ensure metabolites exchanges; moreover, nerve terminals from motor-neurons are contacting myofibers in specialized synapses called neuromuscular junctions (NMJs) which allows the stimulus required for

contraction. Skeletal muscles are also connected to bones through tendons, specialized structures mainly composed by extra cellular matrix (ECM) proteins which couple muscle contraction to movement generation (Figure 1).

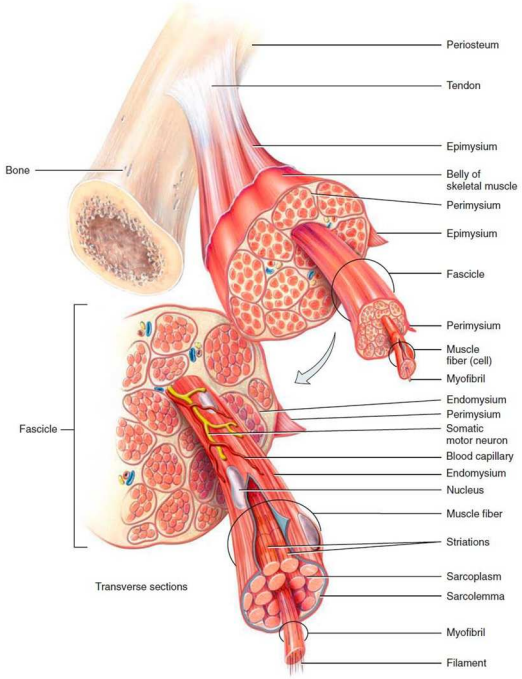

FIGURE 1 SCHEMATIC REPRESENTATON OF SKELETAL MUSCLE STRUCTURE

From a histological point of view, skeletal muscle is a complex post-mitotic tissue formed by a tight organisation of myofibers, long cylindrical multinucleated cells. The nuclei of muscle cells are situated under the plasma membrane called sarcolemma just at the periphery of the myofibers. Muscle cells present a small cytosol with all the space occupied by many myofibrils packed in parallel. This tight organization allows its particular function of contraction. Myofibers are composed by long series of sarcomeres, the functional unit of skeletal muscle cell. A sarcomere is a big protein complex composed by regularly alterned actin and myosin filaments oriented in parallel, kept in the correct position by several important structural and regulatory proteins such as troponin, tropomyosin, titin and desmin. The sarcomere length is about 4µm in resting condition but when is contracted its length is reduced into 2,7 µm.

Sarcomeres were described for the first time thanks to microscopy techniques that discovered the presence of isotropic (light band) and anisotropic (dark band) zones, forming the specific striated aspect of skeletal muscle. After that electron

microscope analysis led to the identification of a precise structural pattern in which two electrodense lines observed across the extremities (Z-lines) define the sarcomeric unit (Figure 2). Thin actin filaments project in either direction off a Z disc but do not cross the entire length of the sarcomere. Z line contains regulatory proteins such as troponin and tropomyosin. From that studies a light band (I-band) and a dark band (A-band) is also observed. Each I-band spans between two adjacent sarcomeres, including the Z-line in its middle and is the region where only actin is present. In addition, in the centre of the A-band, there is a lighter region called the H-band that do not contain actin. An M line is on the middle of the H zone perpendicular to the filaments. Thick myosin filaments are found between actin filaments.

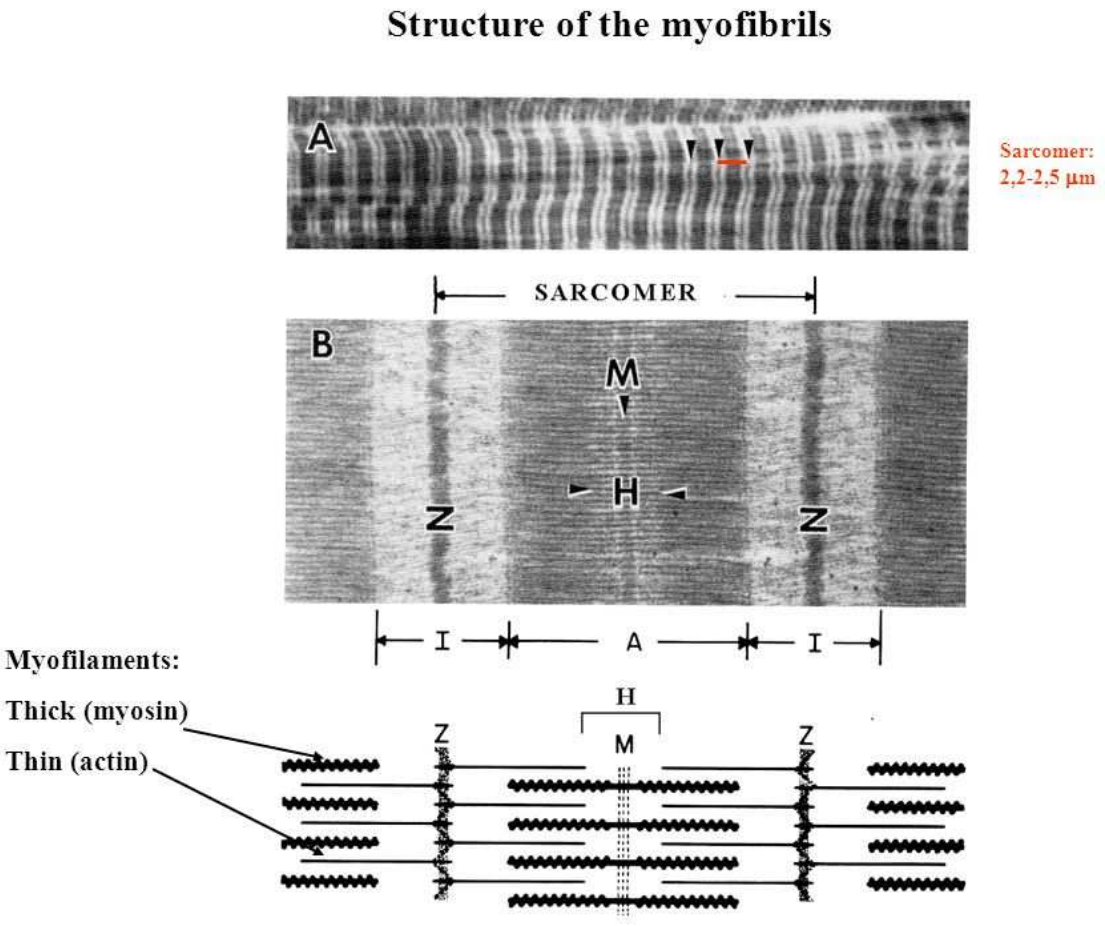

FIGURE 2. SCHEME OF SARCOMER ORGANIZATION

In the Z-line and the M band of the sarcomere there are several important proteins for the stability of the sarcomeric structure (Figure 2). The Z-line protein alpha-

actinin acts as a cross-link between actin filaments and titin molecules in the Z-disk. M proteins and the M-band myosins bind the thick filament system to the M-band part of titin. Moreover, several regulatory proteins, such as tropomyosin and troponin bind myosin molecules, modulating their contraction properties

Contraction is the typical earmark of muscle fibers, which are able to transform chemical energy into mechanical force generation. This is determined by a mechanism called excitation-contraction coupling. Excitation comes from a motor neuron that connects myofibers at the neuromuscular junction. Motor neuron generates an action potential that travels from the neuron to the sarcolemma of the post synaptic cell producing cell depolarization. This allows an increase in cytosolic calcium which activates calcium-sensitive contractile proteins leading myosin head to contact thin filaments pulling them towards M-line due to ATP hydrolysis. As a result, the electrical stimulus is converted in a signal cascade that brings chemical energy to be changed in mechanical force which leads to muscle contraction.

To allow a simultaneous contraction of all sarcomeres, muscle fibers have a particular structure in which the sarcolemma penetrates into the cytoplasm between myofibrils, forming membranous tubules running parallel to the Z-line, the transverse tubules (T-tubules) (Figure 3). T tubules are electrically coupled with the terminal cisternae particular expansions of the sarcoplasmic reticulum (SR). SR is the enlargement of the smooth Endoplasmic Reticulum (ER) and contains the majority of calcium ions required for contraction. This structure formed by T tubules surrounded by two smooth ER cisternae, called Triad, allows the transmission of membrane depolarization form the sarcolema to the ER. The contraction begins when the action potential diffuses from the motor neuron to the sarcolemma through T tubules until it reaches the sarcoplasmic reticulum. The synaptic terminal releases acetylcoline (Ach) inducing changes in the permeability of sarcoplasmic reticulum. This leads to the release of calcium into the cytosol between myofibrils which induces the myosin heads to interact with actin, allowing

muscle contraction. Energy in skeletal muscle is provided by mitochondria, which are locate closed to Z lines (Figure 3).

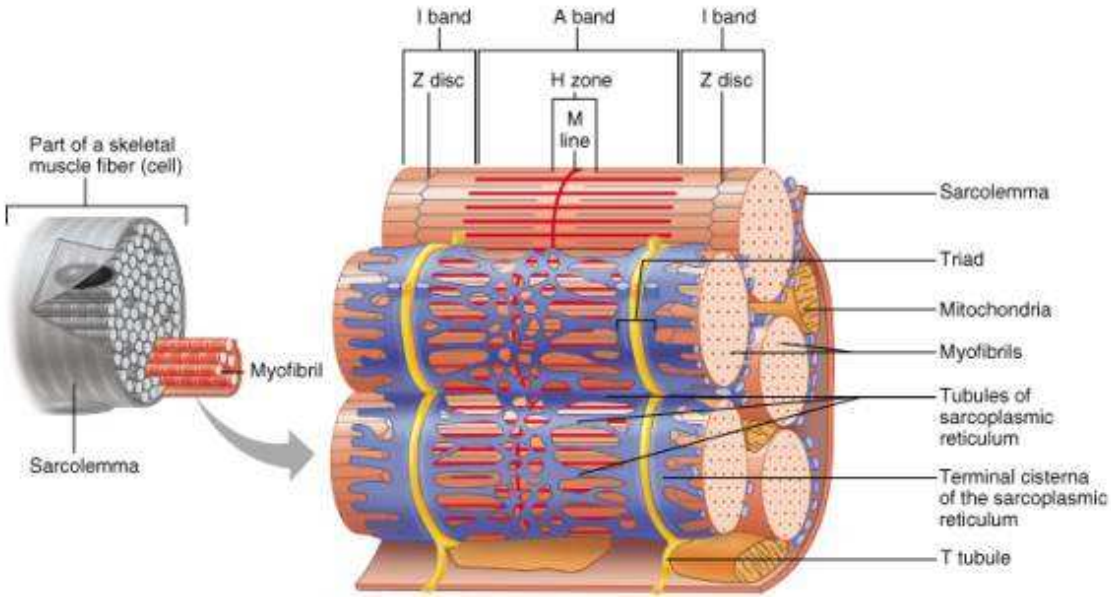

FIGURE 3 T-TUBULES AND TRIAD ORGANISATION

3.1.2. MUSCLE FIBER DIVERSITY

Contractile properties of skeletal muscle depend principally on their fiber type composition. Mammalian muscle fibers are divided in two different classes: type one (slow-twitch fibers) and type II (fast-twitch fibers) (Figure 4). This classification depends on the speed of tension development and relaxation. Type II fast fibers are divided in three different groups depending on which myosin isotype is expressed, indeed different genes encode for MHC IIa, IIx and IIb. IIa fibers are faster than type I but are still relative fatigue resistant. IIa fibers are relatively slower than IIx and IIb and have oxidative metabolism due to the rich amount of mitochondria[4,5]. These are the main characteristics of the different fibers types:

1. The type I fibers are also called slow oxidative fibers. They are small and contain high amount of myoglobin. They are specialized in aerobic activity due to their high content of mitochondria and are fatigue resistant motor units. The muscles of the deep back that are responsible to maintaining the posture are mostly made of type I slow oxidative fibers.

2. The type IIa muscle fibers are known as fast oxidative glycolytic fibers. They contain many mitochondria and because of that have a higher myoglobin content than type IIb fibers. However, unlike type I fibers, type IIa fibers contain high amounts of glycogen and due to this fact, they can do also anaerobic glycolysis and make a fast-twitch. They are more fatigue resistant than type IIb fibers and are used in movements that require high sustained power.
3. The type IIb/x fibers are also called fast glycolytic fibers. They contain fewer mitochondria and lower amount of myoglobin. They have high amount of glycogen and show high anaerobic enzyme activity. That is why these fibers are more prone to fatigue and are found in muscles used for a short, rapid, burst of contraction such as gastrocnemius.

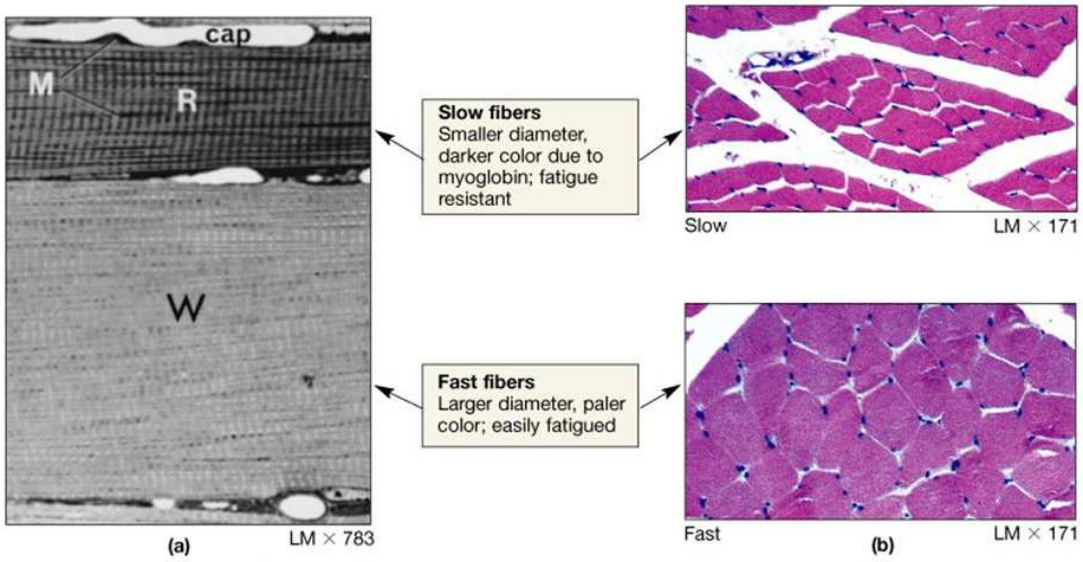

FIGURE 4 . FAST VS SLOW FIBERS

The fiber-type profile of different muscles is initially established during development independently of neural influences. During postnatal development and regeneration, a default nerve activity-independent pathway of muscle fiber differentiation leads to the activation of the fast gene program. On the contrary, postnatal induction and maintenance of the slow gene program is dependent on slow motorneuron activity. Thus, nerves have an impact on fiber type

determination and modulation of nerve activity can result in a switch of fiber type in adult skeletal muscles[6] .

3.2. PLASTICITY OF SKELETAL MUSCLE

Skeletal muscle has the capacity to adapt to the demands imposed to it including not only nutritional status, but also mechanical overload, nerve activity, exercise and stimulation by growth factors and hormones[7]. This term is called plasticity and means that skeletal muscle could increase or decrease its size depending on its activity. For example, as a result of endurance or aerobic exercise training there is an increase of the number and size of mitochondria, as well as enzymes involved with oxidative energy metabolism. On the other hand, as a result of resistance exercise skeletal muscle has a higher amount of contractile proteins leading to a bigger fiber size. This increase in size is called hypertrophy. On the other hand, inactivity, malnutrition or denervation would lead to an increased protein breakdown and decrease of muscle fiber size, a situation called atrophy. Excessive muscle loss (atrophy) aggravates diseases and increases morbidity and mortality.

Muscle integrity depends on a balance between protein synthesis and protein degradation. An excessive and sustained degradation of proteins results in muscle loss. This occurs during aging (sarcopenia) and also in diseases such as cancer (cachexia), AIDS, denervation, sepsis, heart failure, diabetes, etc.

3.2.1. MUSCLE HYPERTROPHY

In response to exercise or upon hormones stimulation there is an increase protein synthesis and a decreased degradation of proteins[8] leading to an increase of muscle mass. The result of this anabolic state is called muscle hypertrophy and is proportional to an increase in the force developed by the muscle during contraction[9] .

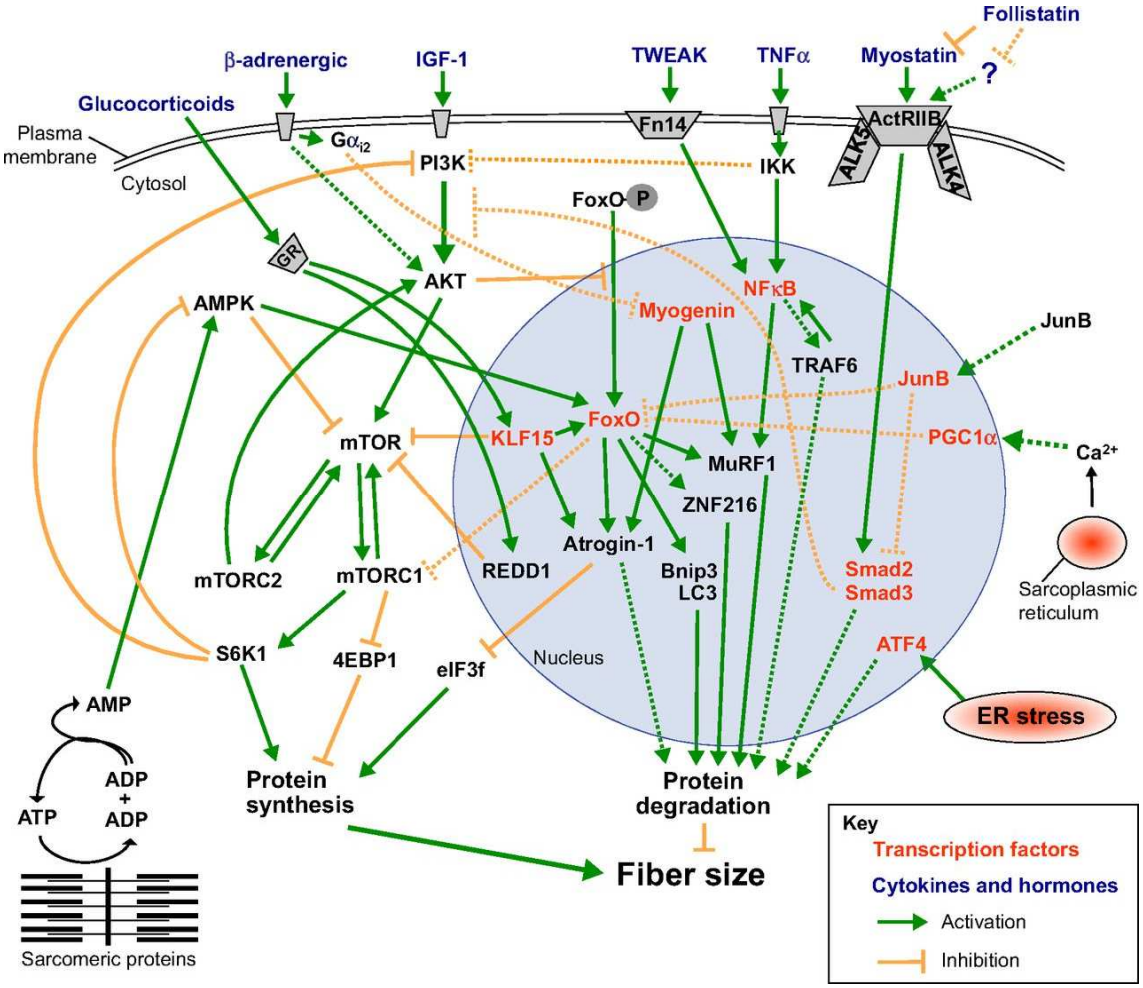

FIGURE 5 SCHEMATIC VIEW OF THE MAIN PATHWAYS CONTROLLING MUSCLE MASS (BONALDO & SANDRI 2013)

The main pathway controlling muscle growth is the IGF1-AKT-mTOR signalling pathway (Figure 5). IGF1 can be produced either by the liver under growth hormone (GH) control or locally by skeletal muscle[10]. IGF1 binds to its receptor and drives to the activation of AKT by phosphorylation. AKT phosphorylate and inhibits TSC1/2, a protein that at the same time inhibits Rheb protein and consequently leading to the inhibition of the mammalian target of rapamycin (mTOR protein)[11]. Thus, AKT activation drives to the activation of mTOR protein. Active mTOR promotes the activation of S6 kinase (S6K) and blocks 4EB-P1, the eukaryotic translation factor 4E (eif4e) inhibitor leading to an increase of protein synthesis and increasing muscle mass. Moreover, the AKT-driven inhibition of GSK3ß stimulates protein synthesis by preventing GSK3ß inhibitory action on eiF2B[12]. Some studies

have clarified better the role of AKT in skeletal muscle hypertrophy. A conditional transgenic mouse was produced in which a constitutively active form of AKT in expressed skeletal muscle after tamoxifen treatment. These mice undergo hypertrophy mainly due to newly synthesised proteins[13] suggesting that AKT activation is sufficient to induce skeletal muscle growth and that IGF1-AKT axis is the major mediator of muscle hypertrophy.

3.2.2. MUSCLE ATROPHY

Muscle atrophy is the decrease in myofiber size mainly due to the loss of organelles, cytoplasm and proteins. This process can occur physiologically, for example during aging or disuse, but also can be induced under pathological conditions such as cancer, diabetes, heart and renal failure. These diseases are accompanied by muscle wasting that could worsen the quality of life of the patients or even increase their mortality. Atrophy is a complex process that can occur due to a variety of stressors such as mechanical unloading, neural inactivity, metabolic stress, inflammation, and high number of glucocorticoids (figure 5). In 1969 Goldberg demonstrated that an increase in protein degradation contributed to the loss of muscle mass during denervation and glucocorticoid treatment[14]. Usually in atrophic animal models there is a decrease in the overall rate of protein synthesis and an increase of protein degradation explaining why it was observed a rapid loss of muscle proteins and muscle mass[1].

Even though exist different catabolic conditions that could lead to atrophy condition, there are common pathways and a common pattern of transcriptional changes that activates in order to transcribe genes involved in atrophy. This includes induction of genes involved in protein degradation and decrease of genes involved in different cellular processes like energy production and growth-related processes. This group of coordinately regulated genes are named “atrogenes” [15]. Recently Sandri’s lab showed that the ForkheadBox O protein family (FoxO family)

which are negatively regulated by AKT kinase and regulate more than 50% of these atrogenes, thus highlighting the role of FoxO in muscle atrophy[16]. Many of the atrogenes participate in the two main proteolytic systems that we have in eukaryotic cells: the ubiquitin-proteasome and the autophagy-lysosome system. In skeletal muscle, both systems are coordinated to degrade proteins and organelles that need to be recycled. Among the upregulated atrophy-related genes there is a dramatic induction of the two muscle-specific ubiquitin ligases, atrogin1/Mafbx and MurF-1 (figure 5), whose induction occurs before the onset of muscle weight loss and seems to be necessary for atrophy [17–19]. Furthermore, FoxO also regulates atrogenes from autophagy-lysosomal pathway such as Bnip3 and microtubule-associated protein 1 light chain 3 (LC3).

Other evidences have shown that TGFß and BMP pathways also contribute to the regulation of muscle mass in adulthood[20,21] (figure 5). Activation of TGFß signalling by myostatin treatment or by TGFß overexpression lead to a decrease phosphorylation of AKT and a decrease activation of the mTOR downstream targets (ribosomal protein S6, p70S6K and 4EBP1)[22]. Bone morphogenetic protein (BMP) signalling through Smad1, Smad 5 and Smad 8, is one of the main hypertrophic signals. Sartori. et al[20] showed that when BMP pathway is blocked or myostatin expression is increased, more Smad4 is phosphorylated by Smad 2/3, leading to an activation of atrophic pathway. Importantly they identify a new ubiquitin ligase, named MUSA1, negatively regulated by BMP SMAD 1-5-8 signal and required for muscle mass loss. In conclusion, Sartori et al. work provided evidences that BMP pathway also have an important role on regulating adult muscle mass in normal and pathological conditions[21] .

Furthermore, NFkB transcription factors are also contributing to skeletal muscle atrophy by upregulating a reduced subset of atrogenes (figure 5). It was shown that NFkB regulates the transcription of inflammatory cytokines, mainly TNFalpha, during cancer cachexia and muscle wasting [1,23].

3.3. PROTEIN DEGRADATION SYSTEMS

Degradation of the damaged components in eukaryotic cells is critical to maintain the balance between anabolism and catabolism; therefore, a huge number of pathways are regulating these systems of degradation. The two main proteolytic systems are the Ubiquitin-Proteasome (UPS) and the Autophagy-Lysosomal (ALS) systems[24]. These machineries are also important to recycle nutrients during starvation, eliminate unnecessary structures and organelles during cell differentiation, to fight against pathogens and to renew tissue components delaying aging[25]. In skeletal muscle protein breakdown occurs not only during pathologies or atrophy but also in physiological conditions in order to remodel the tissue during development or to remove damaged components[26]. An accumulation of damaged organelles or misfolded proteins leads to aggregates accumulation that are harmful for muscle function[1].

3.3.1. THE UBIQUITIN-PROTEASOME SYSTEM

The Ubiquitin Proteasome system (UPS) mainly regulates the degradation of intracellular short-lived proteins. Proteins that degrade with this system are marked by the linking to the polypeptide co-factor ubiquitin. This ubiquitination occurs through a sequential action of different enzymes: E1 (ubiquitin-activating enzyme), E2 (ubiquitin-conjugating enzyme) and E3 (ubiquitin-protein-ligase) (Figure 6). This process allows the activation of the 26S proteasome, a multicatalytic protease complex that degrades the ubiquitinated protein into small peptides and free aminoacids. These small components can be reused for synthesis of new proteins or for energy production[27] .

E3 is the rate limiting enzyme that catalyses the transfer of ubiquitin from E2 to the substrates. However, this reaction is very specific. In fact, the type and the amount of proteins degraded are dependent on which E3 ligases are activated[17].

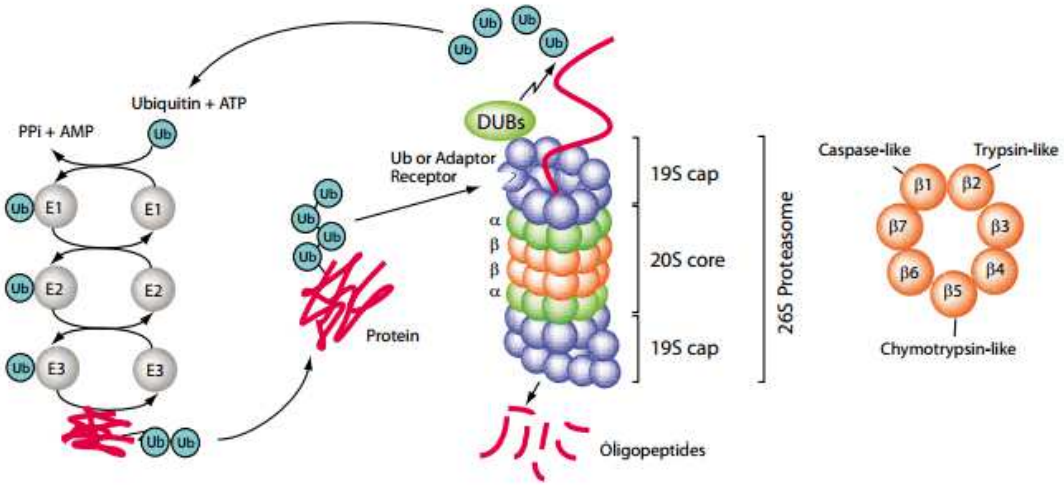

FIGURE 6. THE UBIQUITIN-PROTEASOME SYSTEM

Chains of ubiquitin molecules are generated by isopeptide bonds formed between the C-terminus of one ubiquitin molecule and a specific lysine residue. Ubiquitin has seven lysine residues, which are all used for polymerization, but polyubiquitin chains formed via lysine at 48 (Lys48) or 63(Lys63) are the best characterized. A polyubiquitin via Lys48 usually is a marker for proteolysis; on the other hand, Lys63-linked polyubiquitin is related to membrane trafficking processes[28].

The ubiquitin-proteosomal pathway is constitutively active in skeletal muscle in order to sustain protein turnover and guarantee correct homeostasis; nevertheless, UPS is the responsible of the breakdown of most soluble and myofibrillar proteins during atrophy[15]. Indeed, the decrease of muscle mass in catabolic conditions is associated with: (a) increased muscular polyubiquitinated proteins; (b) increased proteasomal ATP-dependent activity; (c) increased protein breakdown that can be efficiently blocked by proteasome inhibitors; (d) upregulated transcripts encoding ubiquitin, some ubiquitin-conjugating enzymes (E2), ubiquitin-protein ligases (E3) and several proteasome subunits. Among the different E3s, only a few have found to regulate atrophy condition and induced in atrophying muscle. The first to be identified were atrogin1/MAFbx and MurRF1 expressed in smooth muscle cells and striated muscle[29].

Atrogin-1/Mafbx contains an F-box domain, a protein motif of about 50 aminoacids that allows protein-protein interaction and belongs to the SCF complex (Skp1,

Cullin, F-box)[17]. The Fbox protein interacts with the substrates directly, while Cul1-Roc1 components are associate with the E2 Ub-conjugating enzymes. Skp1 is an adaptor that brings F-box protein to the Cul1.Ric1-E2 complex.

MuRF1 belongs to the RING finger E3 ligase subfamily, characterized by three RING-finger domains[30] which are required for ubiquitin-ligase activity[31]. These domains include a B-box and a coiled-coil domain, which may be required for the formation of heterodimers between MuRF1 and MuRF2. Knockout animals lacking either MuRF1 or Atrogin1 protected from atrophy after denervation[29] confirming that these two ligases are necessary for inducing atrophy.

Since two ubiquitin ligases cannot effort for the degradation of all the sarcomeric and soluble proteins, additional E3s are involved in muscle loss. Indeed, recent studies discovered new E3 ligases under FoxOs control transcription factor control whose activity is inducing muscle mass loss in fasting and denervation[16,21]. For this reason, identification and characterization of E3 enzymes, together with their respective substrates may be important for understanding the mechanism that control muscle mass loss and thus, being the first step to identify molecular targets for pharmacological intervention in muscle diseases.

3.3.2. THE AUTOPHAGOSOME-LYSOSOMAL (ALS) SYSTEM

Lysosome system degrade large intra or extracellular structures, such as huge protein complexes, organelles and pathogens. Extracellular material is degradated by lysosomes in a process called endocytosis in which substrates are engulfed by portions of the plasma membrane forming endocytic vesicles that then fuse with lysosomes for degradation. Lysosomes are organelles that contain hydrolytic enzymes specialized in the digestion of endocytosed material and the release of the constituents to the cytosol[32] .

On the other hand, autophagy is a highly conserved lysosome-mediated process by which cells recycle cytosolic cargo[33]. This process is induced mainly under nutrient poor conditions to ensure cellular homeostasis. This is due because through protein and organelles degradation the obtained metabolites are needed for biosynthesis and metabolic processes.

It exists different types of lysosome-mediated self-digestion: microautophagy, chaperone-mediated Autophagy (CMA) and macroautophagy.

The microautophagy is a process where a small portion of cytosol are engulfed directly by the lysosome without intervention of other vesicles[34]. In particular in skeletal muscle microautophagy seems to play a role in the glycogen uptake into lysosomes[35]

Chaperone-Mediated-Autophagy is mediated instead by the chaperone protein Hsc70 (Heat shock protein cognate 70). This chaperone recognizes a specific aminoacid sequence (KFERQ) exposed on the surface of a misfolded protein and is able to help protein translocation directly into lysosomal lumen where degradation takes place[36]. This process has a role in neurodegenerative disorders and lysosomal storage diseases[37]. However, this process in skeletal muscle homeostasis is still unknown.

Macroautophagy is the most studied process in skeletal muscle. It degradates the damage organelles and supramolecule complexes. It was firstly studied in Saccharomyces cerevisiae, leading for the identification of more than 30 genes involved in this process[38] named autophagy-related genes (ATG). For the most of ATG the mammal counterparts have been identify thus demonstrating that this mechanism is highly conserved during evolution[39] . This process is characterized by the formation of a double-membrane vesicle that can engulf cytoplasmic material and intracellular organelles and deliver them into lysosomes for degradation. In yeast autophagosomes originate from pre-autophagosome structure (PAS) where most of the ATGs are recruited. Basal autophagy rates are present in all tissues, even in stress conditions, such as nutrient deprivation, oxidative stress and hypoxic conditions can activate autophagy at different levels in a tissue specific manner. Even though different stressors could activate autophagy by different signalling pathways, most of them converge on the kinase mTOR, which plays a central role in integrating cellular inputs and autophagy regulation[40]. During nutrient deprivation for example, AMPK and p53 signalling pathways are activating and thus inhibiting mTOR. On the other hand, during anabolic conditions or in response to

extracellular response AKT and MAPK are active and thus activate mTOR. The target of mTOR kinase is ULK1, a crucial protein that initiates autophagy (figure 7). When mTOR is active phosphorylates ULK and inhibits its function. Thus, by nutrient deprivation mTOR is inactive and consequently ULK can initiate autophagy process. ULK1 participates in a heterotetrameric complex with FIP200, ATG13 and ATG101 (figure 7). Both FiP200 and ATG13 stabilize ULK1 increasing its kinase activity and encourage translocation from the cytosol to subdomains of the ER, called omegasomes, until formation of the phagophore. ATG101 maintains basal phosphorylation of ULK promoting its stabilization as ATG13 does [41]. ULK1 subsequently activates omegasome bound- VPS34, that translocates to ER puncta soon after ULK and generates pools of PI3P to drive autophagosome formation. VPS34 does not work alone but it forms a complex with Beclin1 and the pseudokinase p150 (figure 7). Depending on the subcellular complex it also binds ATG14 or UVRAG defining the PI3K complexes 1 or 2 respectively[42]. One of the firsts proteins recruited to PI3P is DFCP1 (double FYVE domain-containing protein 1). DFCP1 does not have an essential role due to its depletion does not affect autophagic flux[43]; however is used as a marker for omegasomes and phagophore-nucleation sites. Phagophore nucleation needs the recruitment of the WIPIs (WD-repeat domain phosphoinositide-interacting proteins)[44] (Figure 7). There are four mammals WIPIs (WIPI1, WIPI2b, WIPI3 and WIPI4) and are members of the PROPPIN family. The first ones to be discovered were WIPI1 and WIPI2b which recent studies have demonstrated to be recruited to the omegasomes to form autophagosomes. Even though the function of WIPI1 is not fully understood it is known to act upstream WIPI2b. On the other hand, WIPI2b is a positive regulator and is essential for autophagosome formation. This protein interacts with ATG16L1 and this is required for autophagic flux[45]. Finally, WIPI3 and 4 bind PI3P through LRRG motifs and helps to autophagosome formation. However, is not known if this interaction is necessary for autophagy flux. Recent studies demonstrated that WIPi4 plays important role in controlling the growth and size of autophagosomes[46]. The elongation of the autophagosomal membranes is a critical step associated with

two ubiquitination-like reactions. The first one ATG7 and ATG10, an E1 and E2-like enzymes respectively, conjugate ATG12 to ATG5. The ATG5-ATG12 conjugates then interact non-covalently with ATG16L1to form a large complex that binds the phagophore through WIPI2b. The complex associates with growing phagophores but dissociates once the autophagosome formation is complete. In this phase, membranes are recruited. In the second ubiquitin-like reaction, LC3 (MAP1LC3, the mammalian homolog of ATG8) after a proteolytic cleavage by ATG4 that generate the cytosolic form of the protein (LC3I), is then conjugated to the lipid phosphatidylethanolamine (PE) with a covalent bond, through the action of ATG7(E1-like) and ATG3 (E2-like) to form LC3-II[47].

The lipidated form of LC3 is finally attached to the growing autophagosome membrane, where is kept during the whole process and is located in the inner and outer membrane of the new autophagosomes. For this reason, LC3 is considered a good marker of the entire process and the quantification of the two isoforms can give us information about autophagy induction and flux. Once the cytoplasmic cargo is completely wrapped, the double membrane structure closes to become the mature autophagosome that finally fuses with lysosomes. This fusion generates the so-called autophago-lysosome which digest the cargo and some of the components of the vesicle itself[39]. Indeed, the fusion between the outer autophagosomal membrane with the lysosomal one determines the degradation of the inner membrane and of the proteins that are associated with it. Because of the transient nature of the autophagosomes, the lifetime of LC3 and its homologues is short.

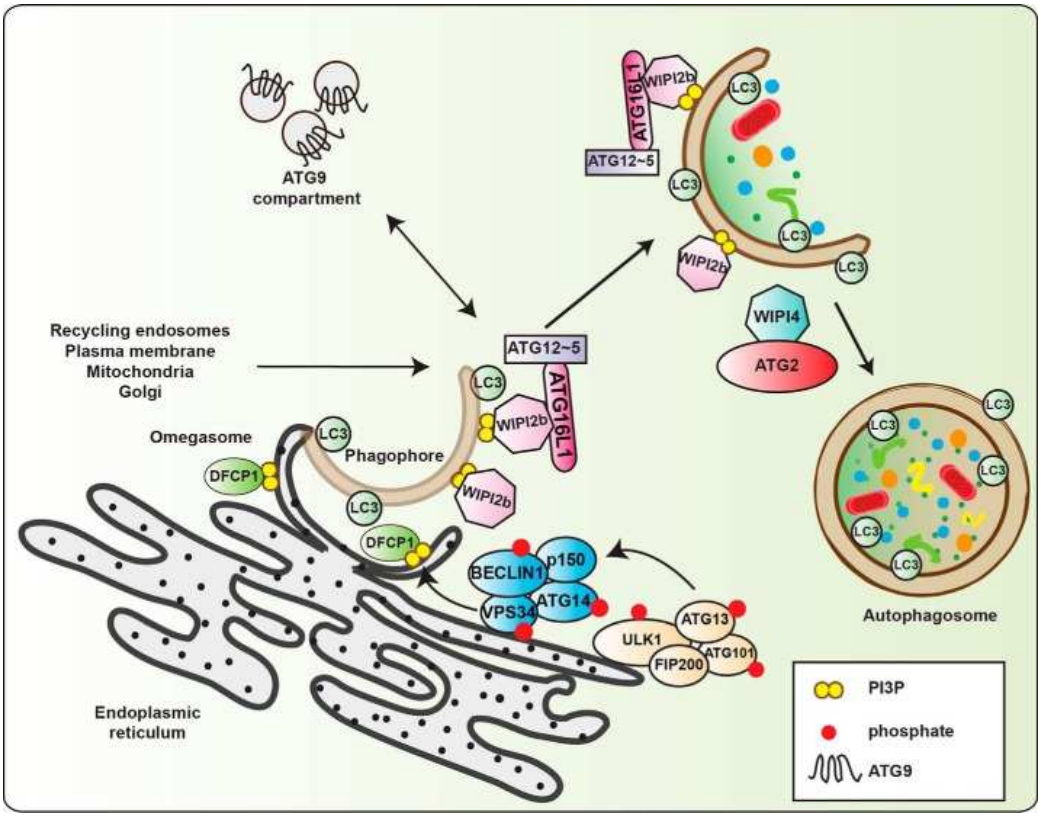

FIGURE 7 **PROCESS OF AUTOPHAGOSOME FORMATION** (MERCER TJ et al. 2018)

One of the differences between ubiquitin-proteasome system and autophagy is that meanwhile ubiquitin are always recycling the ubiquitin molecules, the autophagy-lysosome system progressively loses the ubiquitin-like proteins (LC3s) forcing the cell to replenish in order to maintain autophagic flux.

Although autophagy was primary considered to be a non-selective process, recently has been found the existence of more selective forms of autophagy. Selective autophagy relies on cargo-specific autophagy receptors that facilitate cargo sequestration into autophagosomes[48]. Autophagy receptors directly interact with the structure that needs to be specially eliminated by autophagy, as well as with LC3 present in the internal surface of the growing autophagosomes. This interaction is mediated through specific aminoacid sequence present in the autophagy receptors and commonly referred to as LC3-interacting region. One of the most important well-known ubiquitin– associated proteins that provide a link between autophagy and selective protein degradation is p62, also called SQSTM1.

In this way p62 acts as a bridge between the substrate and the LC3-II located in the inner membrane of the autophagosome[49]

P62 is more linked to the autophagome-lysosome system rather than to ubiquitin-proteasome system, being required in the targeting of disfunctional mytochondria for lysosomal degradation in a specific form of the process called mitophagy. Recently, Hsp70 has been found to not only have a role in the chaperone-mediated autophagy but also in the PINK-mediated mitophagy by stabilizing PINK protein[50]. Moreover other organelles can be specifically targeted for autophagic degradation (nucleophagy, reticulophagy, ribophagy..) supporting the idea that the cell presents high specificity for self-eating.

Autophagy can produce cell death or cell survival depending on the situation. Indeed, both excessive and defective autophagy could induce loss of muscle mass[51]. An excessive autophagy causes an exacerbated protein degradation inducing atrophy. On the other hand, defective autophagy also leads to atrophy condition. This occurs because there is an accumulation of abnormal mitochondria, sarcoplasmic reticulum and a disorganization of the sarcomere that are toxic for the cell. This was seen in our lab using a muscle-specific ATG7 KO mice where autophagy inhibition resulted in muscle atrophy and age-dependent weakness[52]. Thus, autophagy is a complex system that needs to be balanced.

3.4. SIGNALLING PATHWAYS CONTROLLING MUSCLE ATROPHY

The molecules and cellular pathways regulating muscle atrophy are still being elucidated. However, in the last decade many researchers have contributed to elucidate key transcription factors, signalling pathways and cellular processes involved in the sustained breakdown of muscle mass under a variety of conditions[16,53,54]

The main pathway implicated in loss of muscle mass is the Forhead Box O (FoxO) pathway. This protein is a transcription factor under the control of AKT. When AKT

is active phosphorylates FoxO and inactivates its function. On the other hand, when active levels of AKT are reduced, FoxO are dephosphorylated and therefore is able to translocate to the nucleus and activate the transcription of several atrogenes. FoxO3 is the member of the family that has firstly been identified to promote the expression of two important muscle specific ubiquitin-ligases: Atrogin-1 and Murf1[17,55,56]. FoxO3 has been also identified to be necessary and sufficient for the induction of autophagy in adult skeletal muscle by the activation of autophagy proteins such as Bnip3 and LC3[57,58] .

3.4.1. THE FOXO FAMILY MEMBERS OF TRANSCRIPTION FACTORS

The FoxO family is a subclass of Forhead transcription factors. In humans they are divided into 19 subgroups which are classified by alphabetic letters from A to S. FoxO proteins contain 80-100 amino that binds DNA: the forkhead motif[59]. In addition, FoxO contain a nuclear localization sequence (NLS), a nuclear export sequence (NES) and a transactivation domain in their C-terminal region in which helical motif (LXXLL) is important for FoxO transcriptional activity[60]. Importantly, while FoxO1, 3 and 6 proteins have similar length of approximately 650 amino-acid residues, the FoxO4 sequence is shorter and contains about 500 amino acids residues (figure 8). FoxO subfamily is conserved from Caenorhabditis elegans to mammalians. Analysis of multiple aligment showed that the most conserved region is the N terminal region surrounding the AKT phosphorylation site (Thr32), the DBD (Dna binding domain), the region containing (NLS) and the COOH-terminal trans activation domain[61]. The core consensus sequence has been determined by using gel shift experiments and it has the following sequence: 5' TTGTTTAC 3'. The family members have been associated in several physiological and pathological processes, including aging, cancer, and neurological diseases and regulate metabolism, cellular proliferation, apoptosis, stress tolerance and possible lifespan.

FoxO1, FoxO3, FoxO4 and FoxO6 mainly differ on the tissue-specific expression. Nonetheless, it is notable that, contrary to FoxO1,3,4, which are expressed relatively ubiquitously, FoxO6 is expressed predominantly in the central nervous system[62], although is also expressed in oxidative muscles[63] .

All these transcription factors are inhibited by growth factor signalling. In the presence of insulin and insulin growth factor (IGF) the phosphoinositide 3 kinase (PI3K) AKT signalling pathway is activated and protein kinase AKT directly phosphorylates FoxO factors at three conserved residues, resulting in inhibition of FoxO preventing its translocation to the nucleus and repression of transcriptional activity[64] .

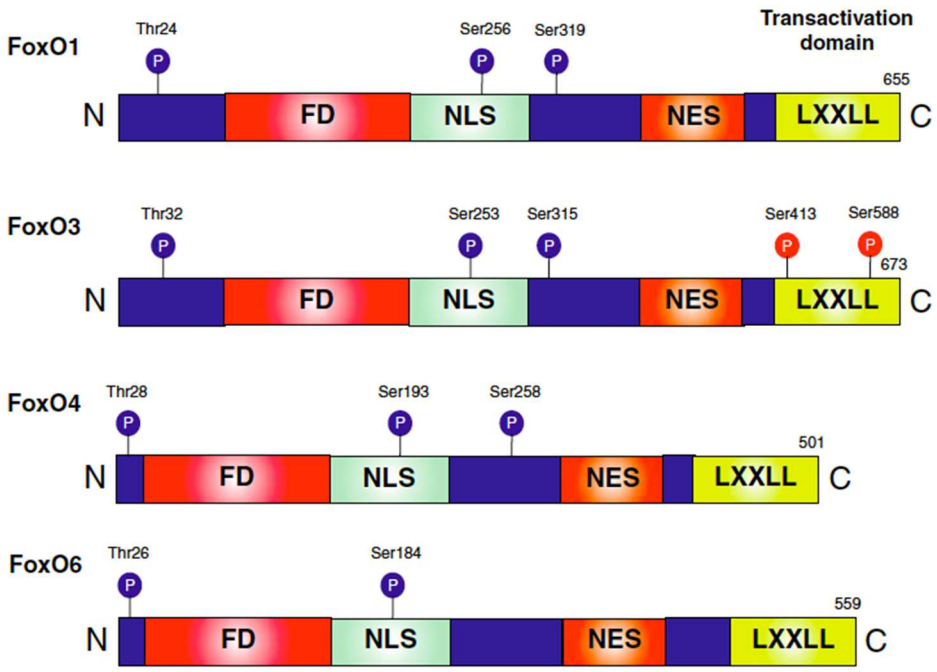

FIGURE 8 **DESCRIPTION OF THE MAMMALIAN FOXO PROTEINS EXPRESSED IN SKELETAL MUSCLE.** The following are indicated: locations of the forhead domain (FD), nuclear localization sequence (NLS), nuclear export sequence (NES) and helical motif (LXXLL), AKT phosphorilation sites (blue circles) and AMPK phosphorilation sites (red circles) (Sanchez et al., 2014)

An exception is FoxO6 which is only phosphorylated in 2 sites and is not regulated by nucleus cytoplasmic shuttling[65]. On the other hand, also the adenosine monophosphate-activated-protein kinase (AMPK) positively regulated by stimuli that decrease cellular energy levels, phosphorylates FoxO3 at six regulatory sites (Thr 179, Ser 399, Ser 413, Ser 355, ser-588 and Ser-626) *in vitro* and promotes its activation[66] (figure 8).

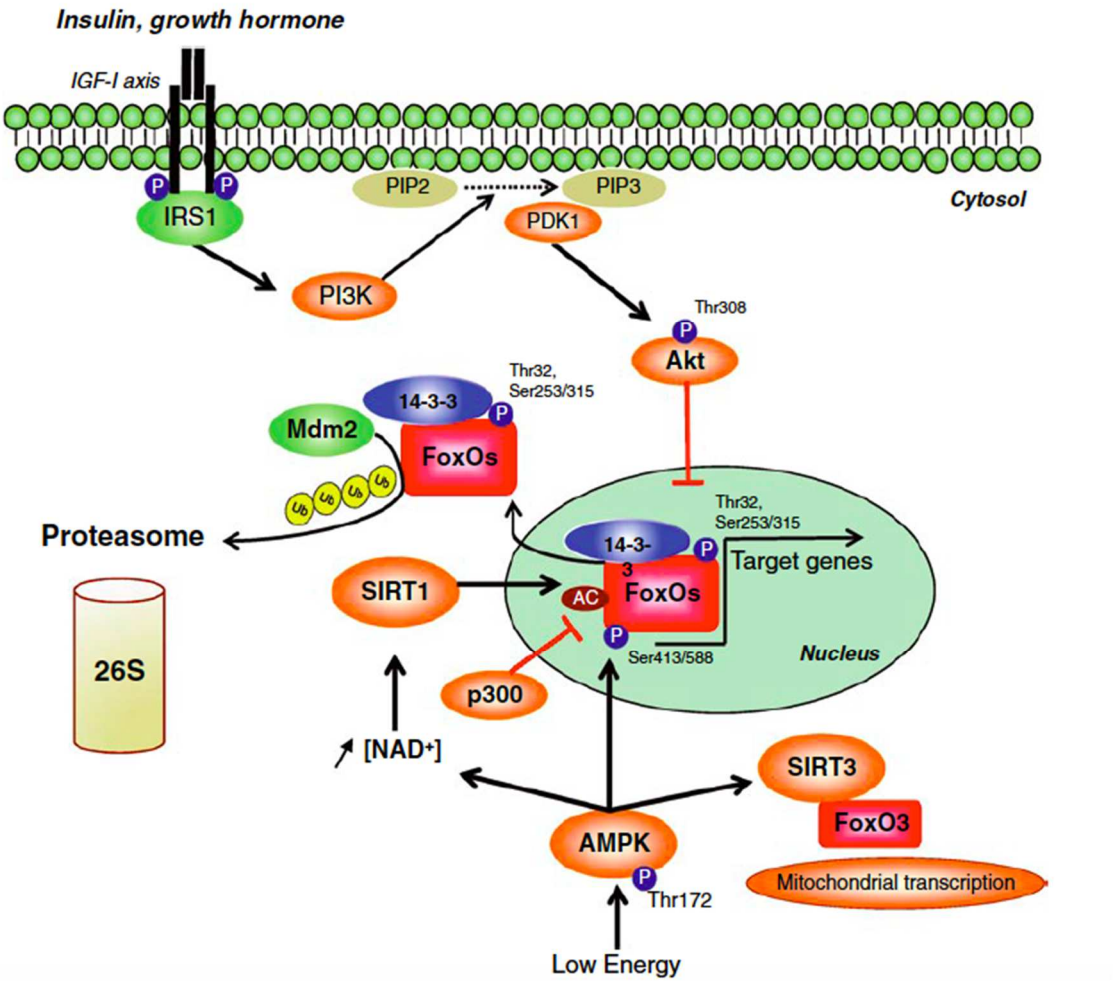

FIGURE 9 ANTAGONIST REGULATION OF FOXO PROTEINS BY THE IGF-1/PI3K/ AKT AXIS AND AMPK (SANCHEZ ET AL.,2014).

FoxO proteins are targeted also by other kinases that phosphorylate FoxO in different sites and regulate FoxO functions. These kinases include JNK[67], MST1[68], ERK and p38 MAPK[69] (Figure 9).

Many post translational modifications (PTMs) such as acetylation/deacetylation, mono or polyubiquitination, glycosylation and arginine and lysine methylation modify the transcriptional activities and also regulate subcellular localization of FoxO family protein, as well as their half-life, DNA binding, etc. In the last decade many interactors that modify FoxO family members have been discovered (Figure 10). For example, It was shown that FoxO3 interacts with the histone acetyl transferase p300 and its acetylation causes cytosolic relocalization and degradation in skeletal muscle[70].

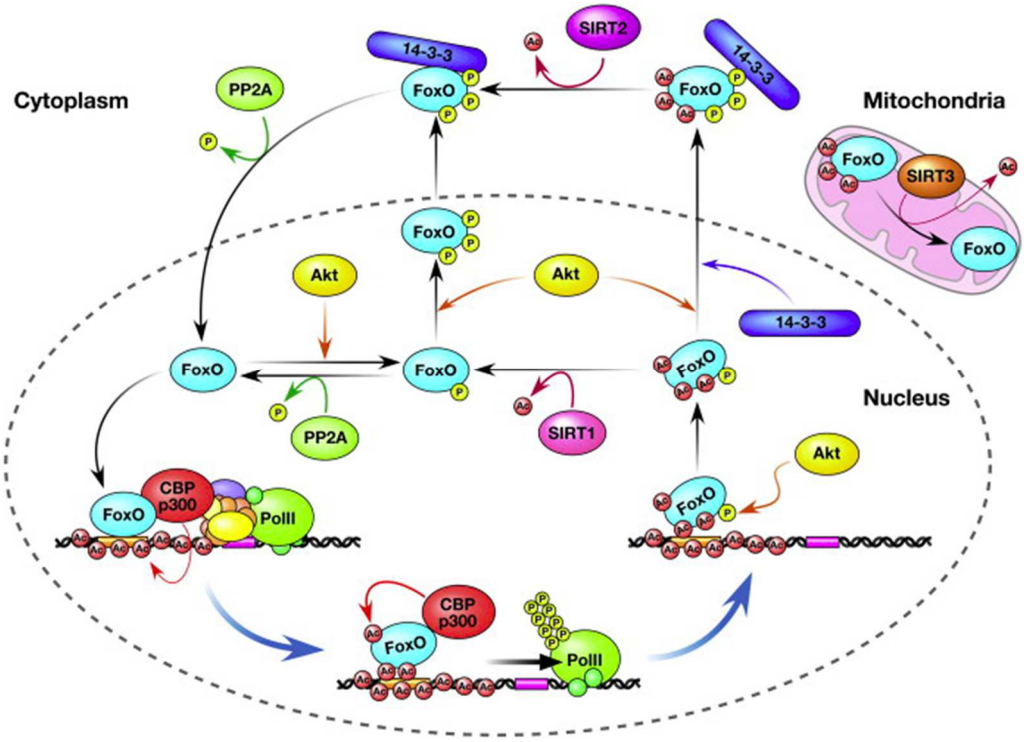

FIGURE 10 SCHEMATIC MODEL FOR THE REGULATION OF FOXO TRASNCRIPTION FACTORS BY REVERSILE PHOSPHORILATION AND ACETILATION

The degradation of FoxOs is mediated by the ubiquitin-proteosome pathway. FoxO proteins are substrates of poly- and mono- ubiquitination. The most important regulators of Foxo transcription factor degradation are several E3 ubiquitin ligases: Skp2, a subunit of the skp1/cul1/Fbox protein that ubiquitinates and promotes the degradation of FoxO1 when is phosphorylated by AKT[71]; MDM2 an ubiquitin ligase able to bind FoxO1 and 3 to promote their poly-ubiquitination and degradation[72] and also promotes FoxO4 nuclear localization by mono-ubiquitination increasing its transcriptional activity under oxidative stress[73] .

The diversity of this upstream regulation suggests the coordination in response of environmental changes such as food deprivation, oxidative stress, growth factor deprivation etc. However, depending on their activation level, FoxO proteins can exhibit ambivalent functions. For example, a basal level of FoxO factors are necessary for cellular homeostasis and to maintain quality control. On the other hand, exacerbated activation may occur in the course of several diseases, resulting in metabolic disorders and atrophy.

3.4.2. Regulation of Skeletal Muscle homeostasis by FoxO proteins

Skeletal muscle shows singular adaptive capabilities in response to stimuli such as nutritional interventions, environmental factors (hypoxia), loading conditions and contractile activity. All of these stimuli induce changes in energy metabolism and muscle mass, specially by altering the balance between synthesis and degradation of proteins or fiber composition. For these reason FoxOs members are taking more in consideration. All four members of FoxO family (FoxO 1/3/4 and 6) are expressed in skeletal muscles. Emerging evidence from multiple systems indicate that FoxOs orchestrate the expression genes involved in protein homeostasis and in cellular quality control. In particular FoxO1 and 3 play a crucial role in the regulation of skeletal muscle mass and homeostasis.

Crosstalk between protein breakdown and protein synthesis is necessary to maintain muscle mass. Activation of FoxO1 or FoxO3 in the skeletal muscle, in catabolic conditions can increase protein breakdown by the regulation of two ubiquitin ligases that have a major role in muscle protein degradation. These two ligases are overexpressed in various atrophy models. The function of E3 ubiquitin ligases is to target specific protein substrates for degradation by the 26 S proteasome.

In vivo studies of FoxO1 inactivation or overexpression have showed that it affects to a great extend muscle mass. One study in mice overexpressing FoxO1 lose their glycemic control due to a decrease in skeletal muscle mass[74]. These effects are mediated by the regulation of three genes: atrogin-1, myostatin and 4EBP1. FoxO promotes the expression of atrogin 1 which along MurF1 controls muscle atrophy[56]. Thus, inactivating FoxO1 in myotubes or rodent muscle decreases both muscle atrophy and atrogin1 expression. FoxO1 also controls myostatin and 4EBP1 by binding to its promoter and inducing its expression. Myostatin is another muscle specific protein causing muscle loss[75] and 4EBP1 is an translational inhibitor whose induction would decrease protein synthesis[76].

On the other hand, FoxO3 is the master regulator of autophagy in adult muscles[57]. Expression of FoxO3 is sufficient and required to activate lysosomal-dependent protein breakdown in cell culture and *in vivo* mouse model. However, the role of FoxOs transcription factors in the control of autophagy is not totally defined. Moreover, several autophagy genes including LC3, Gabarap, Bnip3, VPS34 and Atg12 are under FoxO3 regulation. Gain and loss of function experiments identified BNIP3, as a central player downstream FoxO in muscle atrophy[57,77]. mTOR and FoxO pathways are playing an opposite role in controlling autophagy. In presence of nutrients IGF1/Insulin pathway is activated and this leads to AKT activation. AKT then activates mTOR and by blocking ULK1 inhibits autophagy. On the contrary, pAKT phosphorylates FoxO and inactivates its transcription function by sequestering it in the cytosol. In low nutrient condition AKT is not activated so now FoxO is free to go to the nucleus and activate the transcription of several autophagy related genes, increasing thus protein breakdown and inducing atrophy (figure11).

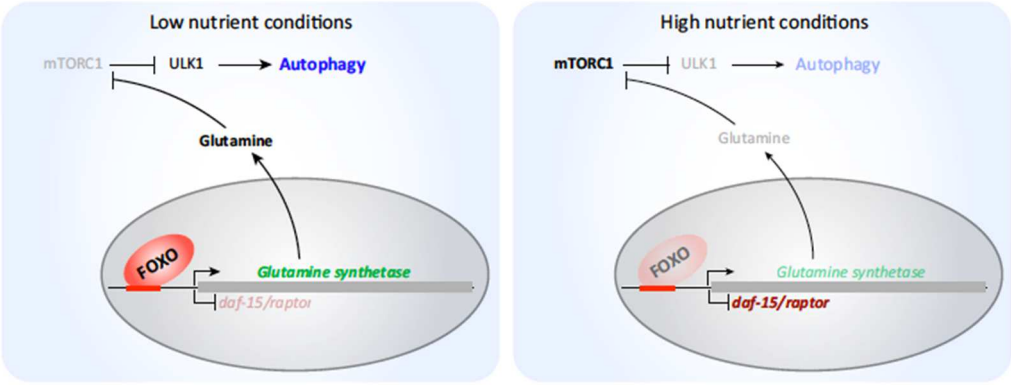

FIGURE 11. **ANTAGONISTIC INTERACTION BETWEEN FOXOS AND THE MTORC1 PATHWAY IN AUTOPHAGY**. (WEBB AND BRUNET 2014)

Furthermore, FoxO1 and FoxO3 have recently been implicated in the regulation of mitophagy through activation of the E3 ligase Mul1[78,79].

Thus, FoxO1 and FoxO3 act through an exacerbation of the ubiquitin-proteasome and autophagy-lysosomal pathways in muscle atrophy. Sandri et al. were the first

to discover that FoxO 3 was sufficient to induce muscle loss through its induction of atrogin1/Mafbx and MurF1 expression[56]. Indeed, KO mice of these two enzymes are partially resistant to muscle atrophy induced by denervation[29]. Moreover, Sandri's lab has found that inactivation of autophagic flux by LC3 silencing partially prevents FoxO3 mediated muscle loss., suggesting the major role of the autophagic pathway in FoxO3 mediated atrophy[57]. Lately, we identified FoxO family members as the master regulators of protein homeostasis in catabolic conditions due to FoxO1/3/4 deletion prevented atrophy and force decline in starved and denervated mice[16]. Gene expression profiling in fasted WT and muscle specific FoxO1/3/4 KO mice showed that FoxOs are required for the induction of more than 50% of the known atrogenes, specifically 29 out of 63 (figure 12).

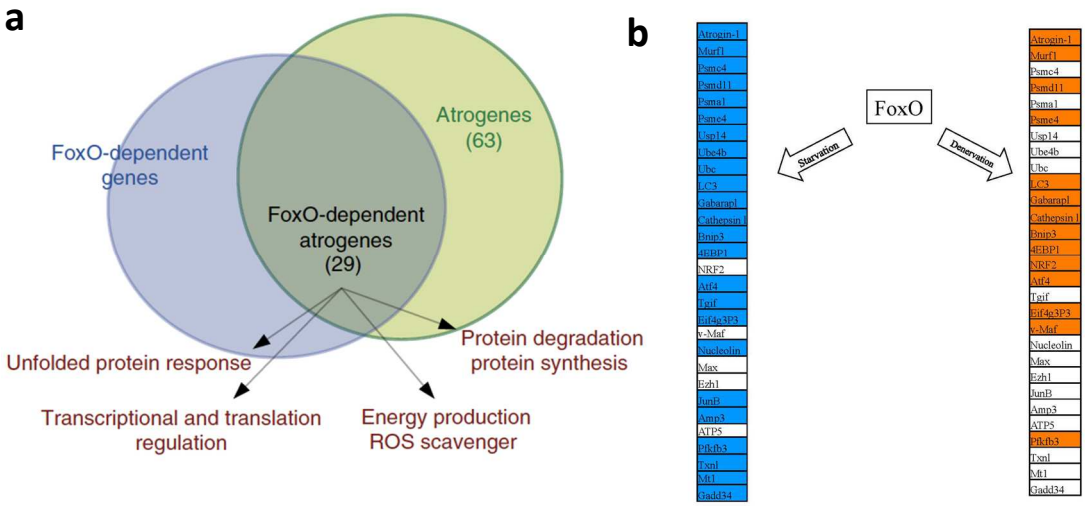

FIGURE 12 **MICROARRAY ANALYSIS COMPARING WT AND FOXO1/3/4 KO IN FED AND FASTING CONDITION**. **a)** Comparison of FoxO-dependent genes with a database from 2006 of the known atrogenes (accessible through GEO series accession number GSE52667) **b)** FoxO-dependent atrogenes during starvation and denervation. Schematic representation showing the genes found to be FoxO-dependent based on microarray analysis. Different colours indicate FoxO-dependent genes that have been validated by RT-PCR in fasting (blue) and in denervation (orange). (Milan et al. 2016)

However, the action of these ubiquitin ligases identified to be FoxO-dependent cannot account for the degradation of all muscle protein, thus many laboratories are trying to discover new ubiquitin ligases E3 that are presumably activated during the process. Our lab has recently discovered MUSA1 as a novel E3 that seems to be critical in muscle atrophy[21]. Moreover Milan et al. have identified a previously uncharacterized ligase termed SMART (Specific of muscle atrophy and regulated by transcription)[16].

4. AIM OF THE STUDY AND BIOLOGICAL SIGNIFICANCE

Muscle homeostasis is essential to the body's integrity and maintenance and the muscle wasting associated with several diseases leads to a poor quality of life. Excessive muscle loss (atrophy) ultimately aggravates diseases and increases morbidity and mortality. Even though there are different catabolic conditions that induces loss of muscle mass, there is a common transcriptional program that activates to increase the expression of genes involved in atrophy. This group of regulated genes, called atrogenes, have an important role in the autophagy-lysosome and ubiquitin-proteasome pathways. An exacerbated activation of FoxO family members (FoxO1/3/4) leads to an increased protein breakdown, muscle wasting and weakness because more than 50% of the atrogenes are under control of this transcription factor[16]. However, the atrogenes identified up to now cannot sustain all protein breakdown during atrophy by themselves. Moreover, the list of atrogenes under FoxO control was obtained using an old database that did not contain all the mouse genome and thus we hypothesized that might exist other genes under FoxO control which are still uncharacterized (whose function is not known) that could have a role in regulating muscle mass (Figure 13).

Thus, the aim of my project is to identify and characterize new genes that were sequenced by the RIKEN consortium and whose functions are yet to be revealed. A better understanding of the precise functions of the genes that are under FoxO control should help us to the development of new therapeutic approaches to prevent or limit muscle wasting.

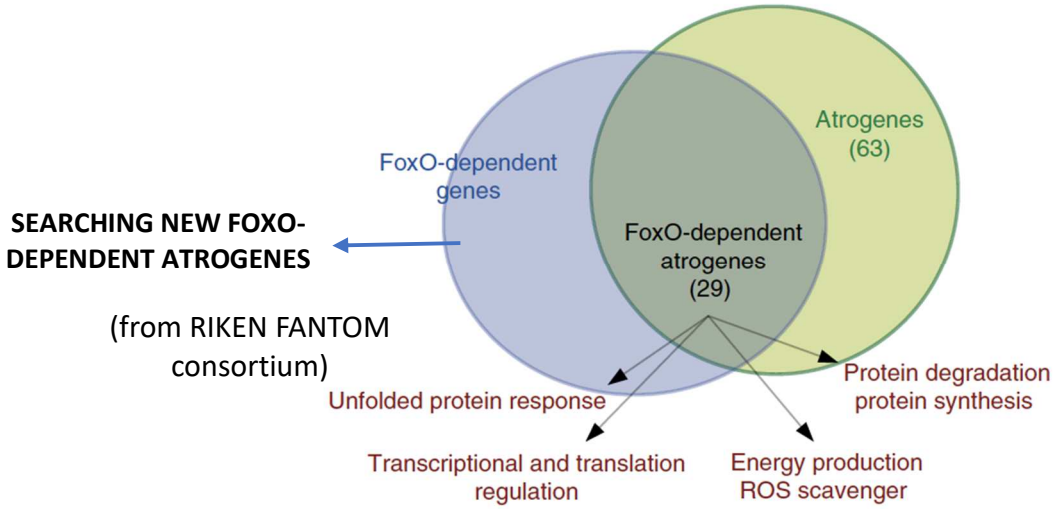

FIGURE 13. **HYPOTHESIS OF THE PROJECT.** We search for uncharacterized genes FoxO-dependent that could regulate muscle mass and be considered as new atrogenes

5. MATERIALS AND METHODS

5.1. GENERATION OF MUSCLE-SPECIFIC FOXO KO MICE AND ATG7 KO MICE

Muscle-specific FoxO1/3/4 knockout mice were obtained in our lab[16]. Mice bearing FoxO1/3/4 floxed alleles (FoxO1/3/4 f/f) were crossed with transgenic mice expressing Cre under the control of a Myosin Light Chain 1 fast promoter (MLC1f-Cre) that is expressed only in skeletal muscle during embryonic development[80].
ATG7 KO mice was generated in our lab[52]. Mice bearing an ATG7 Flox allele[81] (Atg7 $^{f/f}$) was crossed with transgenic expressing Cre under the control of *Myosin Light Chain 1 fast* promoter (MLC1f-Atg7)[57,80]. Cre-mediated recombination was confirmed by PCR with genomic DNA from gastrocnemius muscles. Tamoxifen-inducible Cre-ER was activated by Intra Peritoneum injection of 5 µg Tamoxifen (Sigma) to 2 months old mice daily for one week.

5.2. ANIMALS AND MOUSE TRANSFECTION EXPERIMENTS BY ELECTROPORATION

Animals were handled by specialized personnel under the control of inspectors of the Veterinary Service of the local Sanitary Service (ASL 16-Padova) and the local officers of the ministry of Health. Mice were housed in individual cages in an environmentally controlled room (23°C, 12h light dark cycle) with ad libitum access to food and water. All procedures are specified in the projects approved by the Italian Ministero Salute, Ufficio VI (authorization numbers 1060/2015) and by Ethics Committee of the University of Padova. All experiments were performed on 2- to 4-month old female (25-28g); mice of the same age were used for each individual experiment. *In vivo* transfection experiments were performed in females of 3 months old with C57BL/6 strain background. The transfection was produced by intramuscular (I.M) injection of expression vectors in TA muscle followed by electroporation. The animals were anesthetized by intraperitoneal injection of

xylazine (Xilor) (20 mg/Kg) and Zoletil (10 mg/Kg). Tibialis anterior (TA) muscle was isolated through a small hindlimb incision and DNA was injected along the muscle length. Electric pulses were applied by two stainless steel spatula electrodes placed on each side to the isolated muscle belly (50 Volts/cm, 5 pulses, 200 ms intervals). For fasting experiments control animals were FED ad libitum; food pellets were removed from fasted animals for 24 or 48 hours before sacrifice the mice early in the morning. For gain or loss of function of the gene of interest, one leg was electroporated with the control vector and the other leg with the vector of interest. Muscles were removed early in the morning 7-10 days after transfection.

For FDB muscle transfection mice was anesthetized and FDB muscle were injected with 10 µL of 1x hyaluronidase solution (2mg/ml) between the skin and the muscle using a sterile 1 ml syringe. 50min later the diluted plasmid DNA (10 µg in a maximum of 10 µL) was injected into the footpad in the same fashion as the hyaluronidase. 10 min later a 27 G needle was placed through the balls of skin near the toes in a position perpendicular to the heal-toe line of the foot. The second sterile 27 G needle was place it horizontally through the skin at the heel parallel to the other 27G needle ~1 cm apart from each other. Electric pulses were applied (100 Volts/cm, 20 pulses, 20 ms intervals).

5.3. CUT OF THE SCIATIC NERVE

The right hindlimbs of 3 months old mice were denervated cutting the sciatic nerve unilaterally. The animals were anesthetized by intraperitoneal injection of ketamine (75mg/Kg) and xylazine (20mg/Kg). The sciatic nerve was unilaterally cut at the level of trochanter. About 0.5-1 cm of the peripheral nerve stump was removed and the proximal stump was sutured into a superficial muscle to avoid reinnervation and obtain a permanent denervation of the lower hindlimb. Mice were sacrificed 3 days or 7 days after operation for gene expression analysis.

5.4. CANCER CACHEXIA ANIMAL MODEL

Seven-week-old male BALB/c mice (Charles River, Italy) were housed in groups of five and maintained under controlled temperature (20±1°C), humidity (55±10%), and illumination (12/12h light cycle with lights on at 07:30 am). Food and water were provided ad libitum. All procedures involving animal care or treatments were approved by the Italian Ministry of Health and performed in compliance with the guidelines of the Italian Ministry of Health (according to the Legislative Decree 116/92), the Directive 2010/63/EU of the European Parliament and the Council of 22 September 2010 on the protection of animals used for scientific purposes. Animals were randomized and divided into two groups: control (mice without tumour inoculation) and C26 (C26-bearing mice). Implantation of C26 tumor solid tissue into the flank of BALB/c mice was performed as previously described[82,83.] Control mice were inoculated with physiological solution[84]. BALB/c mice were sacrified and their tissues quickly collected at the experimental endpoint, determined by ethical criteria (loss of ~25% initial body mass). In particular, skeletal muscles were excised, weighed, and frozen in cooled isopentane with liquid nitrogen and stored at −80°C for subsequent analysis.

5.5. HUMAN SKELETAL MUSCLE SAMPLES COLLECTION

The study enrolled patients with colorectal and pancreatic cancer surgically treated at the 3rd Surgical Clinic of Padova University Hospital. The study also enrolled control, healthy donors undergoing elective laparotomy for non-neoplastic and non-inflammatory diseases, matched by age and gender to the cancer patients. All patients joined the protocol according to the guidelines of the "Declaration of Helsinki" and the research project has been approved by Ethical Committee for Clinical Experimentation of Provincia di Padova (protocol number 3674/AO/15). The biopsies were performed during elective laparoscopic surgery by cold section of a rectus abdominal fragment of about 1×0.5 cm. Each fragment was immediately split in two pieces. One was immediately frozen and conserved in liquid nitrogen

for biochemical and molecular and gene expression analysis, the other was frozen in isopentane cooled in liquid nitrogen and stored at -80°C until use for morphological and histological analyses.

5.6. HISTOLOGY ANALYSIS

Muscles were collected and directly frozen by immersion in liquid nitrogen. Then we cut muscle cryosections by using Cryostat (LEICA CM 1950). 10 µm thick slices were used to analyse tissue morphology. Frozen muscle sections (10 µm) were fixed in 4% paraformaldehyde in PBS for 10 min, washed twice in PBS (Sigma-Aldrich) for 5 min at room temperature and incubated in 0.3% triton-100 in PBS for 2 min at RT. After washing in PBS sections were incubated in blocking solution (10% normal goat serum, 5% BSA in BSA) for 1h RT. Anti-flag (Sigma Aldrich) or anti-RIKEN1P7 (Peptide facility Padova) were added for 24h at 4°C. Sections were washed next day twice in PBS, incubated with anti-rabbit Cy3 (Jackson Immunoresearch) for 1h at RT, washed twice, incubated with DAPI and then mounted with Mounting medium.

Cross-sectional area was measured using ImageJ software and compared with the area of age-matched control. The fiber diameter was calculated as caliper width, perpendicular to the longest chord of each myofiber. The total myofiber number was calculated from entire muscle section based on assembled mosaic image (_20 magnification). Stadistics were made by using t test with *P<0.05 being considered statistically significant.

5.7. FDB FIBER ISOLATION

FDB fibers were isolated enzymatically with collagenase (3mg/mL) for 1 h 37°C and then mechanically. Finally, the fibers isolated were plated in Matrigel overnight at 37°C. Cells in Matrigel then were fixed using paraformaldehide 4% in PBS for 20 min at RT. Fibers transfected were fixed

5.8. IMMUNOBLOTTING

Cryosections of 20 µm of TA muscles were lysed with 100 µL of a buffer containing Lysis buffer (50 mM Tris pH 7.5, 150 mM NaCl, 10mM MgCl2, 0.5 mM DTT, q mM EDTA, 10% glycerol, 2%SDS, 1%Triton X-100) and the addition of a protease Inhibitor cocktail and phosphatase inhibitors cocktail I and II (Roche). Protein quantification was determined with BCA kit (pierce). 20 µg of total protein lysate were run through a SDS-Page and electroblotted into a Nitrocellulose membrane. The transfer buffer (Biorad) was prepared as following: 10XTRISglycine, 20% methanol in H20. The membranes were saturated with blocking buffer (5% non-fat milk powder solubilized in TBS 1X with 0.1% Tween). The following antibodies were used: antiGapdH (cat sc 32233), anti-flag rabbit or M2 (Sigma), anti LC3B (cat L7543), anti p62 (cat P0067, Sigma), antiTOM20 (FL-145 Santa Cruz), antimyogenin (sc 12732 Santa Cruz), anti MF20 (DSHB), anti C16orf70 (abcam).

5.9. GENE EXPRESSION ANALYSIS

5.9.1. PRIMER DESIGN

NAME OF THE PRIMER m (mouse), h (Human), F(Forward), R (Reverse)	PRIMER SEQUENCE
mGAPDH F	TGCACCACCAACTGCTTAGC
mGAPDH R	TCTTCTGGGTGGCAGTGATC
mRIKEN1 F	TACAGCAAGTGGGACAGCAT
mRIKEN1 R	TGAGGCAATGTGGTTGTTCT
hGAPDH F	CACCATCTTCCAGGAGCGAG
hGAPDH R	CCTTCTCCATGGTGGTGAAGAC
hRIKEN1 F	TGGGCAATGTCTATGCTGAG
hRIKEN1 R	CTTTGTGTGGAGAGCCAAGC
mRIKEN2 F	ACCCCTGCTTCATTTACCTG
mRIKEN2 R	ATGCGTGGGAGAATCCAAT
mRIKEN3 F	ACCCAATCACAAAAGAAGTCA
mRIKEN3 R	GGGCAGTCTCTGGATGGT
mRIKEN4 F	GTGTCCCTCTTGAACCTAG
mRIKEN4 R	GTGGTCTGCCTATAATCTCAG
mRIKEN5 F	TTGTGTCAGGAGTTTC
mRIKEN5 R	AGGCAGGAAGTGAGTTTC
mRIKEN6 F	TGCGTGAACAAGACTATCC
mRIKEN6 R	AGGGCTACACAGAGAAAAC
mRIKEN7 F	GGGATTCTTACGGTTCTCTG
mRIKEN7 R	CGGAGACAAGCCACATAG
mRIKEN8 F	ACTTGGCTGAAATCTCCG
mRIKEN8 R	TGTACTCGCACAGGAAAC
mRIKEN9 F	GCATTCTGGTTGCTCTGGT
mRIKEN9 R	AATACACTTTCATTGTTTCTTGGAA
mRIKEN10 F	GCACAGGCAGAAAGAGTCAG
mRIKEN10 R	GGCTGGCAAAGCAGATTAT

5.9.2 EXTRACTION OF TOTAL RNA AND REAL TIME-PCR

Total RNA was isolated from Tibialis Anterior (TA) or Gastrocnemius using Trizol (Life technologies) following the manufacturer's instructions. 400 ng of total RNA was reversely transcribed with SuperScript IV (Life Technologies). First the 400 ng were mixed with random primer hexamers, dntPs in a total volum of 11uL. Then the samples were incubated for 5 min at 65 °C to prevent secondary structures of

RNA. RNase Out (Life technologies), DTT and SuperScript IV were added in a final volume of 20 uL. The used reaction program was: 23 °C 10 min, 55 °C 10 min and 80 °C 10 min.

Quantitative real-time PCR was performed with SYBR Green chemistry (Applied Biosystems). All data were normalized to GAPDH expression. Fold change values were calculated using the ΔΔCt method. An unpaired t-test was used to calculate statistical significance.

5.10. PLASMID CLONING

5.10.1. 3XFLAG PLASMID

RIKEN1 gene coding sequence was cloned in p3XFlag-Myc-CMV (6.4Kb). RIKEN1 was amplified from cDNA of cancer cachexia mouse model and cloned in the 3xflag plasmid using KOD Hot Start DNA polymerase (Merck Millipore) using the following primers with sticky ends:

FW 5' AAA GAT CTA CTG GAC CTG GAG GTG GT 3'

Rw complem 5' TTT GAT ATC TTA GGG CAG CTC TGC TGT TCT 3'

Vector peGFP and insert were digested using the restriction enzymes BglII and EcorV using buffer 3 (NEB) at 37 ^{o}C for 2h and from 1%TBE gel the digested vector and insert were purified using PCR gel DNA clean (Merck Millipore). The ligation reaction was done with 50ng of vector with 3-fold molar excess of insert using the Quick ligation kit (NEB).

5.10.2. GFP-N3 PLASMID

RIKEN1 gene coding sequence (1239bp) was cloned in peGFP-N3 vector (4.7 kb). RIKEN1 was amplified from 3xflag plasmid using KOD Hot Start DNA polymerase (Merck Millipore) using the following primers with sticky ends:

Fw 5' AAAGCTAGCATGCTGGACCTGGAGGTGGT 3'

Rw compl 5'TAAGGATCCGGGCAGCTCTGCTGTTC 3' (eliminate stop codon)

Vector peGFP and insert were digested using the restriction enzymes NheI-HF and BamHI (NEB) at 37 ^{o}C for 2h and from 1%TBE gel the digested vector and insert

were purified using PCR gel DNA clean (Merck Millipore). The ligation reaction was done with 50ng of vector with 3-fold molar excess of insert using the Quick ligation kit (NEB).

5.10.3. PBI3XFLAG YFP PLASMID AND PBI3XFLAG LC3YFP

RIKEN1 gene coding sequence (1239bp) was cloned in PBI3xflag YFP vector and PBI3xflag LC3-YFP vector. RIKEN1 is cloned in cterminal of 3xflag. RIKEN1 was amplified from 3xflag plasmid using KOD Hot Start DNA polymerase (Merck Millipore) using the following plasmids with sticky ends:

Fw 5' AAAGCTAGCATGCTGGACCTGGAGGTGGT 3'

Rw compl 5' GGTGATATCTTAGGGCAGCTCTGCTGTTCTCA 3'

Vector PBI and insert were digested using the restriction enzymes NheI-HF and EcorV-HF (NEB) at 37 ^{o}C for 2h and from 1%TBE gel the digested vector and insert were purified using PCR gel DNA clean (Merck Millipore). The ligation reaction was done with 50ng of vector with 3-fold molar excess of insert using the Quick ligation kit (NEB).

5.10.4. *IN VIVO* SHRNA

In vivo RNAi experiments were performed using at least three different sequences for each gene (Invitrogen BLOCK-iTTM Pol II miR RNAi Selected).

Sequence (5' to 3'): TGC TGT AAG GAT GAG GTCATG GCT TAG TTT TGG CCA CTG ACT GAC TAA GCC ATC CTC ATC CTT A.

For the validation of shRNA constructs, HEK cells were maintained in DMEM/10% FBS and transfected with shRNA constructs using Lipofectamine 2000 (Invitrogen). Cells were lysed 24 h or 48 h later and immunoblotting was performed.

5.11. SITE DIRECTED MUTAGENESIS

Prediction of LIR motifs was done with iLIR Autophagy database [75]. Site-directed mutagenesis of LIR motifs in RIKEN1-gfp plasmid was performed using Q5-site directed mutagenesis kit (NEB) following the manufacture instructions. Design of primers with mutation in the crucial aminoacids are shown below.

	MOTIF	SITE DIRECTED MUTAGENESIS	PRIMERS DESIGNED
LIR 1	LKYCGV	Y91A/V94A	Forward 5' AAA GTA AAG TTA AAG GCT TGT GGA GCT CAT TTT AAC TCT CAG GCC 3'
LIR 2	LNFRGL	F131A/L134A	5'CTC TTC CAC CTC AAC GCT CGA GGA GCT TCT TTC TCT TTT CAG 3'
LIR 3	FNYFTL	Y288A/L291A	5' GAC TAC TTT TTT AAC GCT TTT ACT GCT GGA GTG GAC ATC CTG 3'
LIR 4	SKWDSI	W351A/I354A	5' ACA ACC TAC AGC AAG GCT GAC AGC GCT CAG GAG CTT CTG 3'

PCR conditions for gene amplification were: 98 ^{o}C for 30 sec (initial denaturalization), 25 cycles at 98 ^{o}C 10 seconds, 72 ^{o}C 30 sec and 72 ^{o}C 2,5min; final extension at 72 ^{o}C 2 min.

After PCR, the product is added to a unique Kinase-ligase-DpnI (KLD) enzyme mix (NEB) for 5 min room temperature for rapid circularization and template removal. Transformation was performed using the high efficiency NEB 5-alpha Competent E. coli.

5.12. CELL CULTURE

5.12.1. *IN VITRO* TRANSFECTIONS

300000 HEK or C2C12 cells were plated overnight in Dulbecco's modified Eagle's medium (DMEM), 10% FBS 1% P/S at 37°C and 5% CO2. At 60-70 % confluence cells were transfected using Lipofectamine protocol (Life technologies). After 24h cells were fixed and used for immunofluorescence or immunoblot. RIKEN1 plasmids were described in plasmid cloning section. Other plasmids used were: LC3-cherry,

LAMP2-cherry, Golgi-GFP and HSP701A—myc-DDK-tagged (RC200270).We mutagenized HSP70 plasmid by site directed mutagenesis (explained in site-directed mutagenesis section) by adding a STOP codon after MYC tag in order to remove the 3xflag expression and be used for transfections with RIKEN1 flag.

5.12.2. IMMUNOFLUORESCENCE

Cells were fixed with PFA and permeabilized with 0.3% triton in PBS. Then blocked using 0.5% BSA, 10% goat serum in PBS and leave overnight with primary ab (1:100). After 3 washes slides were incubated with secondary antibody (1:200) for 1h. Nucleus were stained with Hoescht 4x and mounted with Dako fluorescent mounting medium. Primary antibodies used for immunofluorescence: antiflag M2 (Sigma), antiP7Riken1 policlonal antibody (Housemade antibody, CRIBI), p62 (Santa Cruz Tecnhologies), antiTOM20 (FL-145 Santa Cruz), MF20 (DSHB), antimyc (M4439 Sigma). Secondary antibodies: cy3 or 488 (Jackson Immunoresearch)

5.12.3. CELL IMMUNOBLOT

Cells were collected after transfection with PBS, centrifuged and then lysed with RIPA buffer for 30 min on ice. Cells were centrifugated for 15 min at 15000g and the supernatant was collected for quantification with BCA kit (Pierce). 10 µg or 20 µg of cell lysate was loaded through SDS-Page and electroblotted into a Nitrocellulose membrane. Antibodies concentrations were explained in immunoblotting section 3.8.

5.12.4 CELL FRACTIONATION MEMBRANE-BOUND AND SOLUBLE

For cell fractionation experiment HEK cells were transfected with 3xflagRIKEN1 or control flag vector and lysed with PBS. Cells were centrifugated at 2000g to pellet the cells and then resuspended with a mild buffer containing 1mM EDTA, 10mM Tris HCl, NaCl 150mM. Cells were sonicated 5x for 5 seconds and 20 sec resting between pulses. Then cells were centrifugated at 13700 rpm for 10 min at 4^{o}C. The supernatant was ultracentrifugated 100000g for 1h at 4^{o}C to separate membrane-bound proteins from soluble proteins.

5.12.5. CELL FRACTIONATION: AGGREGATES AND SOLUBLE PART

Cells were homogenized in five volumes of ice-cold 0.25 M sucrose buffer (50 mM Tris-HCl pH 7.4, 1 mM EDTA) with protease inhibitors. Homogenates were then centrifuged at 500g for 10 min at 4 °C. The resulting supernatants were lysed with an equal volume of cold sucrose buffer containing 1% Triton X-100. Protein concentration were measured and equalized by amount of protein in each sample. Then lysates were centrifugated at 13,000g for 15 min at 4 °C to separate supernatants (fractions soluble) and pellets. Pellets were resuspended in 1% SDS in PBS with equal volume than its respective soluble fraction. 7 µg of soluble fraction and equal volume of pellet fraction was loaded on the SDS polyacrylamide gel.

5.13. KO RIKEN1 LINE USING CRISPCAS9

RIKEN1 KO C2C12 line was obtained by using Transedit CRISPR all-in-one lentiviral expression vectors (pCLIP-ALL-EFS-Puro). 4 clones were pulled together for performing experiments.

Clone 2	Deletion 1 bp
Clone 8	No band
Clone 13	Insertion 1 bp
Clone 16	Deletion 1 bp

300000 C2C12 cells were plated overnight in DMEM 10% FBS 1% P/S. Myoblast were treated with chloroquine 75 µm for 24h before collection for analysis of autophagic flux by immunoblot (see immunoblot methodology). For differentiation experiment, 300000 cells were plated and two days after we changed the medium for differentiation (DMEM with 1% P/S and 2% Horse serum). C2C12 cells were collected after 1day, 2 days and 3days with differentiation media for immunoblot analysis.

5.14 AUTOPHAGIC FLUX QUANTIFICATION

We monitored autophagic flux in fed and 24h starving mice by using colchicine as previously described (Milan et al 2015). Briefly WT mice in FED and STV mice were treated with 0.4 mg/kg colchicine or vehicle by intraperitoneal (I.P) injection each 12 hours. The treatment was repeated two times before muscle harvesting.
For monitoring autophagic flux *in vitro* we treated the cells for 24h with chloroquine (75 μM) before cell collection.

5.15. LC3-VESICLE QUANTIFICATION

FDB muscle transfected with PBILC3YFP overexpressing RIKEN1 or control was used for LC3 quantification. The dots of LC3 was observed by using confocal microscope LEICA. The fluorescent dots were counted using ImageJ program and normalized for cross-sectional area of the fiber.

5.16. MICROSCOPY

5.16.1. FLUORESCENCE AND CONFOCAL MICROSCOPY

Fluorescence Images were collected with an epifluorescence LEICA DM5000B microscope, equipped with a LEICA DFC300-FX digital charge-coupled device camera, by using LEICA DC Viewer software. Confocal images were collected using TCS SP5 Leica at 63X oil zoom 3.

5.16.2. 2-PHOTON MICROSCOPY

Mice 10 days after transfection were anesthetized and tibialis anterior was exposed for scanning under the HyperScope 2 photon microscope (Scientifica) with a 20x objective. This microscope provides advantages for three-dimensional and deep tissue imaging. The software used for acquisition was SciScan.

5.17. STATISTICAL ANALYSIS

Data are expressed as mean values ±SE. Results were evaluated by repeated-measures ANOVA, multivariate analysis of variance (MANOVA) or student's two tail t test. A P value <0.05 was considered statistically significant. In all figures *p<0.05, **p>0.01, ***p<0.001

6. RESULTS

6.1. MICROARRAY ANALYSIS AND SELECTION OF NOVEL FOXO-DEPENDENT CANDIDATES

Gene expression profiling in fasted WT and muscle specific FoxO1/3/4 KO mice showed that FoxOs are required for the induction of more than 50% of the known atrogenes. However, with the list of atrogenes was obtained with an old database that did not contain all the mouse genome and thus we hypothesized that there are other atrogenes, still uncharacterized, that could have an important role during atrophy. We detected 10 candidate genes putative to be FoxO-dependent in the gene expression profile due to its higher expression in starvation (STV) but a downregulation in FoxO1/3/4 KO mice. Since the only information that we have is the DNA sequence obtained in the FANTOM RIKEN consortium database[85,86], these novel genes were named initially RIKEN genes (from RIKEN1 to RIKEN10) (Figure 14a).

We confirmed the results obtained with microarray by performing RT-PCR analysis in WT and FoxO1/3/4 KO mice. RIKEN1 and RIKEN4 were the most interesting candidates as they were highly induced in starved WT mice, but its expression is inhibited in starved KO animals indicating that this gene is positively controlled by FoxO in starvation. On the other hand, RIKEN2, RIKEN3, RIKEN8 and RIKEN9 increases its expression in KO mice in basal condition suggesting that these genes are negatively controlled by FoxO in basal conditions (Figure 14b).

For this thesis, we decided to focus our attention in RIKEN1 due to its higher expression in starvation in WT mice, condition where FoxO is activated, and because of the clear reduction in FoxO KO mice.

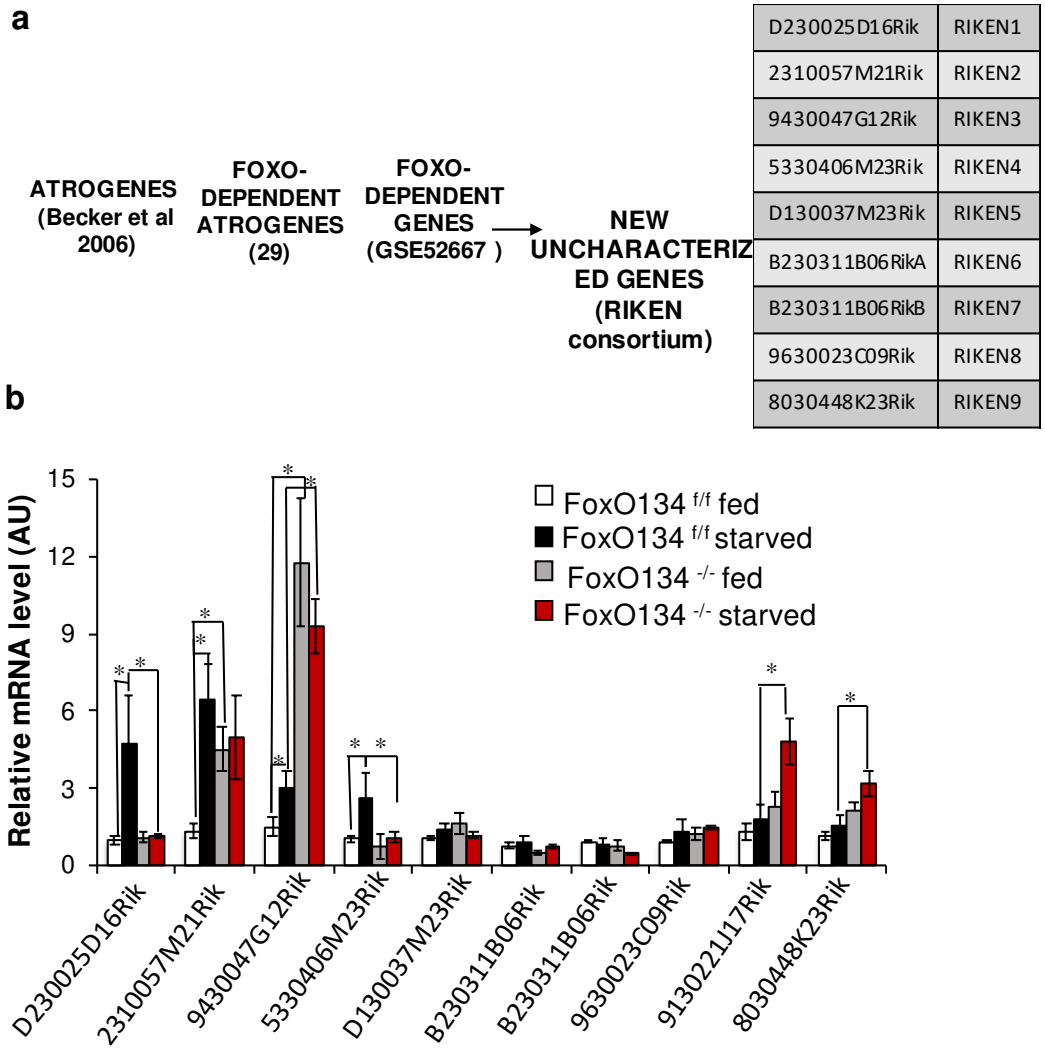

FIGURE 14: GENE EXPRESSION PROFILE: SELECTION OF NEW FOXO-DEPENDENT ORPHAN GENES. (a) The scheme shows the overlap between Foxo-dependent genes, identified by gene expression profiling of fed (n.4) and fasted (n.4) muscles from FoxO1/3/4 f/f and FoxO1/3/4 -/- (GSES2667) and atrophy-related genes or atrogenes (Becker et al 2006). From our gene expression profile we selected 9 orphan genes that showed to be FoxO-dependent. (b) quantitative RT–PCR of atrogenes from fed and 24-h starved tibialis anterior of control and FoxO1/3/4 -/-mice. Data are normalized to GAPDH and expressed as fold increase of control-fed animals. N=4 muscles in each group. Error bars indicate s.e.m. *p <0.05, **p<0.01 (student's t-test).

6.2. BIONFORMATIC ANALYSIS OF RIKEN1

D230025D16RIK (RIKEN1mouse) gene is located in chromosome 8: 105,225,145-105,253,053. It has 6 possible transcripts (splice variants) (Figure 15a) which includes two predicted protein coding genes. These two transcripts are D230025D16Rik-201 and 203 with 422aa and 117aa respectively. D230025D16Rik-205 and 202 are transcripts that activate the nonsense mediated decay pathway and thus are targeting for degradation. On the other hand, D230025D16Rik-206 and 204 are transcripts with retain intron and do not codify any protein. As we were interested in genes codifying proteins, we focused our attention in the first transcript (D230025D16Rik-201, here called RIKEN1).

a ENSMUSG000031889-2

Name	Transcript ID	bp	Protein	Translation ID	Biotype	CCDS	UniProt
D230025D16Rik-201	ENSMUST00000034361.9	2916	422aa	ENSMUSP00000034361	Protein coding	CCDS22593	Q922R1
D230025D16Rik-203	ENSMUST00000132964.1	513	117aa	ENSMUSP00000123583	Protein coding	-	D3YYD8
D230025D16Rik-205	ENSMUST00000141957.7	2460	165aa	ENSMUSP00000119148	Nonsense mediated decay	-	D6RCI5
D230025D16Rik-202	ENSMUST00000124113.7	2364	121aa	ENSMUSP00000119743	Nonsense mediated decay	-	D6RI91
D230025D16Rik-206	ENSMUST00000156561.7	2937	No protein	-	Retained intron	-	-
D230025D16Rik-204	ENSMUST00000133035.1	707	No protein	-	Retained intron	-	-

b ENSG00000125149

Name	Transcript ID	bp	Protein	Translation ID	Biotype	CCDS	UniProt
C16orf70-201	ENST00000219139.7	2865	422aa	ENSP00000219139	Protein coding	CCDS10828	A0A024R6W4 Q9BSU1
C16orf70-208	ENST00000569600.5	1353	422aa	ENSP00000455182	Protein coding	CCDS10828	A0A024R6W4 Q9BSU1
C16orf70-203	ENST00000563853.6	1025	320aa	ENSP00000456688	Protein coding	-	H3BSG0
C16orf70-211	ENST00000569914.5	768	222aa	ENSP00000456549	Protein coding	-	H3BS58
C16orf70-205	ENST00000566026.1	525	165aa	ENSP00000456154	Protein coding	-	H3BRA5
C16orf70-207	ENST00000569277.1	519	98aa	ENSP00000464242	Protein coding	-	J3QRI8
C16orf70-210	ENST00000569683.5	905	No protein	-	Processed transcript	-	-
C16orf70-202	ENST00000561683.1	476	No protein	-	Processed transcript	-	-
C16orf70-209	ENST00000569626.1	2835	No protein	-	Retained intron	-	-
C16orf70-206	ENST00000567162.2	695	No protein	-	Retained intron	-	-
C16orf70-204	ENST00000565900.1	655	No protein	-	Retained intron	-	-

FIGURE 15. RIKEN1 TRANSCRIPTS IN MOUSE AND HUMAN. Data exported from ENSEMBL database **(a)** (mus_musculus_gene_summary_ensmusg00000031889-2 and **(b)** homo_sapiens_gene_summary_ensg00000125149

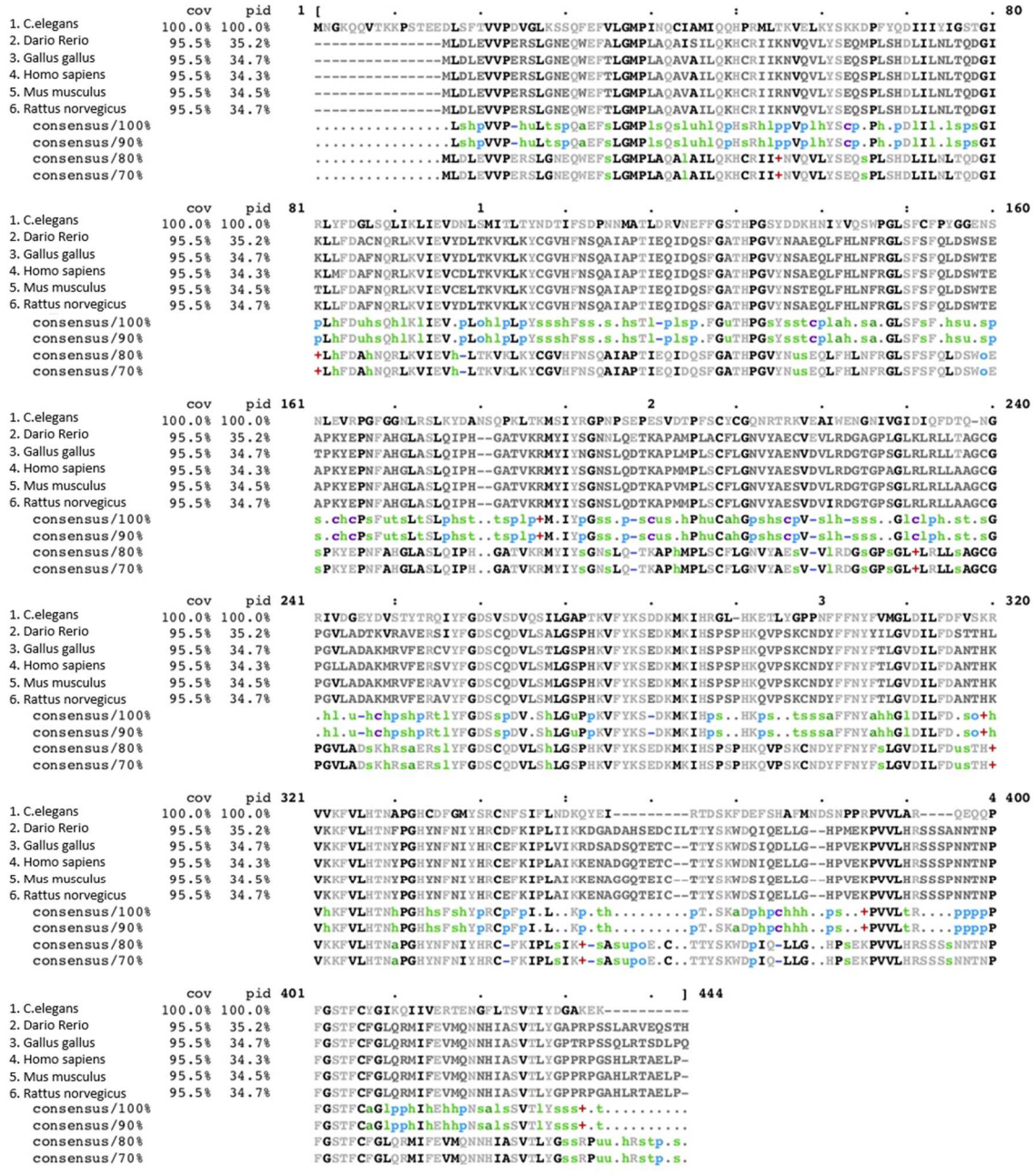

FIGURE 16. **CONSERVATION OF RIKEN1 PROTEIN SEQUENCE AMONG SPECIES.** BLASTp alignment of RIKEN1 between *C.elegans, Dario Rerio, GallusG, Homo sapiens Mus Musculus and Rattus Norvegicus*. Cov (sequence covered) pid(% of identity).

The human homolog of D230025D16Rik is C16orf70, located in Chromosome 16: 67,109,988-67,148,539 forward strand. This gene has 6 splice variants/transcripts that codify for proteins, 3 transcripts that contain retain intron and do not translate

into proteins and 2 processed transcripts that do not contain an ORF (lncRNA, ncRNA etc.) (Figure 15b).

RIKEN1 protein is conserved from *C.elegans* to *Homo sapiens* as seen in the multiple alignment performed with *Clustalw* (Figure 16). The human gene has a 30% homology with *C.elegans*, 70% with *Dario Rerio* (zebrafish) and 99% homology with mouse gene. As conserved sequences are thought to have important biological functions this increased our interest in studying this gene.

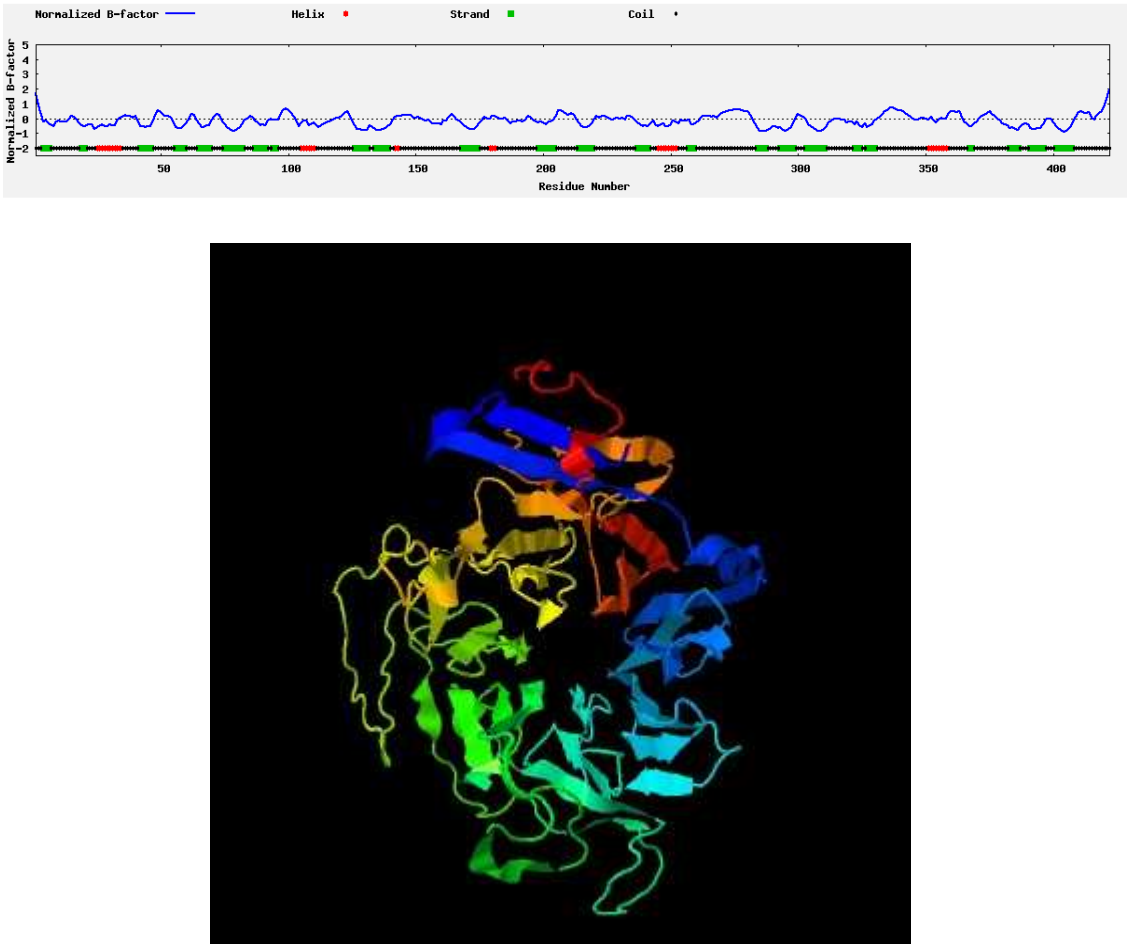

FIGURE 17. **RIKEN1 STRUCTURE PREDICTION WITH I-TASSER**. Upper image shows the UPF0132 domain with the predicted secondary structures: helix (red), strands (green) and coils (black). Lower image represents the predictive RIKEN1 3D model structure by I-TASSER database. Images were taken from the output of the I-TASSER database[87].

RIKEN1 protein forms part of an uncharacterized protein family called UPF0183. Members of this family are proteins of unknown function. For this reason, RIKEN1 does not have domains that could resemble other proteins studied and consequently the predictable structure modelling may not resemble the real one. However, RIKEN1 has an 72% of hydrophobicity and 82% of the protein is ordered meaning that it might form helix, sheets and coils. Basing on I-TASSER server[87] we predicted the model of RIKEN1 structure (figure 17).

We were interested in knowing whether the expression of this gene was exclusive in the muscle or if it was ubiquitously expressed in all organs. The mouse ENCODE transcriptome data (Figure 18a) shows that this gene is expressed ubiquitously in all organs and in particular is highly expressed in the lungs and the liver. We confirm that data by analysing RIKEN1 protein expression (Figure 18b,c,d) by immunoblot and also by comparing different cell lines we could appreciate a higher RIKEN1 mRNA expression in HEK cells (human embryonic kidney cells) compared with myotubes or myoblast (figure 18e).

Muscledb database[88] showed that RIKEN1 was expressed in striated muscle, smooth muscle and skeletal muscle. There were not particularly differences between soleus, gastrocnemius and tibialis anterior muscles. Curiously, RIKEN1 was higher expressed in the tongue and the diaphragm (figure 18f).

Overall, bioinformatic analysis suggest that RIKEN1 is not a specific gene from muscle but that may have a role also in other organs. However, as FoxO proteins are key factors of muscle atrophy, we first decided to study this gene in a muscle scenario.

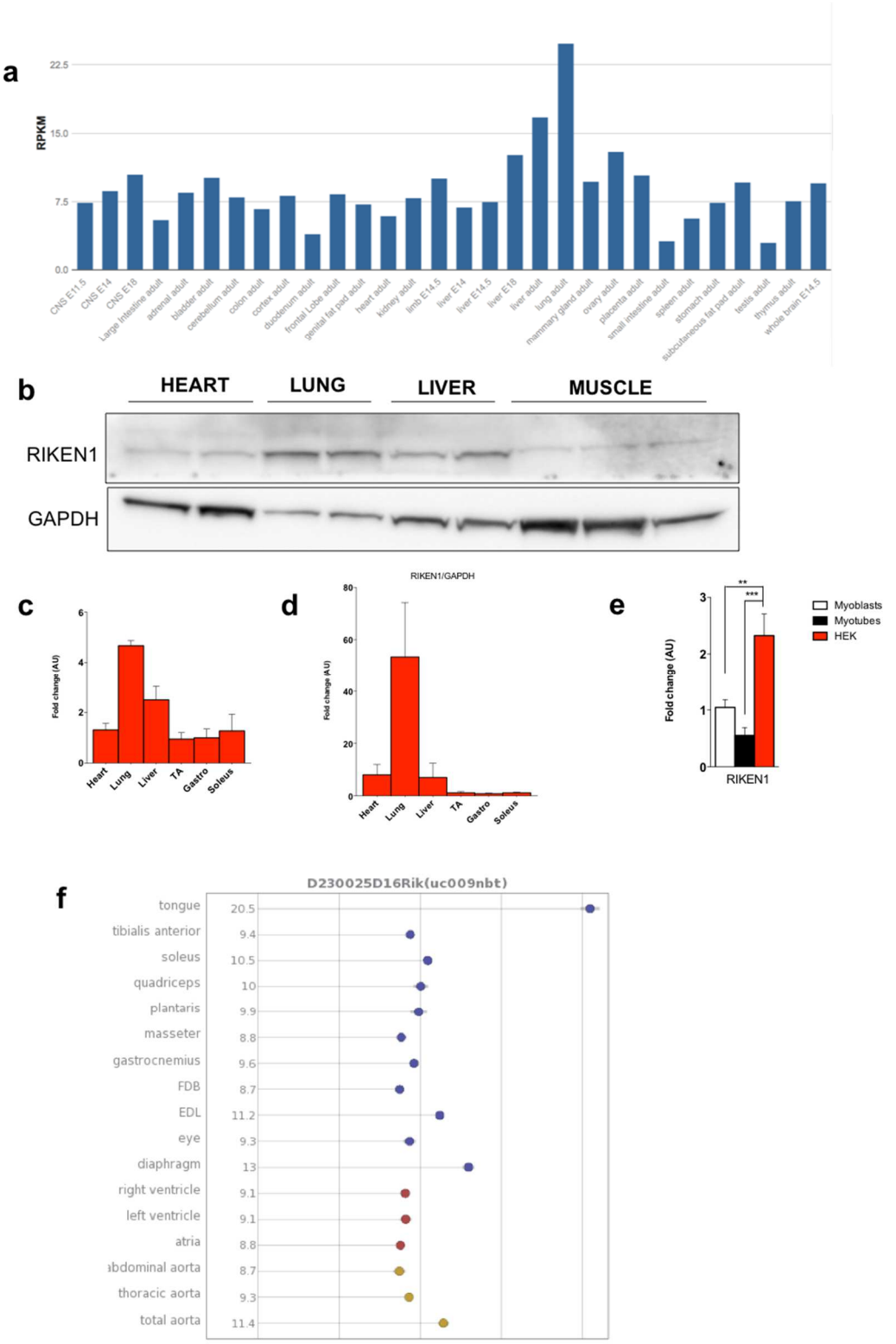

FIGURE 18. RIKEN1 EXPRESSION PROFILE. **(a)** RNA profiling data sets generated by the mouse encode project (PMID 25409824) **(b)** immunoblot analysis of RIKEN1 in homogenates of different WT mouse organs (heart, lung, liver and muscle). Quantification of the blot was done by loading **(c)** or by normalizing for GAPDH **(d)** N=3. **(e)** Real-Time PCR of RIKEN1 gene expression in Myoblasts, Myotubes and HEK cells. Results were normalized by GAPDH (n=5) **(f)** *Muscledb* database showing the expression of RIKEN1 in the different muscles including skeletal, smooth and cardiac muscles.

6.3. RIKEN1 IS A NEW ATROGENE UPREGULATED IN CATABOLIC CONDITION

RIKEN1 upregulates during starvation (figure 14b and 19a). However, studies clearly indicate that the signaling network controlling the atrophy program is specific for each catabolic condition and thus we wondered if RIKEN1 was upregulated during different catabolic conditions or it was only a nutrient-dependent gene.

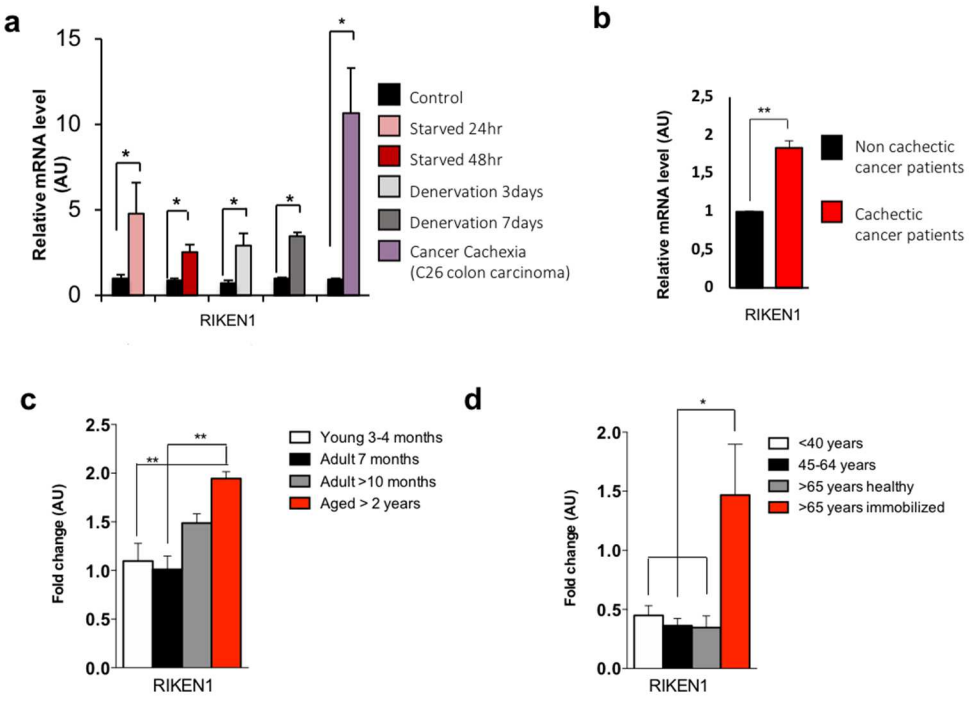

FIGURE 19 **RIKEN1 IS EXPRESSED IN DIFFERENT CATABOLIC CONDITIONS**. Quantitative real time PCR in different catabolic conditions **(a)** gastrocnemius homogenates from starved 24h and 48h, denervated 3days, 7 days and cancer cachexia mouse models n=3 **(b)** homogenates from vastus medialis muscle of cachectic cancer patients n=? **(c)** aging mice (3-4months, 7 months, 10 months and >2 years old mice) **(d)** human biopsies of man and woman of different ages. The 4 groups considered were <40 years old, 45-64 years old, >65 years old healthy aging and >65 years old people with hip fracture (unhealthy aging). Data are normalized to GAPDH and expressed as fold increase of control-fed animals. N=4 muscles in each group. Error bars indicate S.E.M. *p <0.05, **p<0.01 (student's t-test).

By RT-PCR RIKEN1 we showed a 5-fold induction after 24h of starvation, 3-fold increase after 48h of starvation and 3-fold during 3 or 7 days of denervation. Our expertise in cancer-cachexia animal models allowed us to study also this gene in this catabolic condition. Interestingly, we observed a 10-fold increase of RIKEN1 in a C26 cancer cachexia mouse model (figure 19a).

We wondered if the induction of RIKEN1 in cancer cachexia mouse model was reproduced in humans muscle biopsies. Accordingly, human biopsies of colon cancer cachectic patients had a significant higher expression of RIKEN1 compared with non-cachectic patients (Figure 19b). Furthermore, Prof. Hussain's lab has observed that this gene is also induced in sepsis condition (data not shown).

Thus, RIKEN1 seems to be a nutrient-dependent gene, inactivity-dependent gene, metabolic-dependent gene and inflammatory-dependent gene.

The next question to address was whether RIKEN1 genes were also induced during aging. Interestingly, RIKEN1 is induced in muscles from aged mice compared with young (3-4 months) or adult mice of <7months indicating that RIKEN1 is also an age-dependent gene (figure 19c). Even more interestingly, the analysis of human muscle biopsies of young versus old individuals (more than 65 years old) with and without hip fracture showed a significant increase expression of RIKEN1 in the group of old hip-fractured subjects compared to the other groups (figure 19d). This supports the idea that adding an extra catabolic factor to aging sarcopenia, such as the immobilization, could promote the expression of genes that makes worsening the atrophic condition.

Taken together, our results suggest that RIKEN1 is a new atrogene induced in different catabolic conditions such as denervation, fasting, cancer-cachexia and aging. Even though its potential significance in the different conditions we decided to first focus our attention in fasting condition for the next experiments.

6.4. RIKEN1mRNA TRANSLATES INTO A CITOPLASMIC PROTEIN WHICH HAS PUNCTA DISTRIBUTION

As predicted in ENSEMBL RIKEN1 has different transcripts. Two of them have a reading frame and therefore may codify for a protein. To confirm that, we overexpressed the longest ORF isoform (422aa) *in vitro* and *in vivo*. We cloned RIKEN1 in different vectors to demonstrate that independently of the tag and whether the gene is cloned in the N-terminal or C-terminal, RIKEN1 have the same localization. We cloned RIKEN1 in 3xflag vector (figure 20a), RIKEN1-eGFPN3 vector (figure 20b) and PBI-eGFP 3xflag RIKEN1 vector (figure 20c). We overexpressed these vectors in HEK cells to then collect the lysates and run an immunoblot. We could observe in cells transfected with 3xflagRIKEN1 vector (Figure 20a), and PBI-eGFP 3xflag RIKEN1 vector that the expressed protein has around 49Kda as predicted bioinformatically. RIKEN1-egfpN3 protein has a higher molecular weight due to the GFP tag of about 28kDa (Figure 20c). We then transfected these vectors in C2C12 cells, HEK cells and also in skeletal muscle to see the localization of the protein by immunofluorescence. Interestingly, we observed that RIKEN1 has a cytoplasmic punctiform distribution both *in vitro* (Figure 20d and 20e) and *in vivo* muscle transfection (Figure 20f) by using different plasmids.

We also created our own antibody antiRIKEN1 (CRIBI peptide facility) that recognise the endogenous protein (anti-RIKEN1 P7) and demonstrated that RIKEN1 has punctiform distribution in the cytoplasm that colocalize with our RIKEN1-flag plasmid (Figure 20g). Finally, RIKEN1-flag plasmid and the endogenous protein has a perinuclear localization as more clearly seen in FDB muscle and C2C12 cells (Fig 20d, h).

These results suggest that independently of the vector RIKEN1 gene translates into a protein of 49 KDa that has a punctiform distribution in the cytoplasm resembling the endogenous protein.

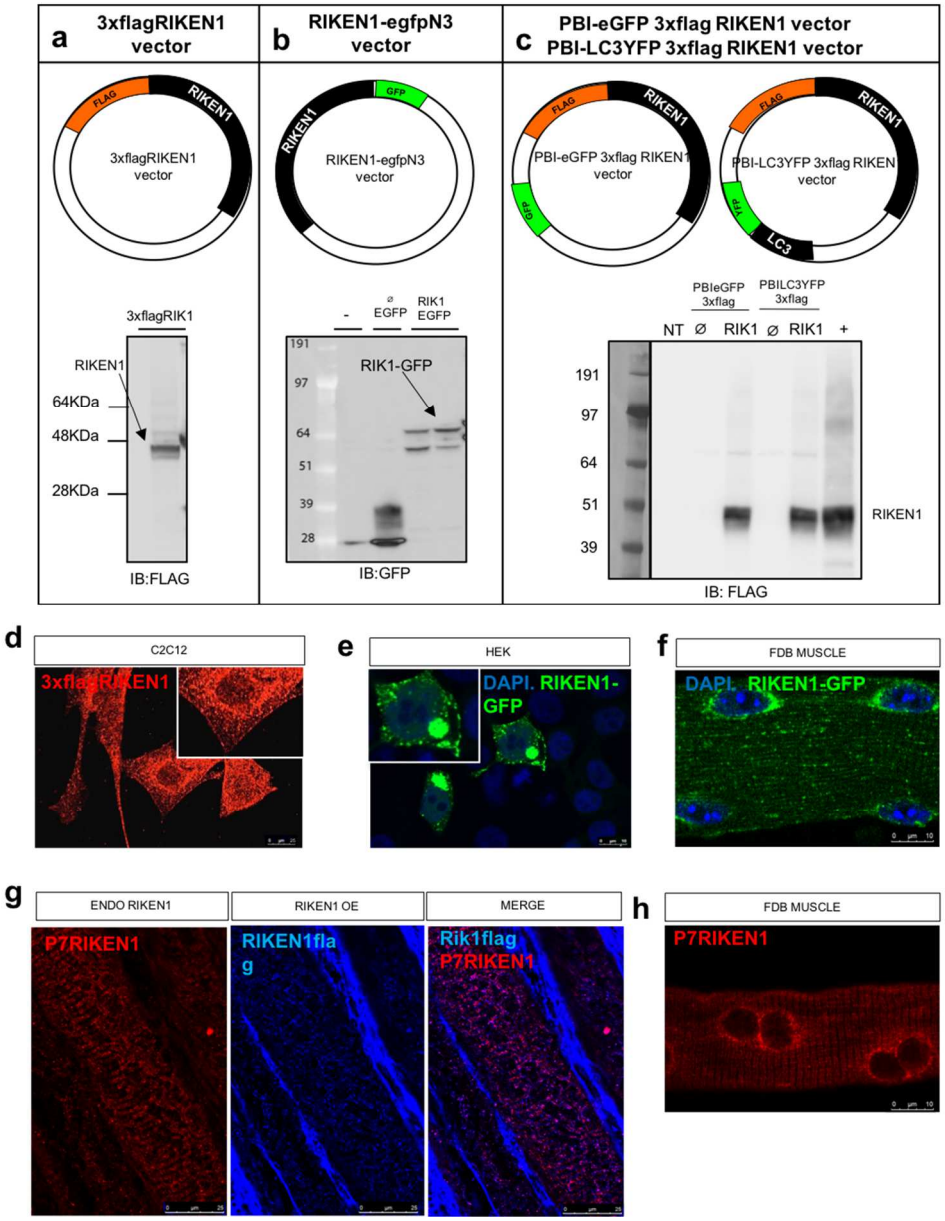

FIGURE 20 **RIKEN1 IS A CYTOPLASMATIC PROTEIN**. Cloning of RIKEN1 in different vectors: **(a)** 3xflag-RIKEN1, **(b)** RIKEN1-gfp and **(c)** PBI-eGFP 3xflagRIKEN1 vector. Immunoblots were performed in HEK cells transfected with the cloned vectors to demonstrate protein expression. **(d)** Immunofluorescence with antiflag of C2C12 transfected with 3xflagRIKEN1. **(e)** HEK cells transfected with RIKEN1-GFP. **(f)** *In vivo* transfection with RIKEN1-GFP in FDB muscle. After 10 days muscles were collected and dissociated to obtain single fibers. **(g)** Immunofluorescence in longitudinal sections of tibialis anterior muscle. Merge between endogenous RIKEN1 (antibody P7RIK1) and overexpressed protein 3xflagRIKEN1 (antibody anti-flag). **(h)** Punctiform and perinuclear localization of the endogenous RIKEN1 (P7 antibody). All images were collected using LEICA confocal microscope.

6.5. RIKEN1 COLOCALIZES WITH THE AUTOPHAGOSOME-LYSOSOME SYSTEM *IN VIVO*

Puncta usually means vesicles and therefore we wondered if RIKEN1 was bound into membrane-bound structures. We perform a fractionation protocol separating soluble and membrane-bound proteins and we found RIKEN1 in both compartments but mostly in the membrane fraction (Figure 21a). We excluded that could be located in the Golgi apparatus by analysing colocalization of endogenous RIKEN1 and Golgi marker (Figure 21b).

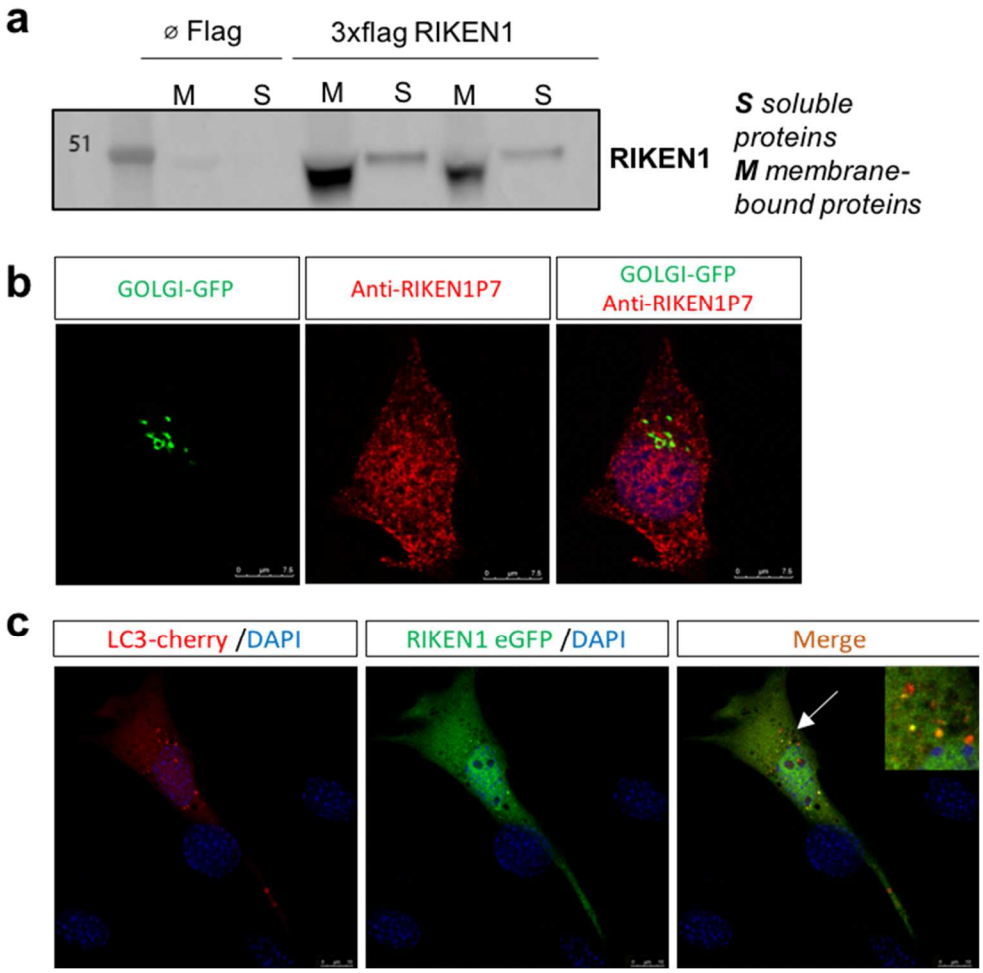

FIGURE 21. **RIKEN1 COLOCALIZES WITH THE AUTOPHAGOSOME-LYSOSOME SYSTEM**. **(a)** Fractionation protocol to separate membrane and soluble proteins in HEK cells overexpressing 3xflagRIKEN1. **(b)** HEK cells transfected with Golgi marker tagged with GFP. Immunofluorescence for the endogenous RIKEN1. **(c)** Representative image from the confocal microscope of C2C12 cells transfected with LC3-cherry (red) and RIK1-gfp (green) in HBSS condition.

As RIKEN1 localizes in membrane vesicles we hypothesised that this protein might be participating in the autophagosome-lysosome system, one of the main pathways of degradation of proteins. This process is characterized by the formation of a double-membrane vesicle that can engulf cytoplasmic material and intracellular organelles and deliver them into lysosomes for degradation. To answer this question, we overexpressed RIKEN1-gfp with LC3-cherry or LAMP2-cherry to see whether RIKEN1 was localized in either autophagosomes or lysosomes respectively in basal (FED) and fasting condition (STV) for 24h. We observed a colocalization with LC3-cherry both *in vitro* (figure 21c) and *in vivo* FED and STV condition (Figure 22b black bars and figure 23). Moreover, RIKEN1 colocalized with LAMP2-cherry mostly in fasting, condition where autophagic flux is increased (Figure 22c black bars and figure 24). To further confirm these results, we could see colocalization of RIKEN1 with LC3-cherry with *in vivo* imaging by 2photon microscopy (figure 25a and b).

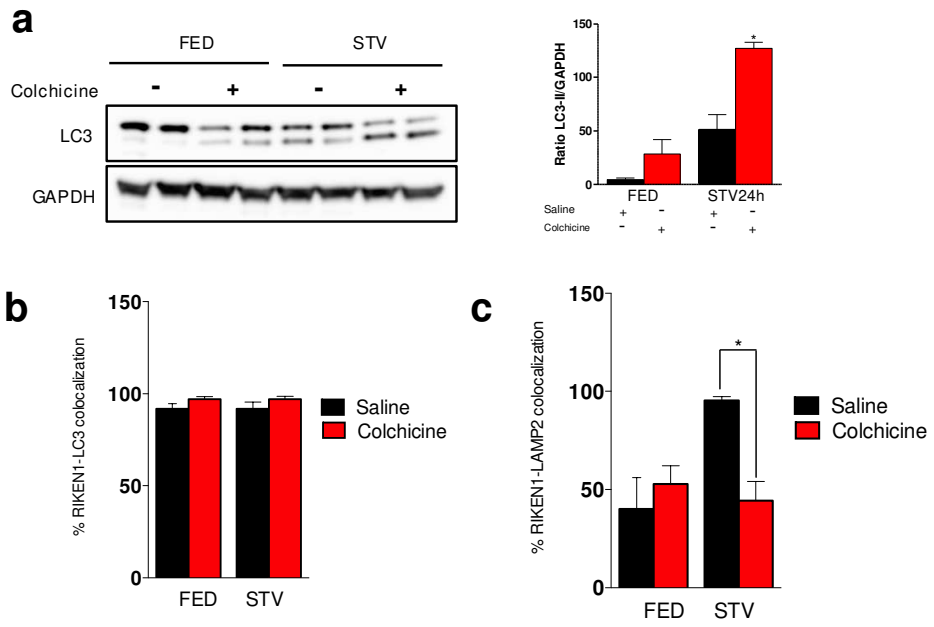

FIGURE 22. **RIKEN1 COLOCALIZES WITH THE AUTOPHAGOSOME-LYSOSOME SYSTEM (a)** homogenates of gastrocnemius muscles from FED and STV animals treated with saline or colchicine. The efficiency of the treatment was quantified by the ratio of LC3II/GAPDH. **(b)** Quantification of the percentage of LC3 dots colocalizing with RIKEN1 in FDB fibers from FED or STV 24h mice treated with saline or colchicine. The number of dots were normalized by the area of the fiber **(c)** Quantification of the percentage of LAMP2 dots colocalizing with RIKEN1 in FDB fibers from FED or STV 24h mice treated with saline or colchicine. The number of dots were normalized by the area of the fiber. Data are shown as mean ±S.E.M. Error bars indicate S.E.M. *P<0.05. (Student's t-test)

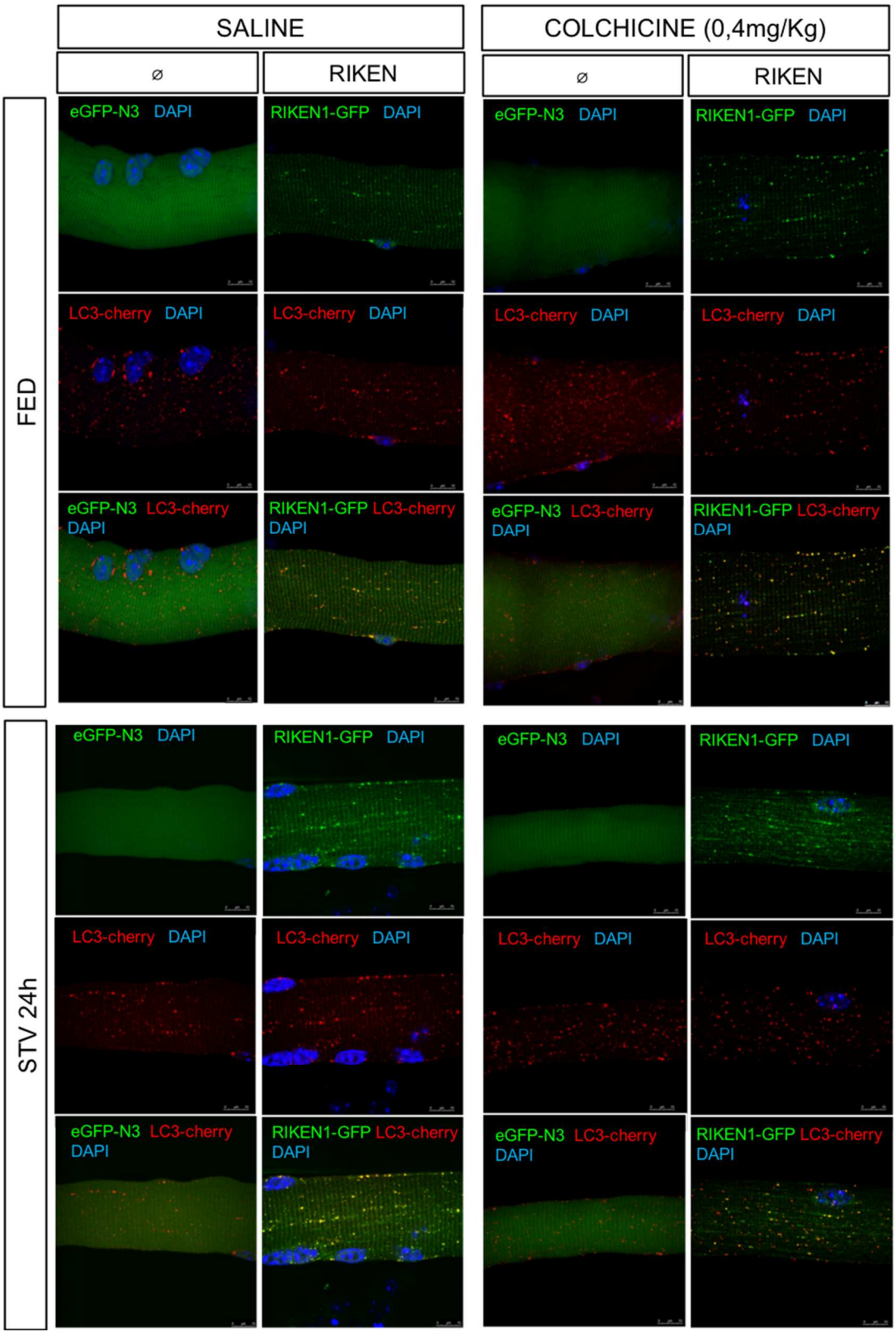

FIGURE 23. **RIKEN1 COLOCALIZES WITH LC3 IN FED AND STV24H CONDITION**. Representative images with confocal microscope showing the colocalization of RIKEN1GFP and LC3-cherry in FED and STV 24h condition with saline or colchicine treatment. Yellow dots mean colocalization. Quantification is in figure 22b

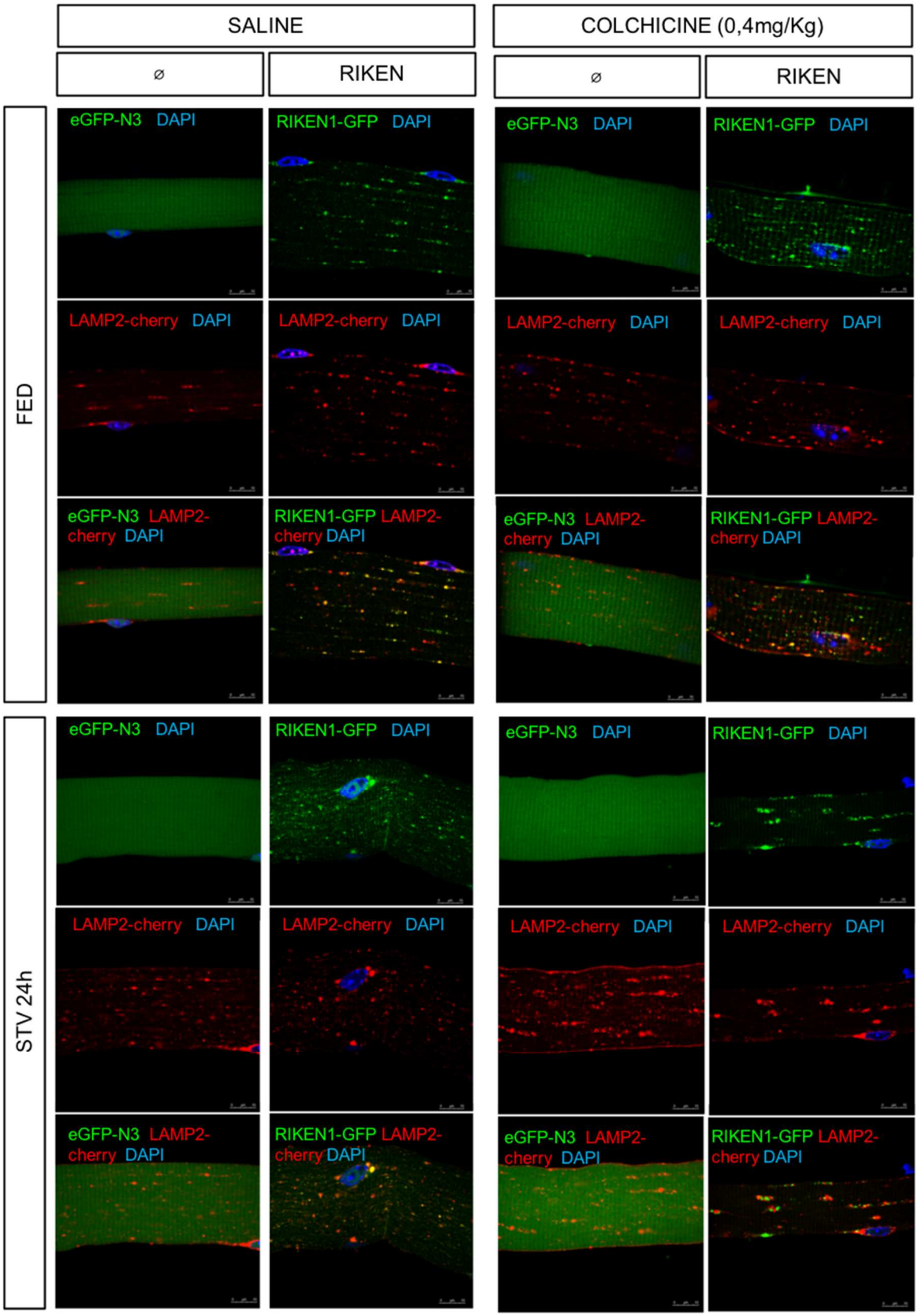

FIGURE 24 **RIKEN1 COLOCALIZES WITH LAMP2 MOSTLY IN STV 24H CONDITION**. Representative images with confocal microscope showing the colocalization of RIKEN1GFP and LAMP2-cherry in FED and STV 24h condition with saline or colchicine treatment. Quantification graph is in figure 22c

During starvation autophagic flux increases and autophagosomes fuse with lysosomes to give rise to autophagolysosomes. Thus, our hypothesis was that RIKEN1 might localize in autophagosomes and when autophagic flux increases more RIKEN1 translocate in autophagolysosomes explaining why we observe colocalization with LAMP2 in starvation but not in basal condition. To investigate our hypothesis, we blocked the fusion of vesicles with colchicine. This drug blocks the polymerization of microtubules and thus prevents fusion of vesicles. We checked the efficiency of colchicine by analysing the accumulation of LC3II in the colchicine-treated mice compared with controls (Figure 22a).

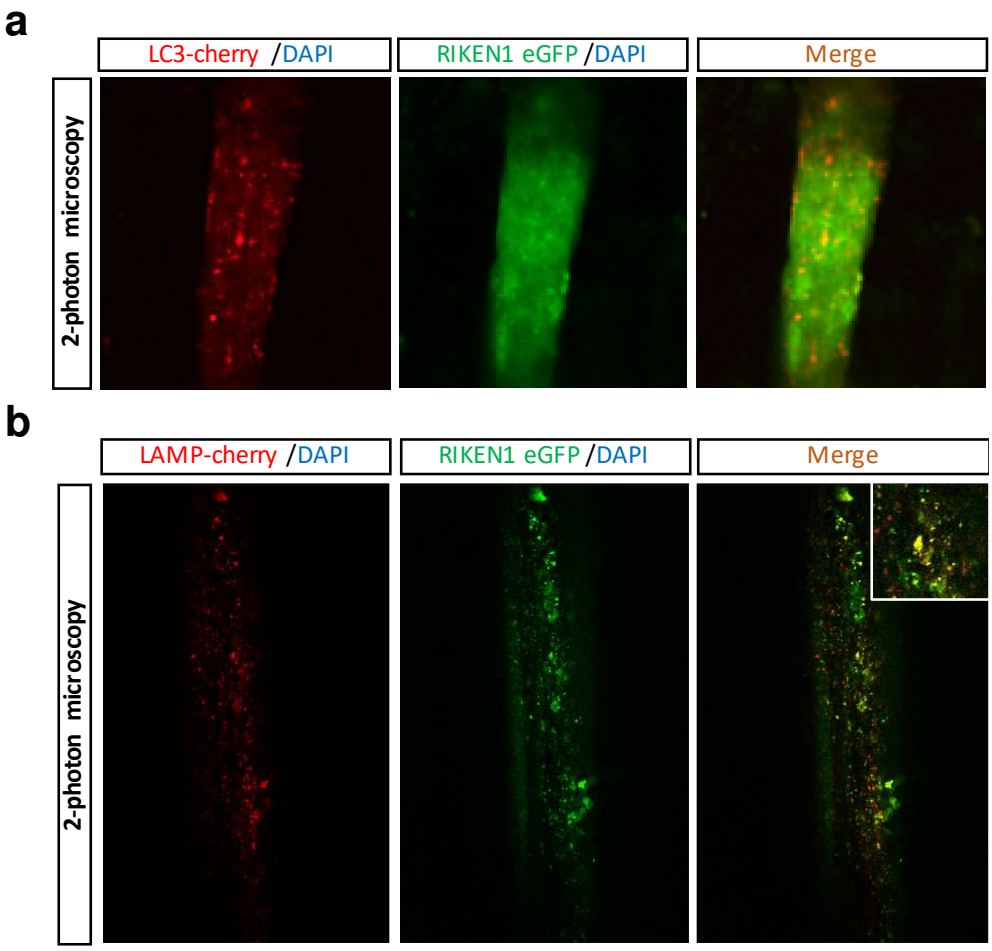

FIGURE 25. **RIKEN1 COLOCALIZES WITH LC3 AND LAMP2 *IN VIVO*.** **(a)** *In vivo* 2photon microscopy images of TA from mice transfected with LC3-cherry and RIKEN-GFP. Pictures were taken with mice anesthetized. **(b)** *In vivo* 2photon microscopy images of TA from mice transfected with LAMP2-cherry and RIKEN-GFP. Pictures were taken with mice anesthetized.

As observed, RIKEN1 maintained the colocalization with LC3-cherry after colchicine treatment (Figure 22b, 23). On the other hand, RIKEN1 significatively decreased the colocalization with LAMP2 after colchicine treatment (Figure 22c, 24). This suggests RIKEN1 is located in autophagosomes and not in lysosomes when we block the fusion of vesicles.

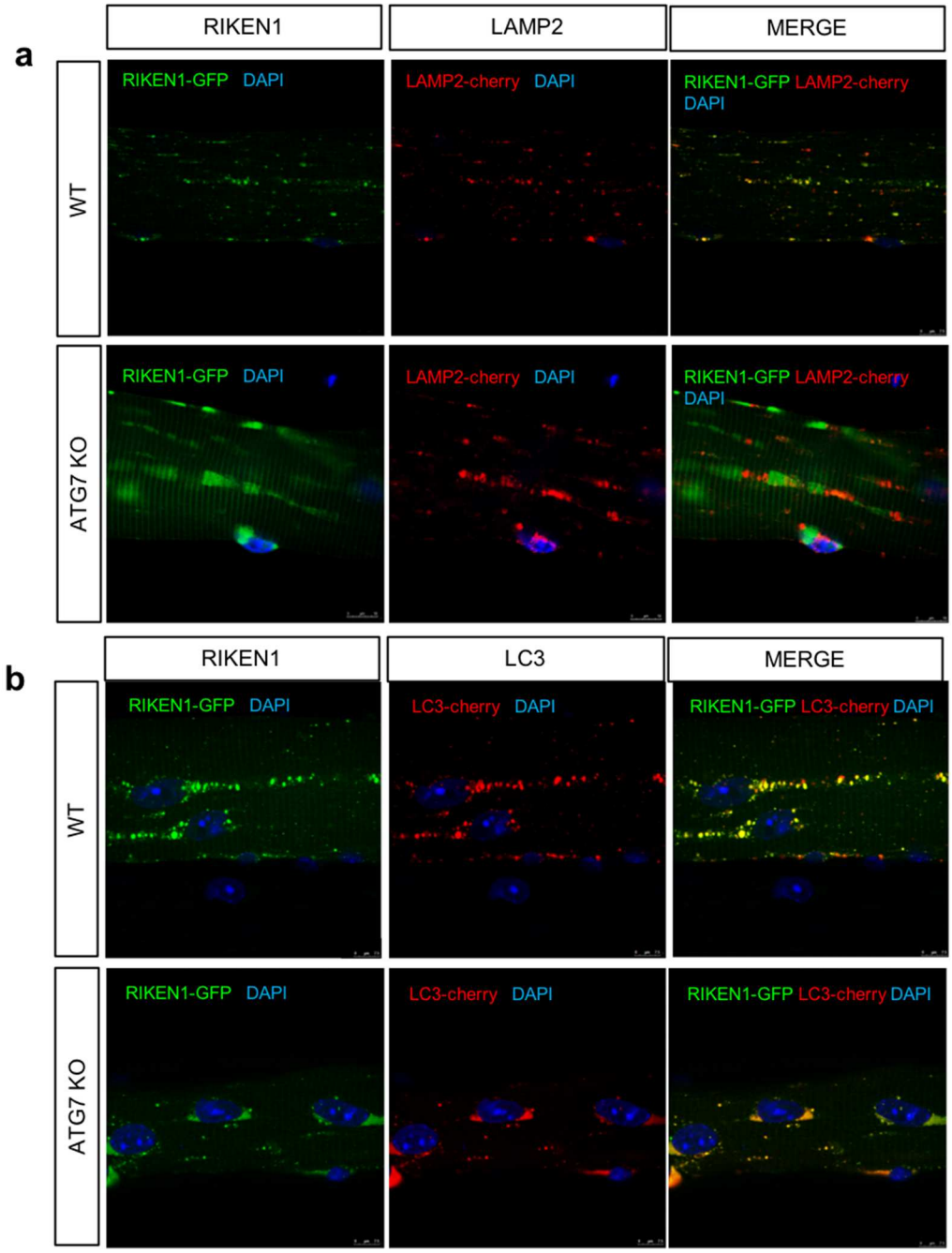

FIGURE 26 **RIKEN1 OVEREXPRESSION IN ATG7 KO MICE. (a)** *In vivo* co-transfection of RIK1gfp and LAMP2 in FDB muscle of WT or ATG7 KO mice. Single fibers were dissociated from the muscle for the analysis. **(b)** *In vivo* co-transfection of RIK1gfp and LC3-cherry in FDB muscle of WT or ATG7 KO mice. Single fibers were dissociated from the muscle for the analysis.

To further confirm these findings, we used an ATG7 KO mice generated in Sandri's lab[89] in which autophagosome formation is impaired. As seen in Figure 26a, RIKEN1-gfp in KO mice changed its localization being more cytosolic and less punctuate compared with the control WT mice.

Moreover, RIKEN1 in ATG7 KO mice did not colocalize with LAMP2 (figure 26a) but aggregates with LC3 in the cytoplasm (figure 26b).

Altogether, these findings strongly suggest that RIKEN1 is located in the autophagosomes and in the autophagolysosomes following the autophagic flux.

Finally, we wondered whether RIKEN1 plays a role at early or late stage of autophagy process. A good marker of early autophagy is DFCP1, a protein located in the omegasomes where autophagosome biogenesis occurs. To answer this question, we analysed the colocalization of the endogenous RIKEN1 with DFCP1-gfp. Our preliminar data *in vivo* (figure27a) and *in vitro* (figure 27b) showed that RIKEN1 is close but not totally overlapping with omegasomes in FDB fibers and HEK cells supporting the idea that RIKEN1 may be adjacent to omegasomes-ER but in a distinct structure.

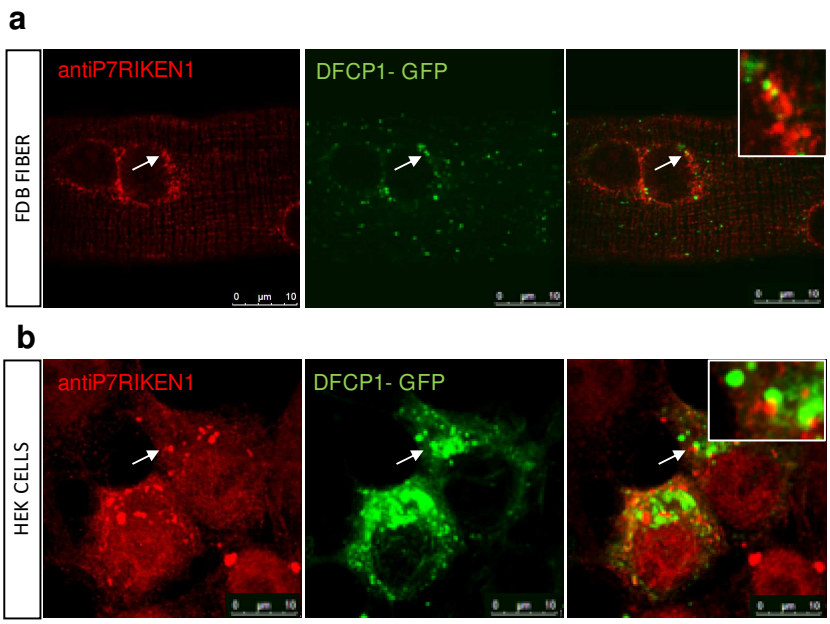

FIGURE 27. **RIKEN1 DOES NOT COLOCALIZE WITH OMEGASOMES. (a)** immunofluorescence anti-P7RIKEN1 of FDB fibers transfected with DFCP1-GFP **(b)** Representative images of HEK cells transfected with DFCP1-GFP. Immunofluorescence anti-P7RIKEN1. Pictures shown are taken by confocal microscope LEICA.

6.6. RIKEN 1 INTERACTS DIRECTLY WITH LC3 THROUGH LIR MOTIFS

Our results demonstrate that RIKEN1 colocalizes with LC3 in autophagosomes and we consequently wondered whether RIKEN1 is directly interacting with this protein. Collaboration with Prof.Dikic laboratory verified this direct interaction by immunoprecipitation (data not shown). Moreover, we wondered if RIKEN1 may be interacting with LC3 through its LIR (LC3-interactive) motifs. To answer this question, we first dissected bioinformatically the predictive LIR motifs. As shown in figure 28a there are 4 predictive LC3-interactive motifs (LIR1-4).

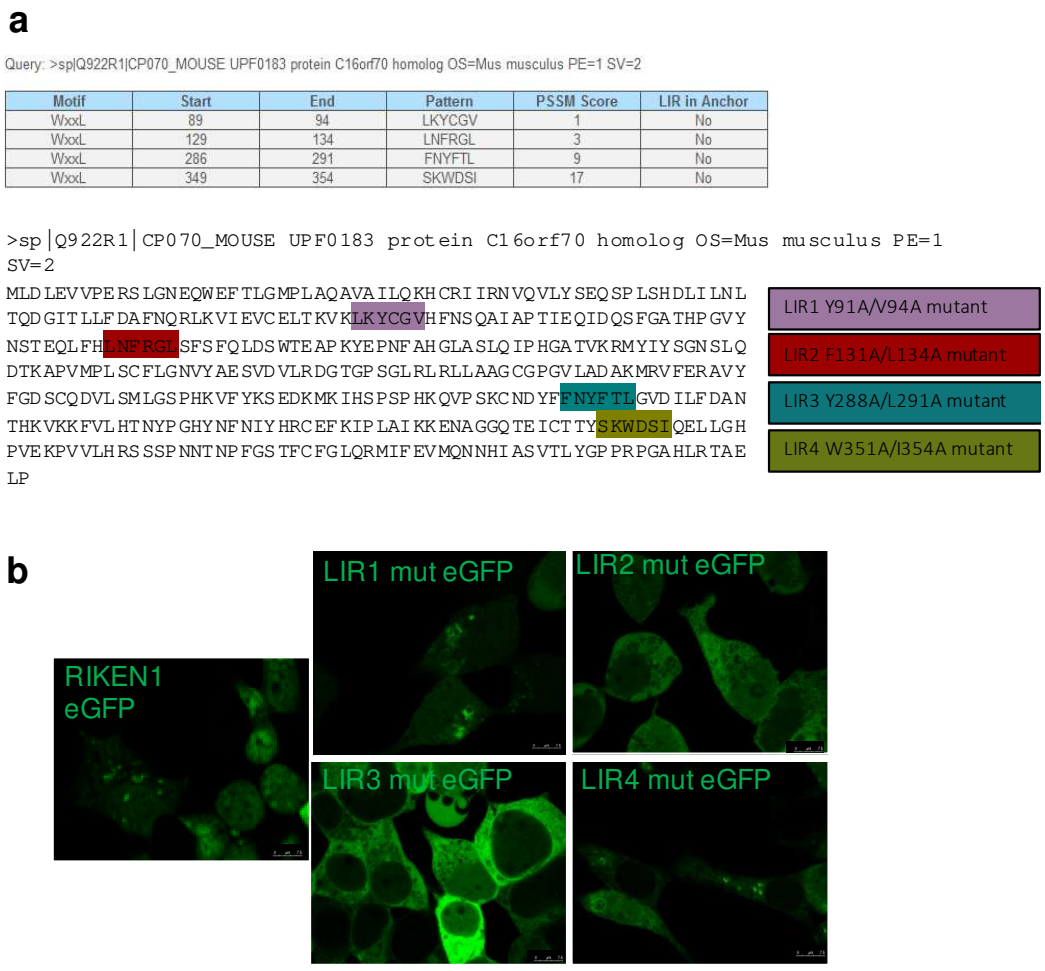

FIGURE 28. **RIKEN1 INTERACTS DIRECTLY WITH LC3 THROUGH ITS LIR MOTIFS. (a)** Prediction of RIKEN1 LIR motifs using iLIR Autophagy database. The 4 LIR predicted were named LIR1-4. The scheme also shows the mutated aminoacids by site-directed mutagenesis. **(b)** Overexpression of the control plasmid and the mutated plasmids (LIR1-LIR4) in HEK cells.

Thus, we performed-site directed mutagenesis in the two critical aminoacids required for the interaction with LC3 (figure 28a). RIKEN1 mutated in LIR1 and 4 did not change the localization of RIKEN1 which still formed puncta. On the other hand, LIR2 and 3 mutation changed RIKEN1 localization and became mostly cytosolic (figure28b). Thus, our results strongly suggest that LIR2 and 3 mutation prevents the interaction with LC3 and its localization in autophagosomes.

6.7 RIKEN1 INCREASES THE AUTOPHAGIC FLUX

Data showed previously demonstrate RIKEN1 colocalization with the autophagosome-lysosome system. For this reason, we wondered if RIKEN1 may regulate this degradation system by analysing the amount of autophagosomes in FDB fibers. As clearly seen in Figure 29a, overexpression of RIKEN1 increases LC3 puncta significatively in FDB muscle.

To analyze the autophagic flux we overexpressed RIKEN1 in HEK cells treated with chloroquine, a drug that prevents lysosomes acidification. We confirmed that blocking the flux LC3II accumulates more in the overexpressing RIKEN1 cells compared with the control (Figure 29b). This result suggest that the flux was increased in RIKEN1 overexpressing cells.

On the other hand, we wondered if RIKEN1 could be critical for autophagic flux. For that purpose, we designed shRNA against RIKEN1 and we verified by RT PCR and immunoblot that the transcript and the protein was ablated before performing experiments (Figure 30a and 30b).

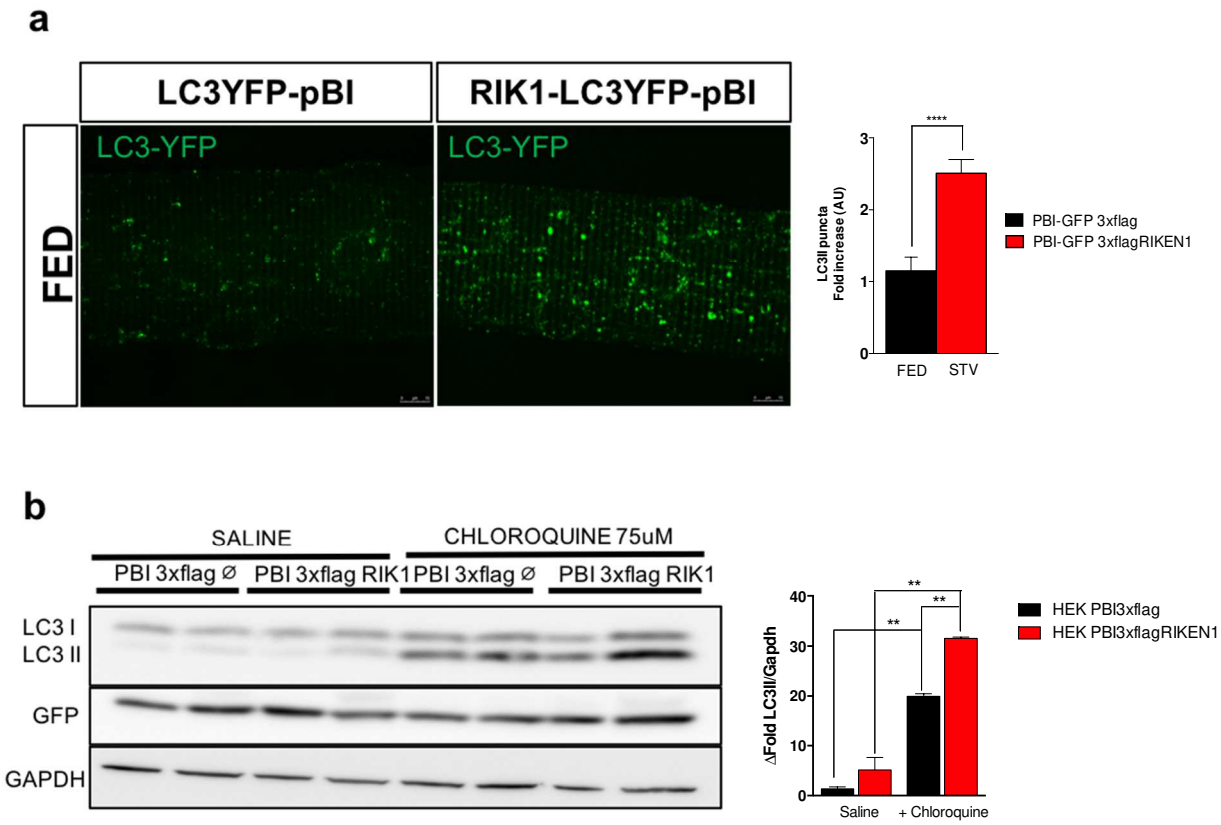

FIGURE 29 **RIKEN1 INCREASES AUTOPHAGIC FLUX**. **(a)** overexpression of PBI 3xflagRIKEN1/Lc3YFP or PBI 3xflag/LC3YFPplasmid in FDB muscle fibers. Fibers were isolated and fixed. Quantification of the green puncta using ImaJ program. **(b)** immunoblot of HEK homogenates transfected with control vector or overexpressing vector PBI 3xflag RIK1 and treated for 24h with chloroquine 75 µM. Data was normalized by GAPDH and expressed as fold increase. Data are shown as mean ±s.e.m. Error bars indicate s.e.m. *P<0.05. (Student's t-test)

To do so, we co-transfect FDB muscles with shRNARIKEN1 and LC3cherry. As observed in figure 30c and 30d RIKEN1 inhibition did not decrease the number of LC3 puncta in basal condition.

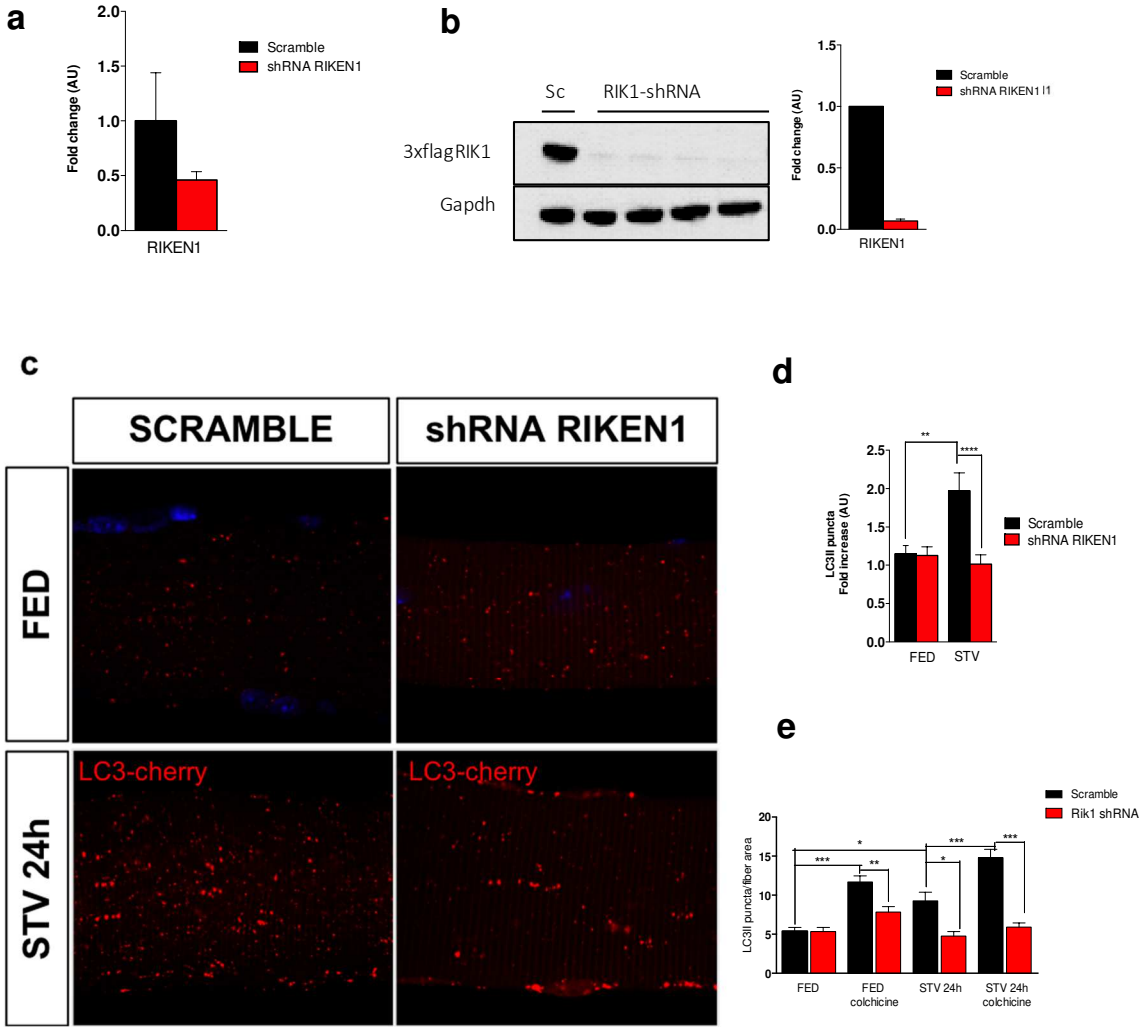

FIGURE 30. **INHIBITION OF RIKEN1 WITH SHRNA *IN VIVO* BLOCKS THE AUTOPHAGIC FLUX. (a)** Quantitative RT-PCR of RIKEN1 transcript in FDB muscle transfected with scramble or shRNARIKEN1. **(b)** Immunoblot with homogenates of HEK cells cotransfected with RIKEN1flag-scramble or RIKEN1flag- shRNARIKEN1 **(c)** Representative images of FDB fibers from mice FED or STV 24h cotransfected with shRNAs and LC3cherry. **(d)** Quantification of LC3-cherry positive vesicles and normalized by the area of the fibers in FED and STV condition. (n=3 per group) **(e)** Quantification of LC3-cherry positive vesicles and normalized by the area of the fibers in FED and STV condition treated with saline or colchicine to block the flux (n=3 per group). Quantification of the puncta was using ImaJ program. Data are shown as mean ±S.E.M. Error bars indicate S.E.M. *P<0.05, **P<0.01 ***P<0.001 (Student's t-test)

However, inhibition of RIKEN1 reduced LC3II puncta in fasted condition suggesting RIKEN1 role is more important during catabolic conditions than in basal condition. At this point, we wondered if the flux was blocked by inhibiting RIKEN1 using colchicine drug. As seen in figure 30e LC3II puncta did not increase after colchicine

treatment in basal and starved condition compared with saline control suggesting a block of autophagy when RIKEN1 is inhibited.

To better understand the role of RIKEN1 in autophagy with the collaboration of Prof. Salviati's lab we created a C2C12 cell line KO for RIKEN1 using the innovative CRISPR-CAS9 technique. We stained the cells with the autophagy marker p62 and as observed in figure 31a we could appreciate an accumulation of p62 in KO cell line.

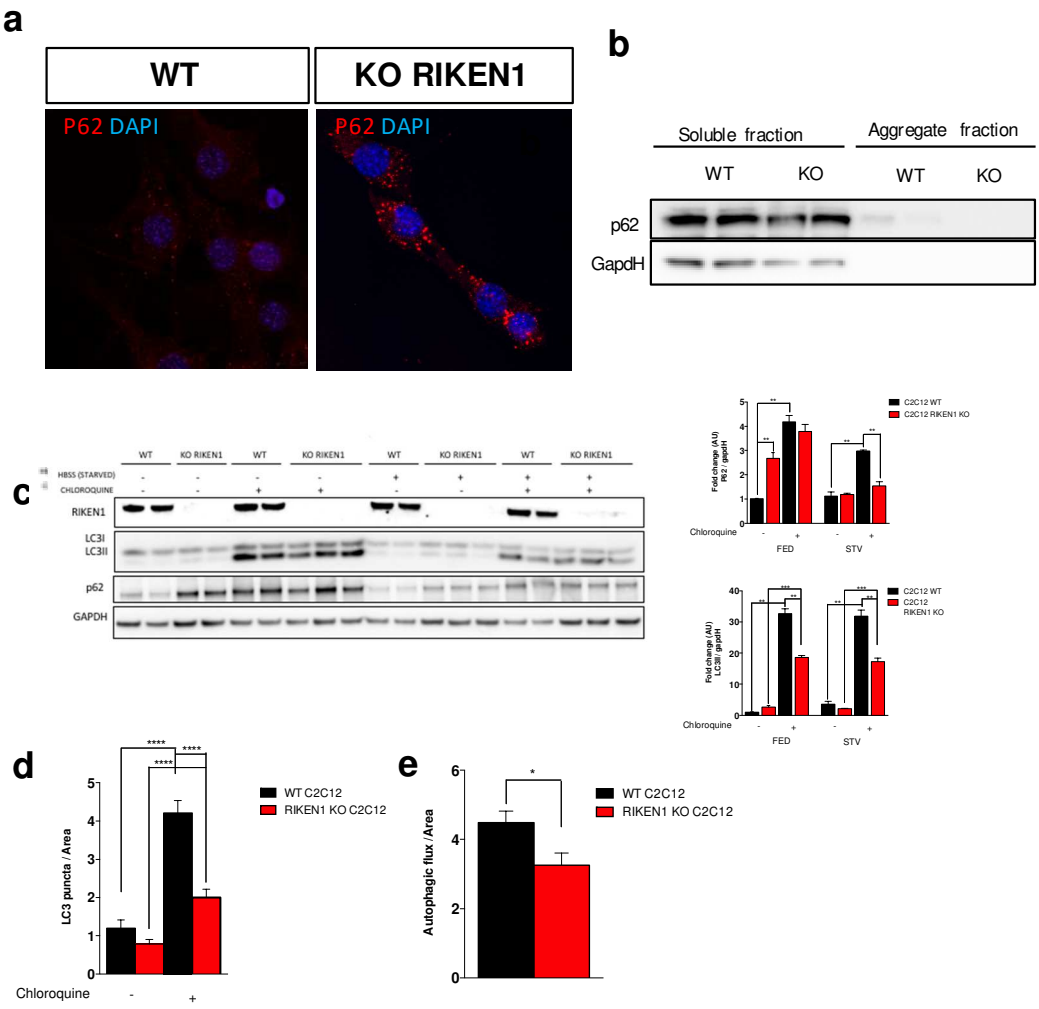

FIGURE 31. **RIKEN1KO CELLS ACCUMULATE P62 AND SHOWED A REDUCED AUTOPHAGIC FLUX.** **(a)**Representative images of an immunofluorescence against p62 in WT and KO C2C12 RIKEN1 myoblasts. **(b)** fractionation protocol to separate soluble and aggregate fraction was performed in WT or KO c2c12 cells. Equal volumes were loaded for aggregate and soluble fraction. Immunoblot anti p62 and GAPDH. **(c)**immunoblot from homogenates of c2c12 WT or KO cells in basal or 2h starved condition treated with/without chloroquine 24h (n=3 per group). Quantification of p62 and lc3II was normalized by gapdh. **(d)** Analysis of LC3 puncta with or without chloroquine 75uM in WT and KO RIKEN1 C2C12 cells normalized by the Area. **(e)** Data showed in figure d was expressed by fold increase of chloroquine-treated cells respect non-treated cells. All data are shown as mean ±S.E.M. error bars indicate S.E.M. *p<0.05 **p<0.01 ***p<0.001 (student's t-test)

We perform a protocol to separate aggregates fraction and soluble fraction in order to see if the accumulation of p62 is mainly due to the formation of aggregates or p62 is not being degraded efficiently by the system in KO cells. As observed in figure 31b p62 are located in the soluble fraction in the KO cells and not into aggregates. Thus, these results suggest that p62 accumulate into autophagosomes because is not efficiently degraded.

Our shRNA data suggested that there was a block of autophagy flux inhibiting RIKEN1. Therefore, to further confirm this hypothesis we performed the same experiment in KO C2C12 cells using chloroquine drug to analyse the autophagic flux.

As seen in figure 31c p62 and Lc3 levels increase in the WT suggesting that the treatment worked efficiently. On the other hand, KO cells after chloroquine treatment did not increase the levels of p62. In addition, LC3II levels were significantly reduced if we compared them with WT cells treated with chloroquine (figure 31c) revealing that basal autophagy flux is reduced in absence of RIKEN1. Consistently with immunoblots for LC3 lipidation, immunofluorescence analyses for LC3 positive puncta also showed a reduced autophagic flux. LC3II positive puncta were counted directly in WT and RIKEN KO C2C12 myoblasts blocking or not the flux with chloroquine for 24h (figure 31d,e).

Overall, our data shows that by inhibiting or depleting RIKEN1 *in vivo* and *in vitro* autophagic flux is reduced and that by overexpressing RIKEN1 autophagic flux is accelerated.

6.8. RIKEN1 IS REQUIRED AND SUFFICIENT TO INDUCE ATROPHY *IN VIVO* MUSCLE

FoxOs orchestrate the expression of genes involved in protein homeostasis and in cellular quality control. FoxO1 and 3 play a crucial role in the regulation of skeletal muscle mass and homeostasis by regulating atrogenes that participate in autophagy-lysosomal system or ubiquitin-proteasome system.

Our results strongly suggest that RIKEN1 is a FoxO-dependent gene induced in catabolic conditions which plays a role in autophagosome-lysosomal system increasing autophagic flux.

Because the enhancement of autophagy flux in catabolic conditions contributes to the shrinkage of muscle cells, we tested the physiological relevance of RIKEN1 inhibition on muscle mass when autophagy is activated by nutrients removal or by cancer growth. For this reason, we transfected TA muscle with shRNA of RIKEN1 or scramble control in starved mice or in tumour-bearing mice in order to compare the area of the fibers. Interestingly, we found that inhibition of RIKEN1 reduced muscle loss in fasted animals (figure 32a) and tumour-bearing mice (figure 32b) confirming the critical role of this factor in protein breakdown. Conversely, overexpression of RIKEN1 reduced around 20% the fiber size meaning that by itself is sufficient to induce atrophy in tibialis anterior muscle transfected (Figure 32c).

Therefore, RIKEN1 is a critical player in autophagy regulation and consequently, plays a physiological role in the control of muscle mass during stress conditions.

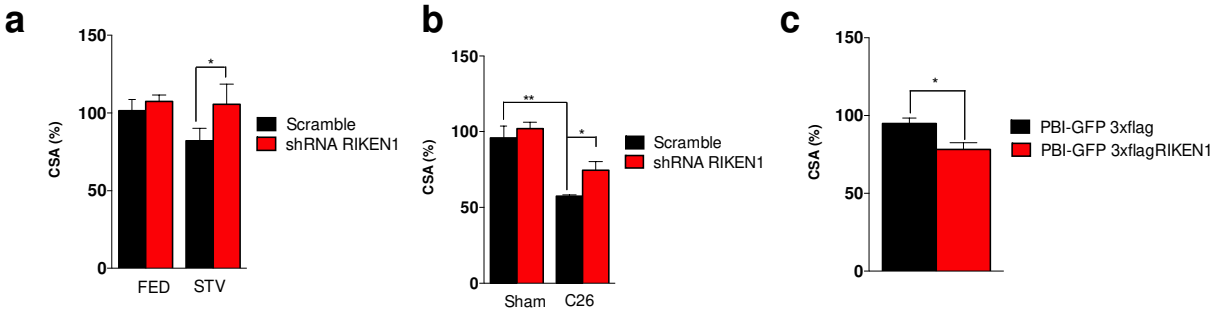

FIGURE 32. **RIKEN1 IS NECESSARY AND SUFFICIENT TO INDUCE MUSCLE ATROPHY *IN VIVO***. Efficiency of shRNARIKEN1 **(a)** Inhibition of RIKEN1 prevents muscle atrophy in FASTED muscles. Adult tibialis anterior muscles were transfected with expressing vectors that encode shRNAs against RIKEN1 or scramble. 10 days later cross-sectional area of transfected fibers, identified by GFP fluorescence, was measured. N=7 muscles for each group. **(b)** Inhibition of RIKEN1 prevents muscle atrophy in C26 tumour-bearing mice muscles. Adult tibialis anterior muscles were transfected with expressing vectors that encode shRNAs against RIKEN1 or scramble. 10 days later cross-sectional area of transfected fibers, identified by GFP fluorescence, was measured. N=3 muscles for each group. **(c)** Overexpression of RIKEN1 induces atrophy *in vivo*. Adult tibialis anterior muscles were transfected with PBI-GFP (one leg) or PBI-GFP 3xflag RIKEN1 (contralateral leg). After 10 days cross-sectional area of transfected fibers, identified by GFP fluorescence, were measured. (n=5). Data are shown as mean ±S.E.M. Error bars indicate S.E.M. *P<0.05. (Student's t-test).

6.9 RIKEN1 IS INDUCED IN POMPE DISEASE- AN AUTOPHAGY RELATED DISEASE

The importance of this protein in autophagy pathway made us reasoned about the possibility of being induced in some autophagy-related diseases. Pompe disease is characterized by the deficiency of lysosomal acid alpha-glucosidase gene which encodes a lysosomal enzyme responsible for the degradation of glycogen. A deficiency of this lysosomal protein allows glycogen accumulation in multiple tissues even though clinical manifestations are mainly due to skeletal and cardiac muscle involvement. It was thought that lysosomal enlargement/rupture was the mechanism of muscle damage in Pompe disease. However, in past years it became clear that this simple view of the pathology is inadequate; the pathological cascade involves dysfunctional autophagy at the termination stage with an impaired autophagosomal-lysosomal fusion[90].

Microarray data on biceps biopsies from untreated patients with infantile-onset Pompe (GDS4410/223440_at) showed an increased expression of RIKEN1 gene in patients with Pompe disease (figure 33a).

In line with microarray database we found that leukocytes from patients with Pompe diseases revealed an increased RIKEN1 protein expression compared with control samples (figure 33b). More research is needed to understand the reason why this gene is upregulated in Pompe patients and whether it has an impact in the pathology of the disease.

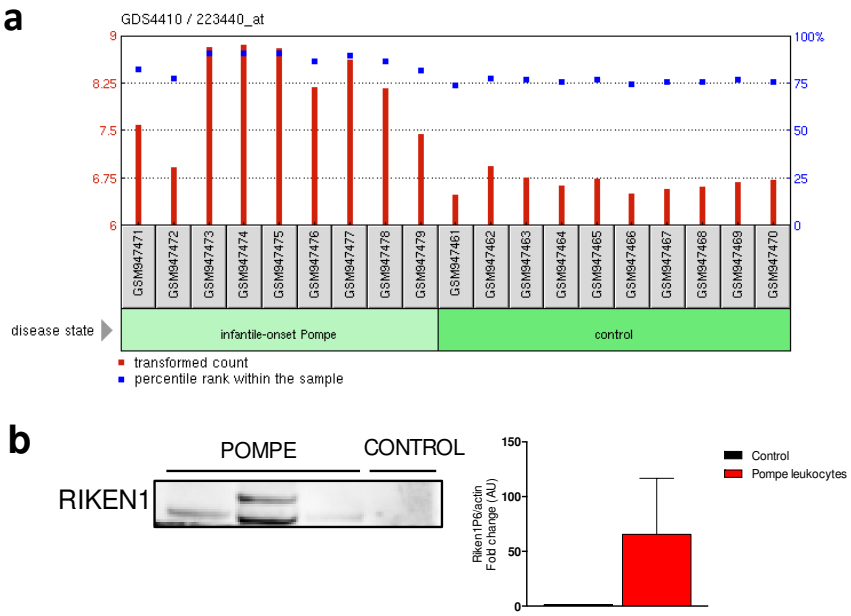

FIGURE 33. **RIKEN1 IS INDUCED IN POMPE DISEASE. (a)** Microarray database (GDS4410/223440_AT). RIKEN1 expression in infantile-onset Pompe vs control patients. **(b)** Immunoblot of RIKEN1 (P7antibody) of homogenates from leukocytes of Pompe patients (n=3) or control.

7. DISCUSSION

Muscle atrophy results from transcriptional adaptations in diseases such as cancer (cachexia), AIDS, denervation/disuse, sepsis, heart failure, diabetes, renal failure, liver failure, burn injury etc. Excessive muscle loss ultimately aggravates diseases and increases morbidity and mortality.

FoxOs are involved in a variety of biological process such as autophagy, apoptosis, ROS detoxification, glucose metabolism, DNA repair, cell cycle, stem cell maintenance and longevity[97,98]. Previous work in our lab demonstrated that muscle atrophy is regulated by a transcription-dependent process that requires the expression of atrogenes. Moreover, FoxO-family members are the key regulators of several atrogenes. Our ambitious goal was to discover new FoxO-dependent genes involved in atrophy and understand its role in the pathology.

This work reveals for the first time the importance of a new gene, here called RIKEN1, as a novel atrophy-related gene under FoxO control that is involved in the regulation of autophagic system that have an impact in controlling muscle mass by leading to atrophy condition. Our hypothesis is that the FoxO-dependent induction of RIKEN1 in catabolic conditions leads to an elevated autophagic flux that degrades excessive amount of proteins and organelles which induces atrophy. Our results showed total protection against muscle wasting in a fasting condition and a reduced muscle mass loss in tumour-bearing mice when RIKEN1 is inhibited. On the other hand, overexpression of RIKEN1 leads to atrophy suggesting that RIKEN1 is required and sufficient for inducing muscle wasting. FoxO deletion does not affect basal autophagic flux and in agreement also the inhibition of RIKEN1 do not show any changes in CSA or autophagic flux in basal condition but only during catabolic condition where this gene is upregulated by FoxO.

RIKEN1 punctuate distribution in the cytoplasm reassembling vesicles, made us think the possibility of having a role in the autophagic-lysosomal system. This work shows *in vivo* that RIKEN1 is bound to autophagosomes and interacts directly with LC3II. Then, after fusion with lysosomes RIKEN1 goes into the autophagolysosomes.

Our *in vivo* and *in vitro* experiments verify that RIKEN1 overexpression significatively increases the autophagic flux and instead, the inhibition of RIKEN1 reduced significantly the flux in basal and starved conditions. Supporting this hypothesis, we showed that RIKEN1 KO C2C12 cells had a reduction of the autophagic flux compared with WT. However, we could appreciate that LC3II accumulates in KO cells after chloroquine treatment although these levels are significantly reduced if we compared them with WT cells treated with chloroquine. Even though this may seem controversial, RIKEN1 may not be essential for LC3 lipidation and binding to the autophagosome but as ATG16L or WIPI2 may regulate the flux significatively to prevent p62 degradation. One hypothesis could be that RIKEN1 have a role at later stages of autophagosome formation. To further confirm the hypothesis that RIKEN1 plays a role at later stages we wondered if we could exclude RIKEN1 localization in omegasomes by analysing the colocalization with DFCP1, a marker of omegasomes. Our preliminar data shows that RIKEN1 is close but not totally overlapping with omegasomes in FDB fibers of HEK cells supporting our idea that RIKEN1 may be adjacent to omegasomes-ER but in a distinct structure. Moreover, mass spectrometry data showed that RIKEN1 binds WIPI2[46] and ATG16L (data not shown) and this interaction was enhanced by amino-acid starvation. Furthermore, preliminary immunoprecipitation results showed interaction of RIKEN1 with LC3 and GABARAP further confirming the hypothesis that RIKEN1 interacts with later markers of autophagosome biogenesis (GABARAP, ATG16L, WIPI2, LC3II) rather than early markers (DFCP1, ULK1). Further studies need to be done to reveal the specific mechanism of action of RIKEN1 in autophagosomes that explain the increased autophagosome biogenesis and how its depletion decrease significatively autophagic flux. Dissecting the role of RIKEN1 in each step of the autophagic flux is crucial to understand their role and to develop strategies to target it in muscle pathologies.

A recent paper explored systematically Human interactome using high-throughput affinity-purification mass spectrometry of HEK cells and we found human RIKEN1 (c16orf70) not only interacting with proteins of the autophagy system (WIPI2 and

BCAS) but also with other systems such as the proteasome (PSMA2 and PSMA3), and SERPINS (SERPINB3 and SERPINB4) (figure 34).

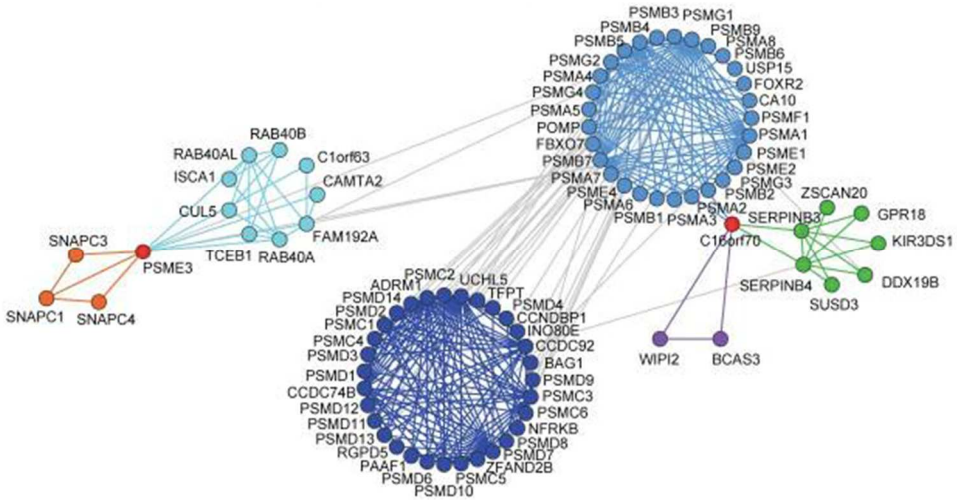

FIGURE 34. **HUMAN INTERACTOME USING HIGH-THROUGHPUT AFFINITY-PURIFICATION MASS SPECTROMETRY** (HUTTLIN ET AL 2016). Proteins are grouped by community membership; communities that initially clustered together and subsequently split are rendered in similar hues; proteins shared among clusters are red. Interactions that span multiple communities are gray while interactions among members of a community share the color of that cluster. Human RIKEN1 (C16orf70) in red showed interaction with SERPINS, Autophagy protein WIPI2 and Proteasomal proteins.

SERPINS are serine/cysteine protease inhibitors that have been reported to contribute to numerous pathological conditions such as inflammatory diseases and cancer. Thus, even though our study was focused into the characterization of RIKEN1 in atrophy, we cannot exclude RIKEN1 may participate in other systems and other pathologies. In line with that, preliminary data in KO RIKEN1 cell line showed also a defect in cell differentiation due to an insufficient amount of myogenin that facilitates cells to fuse suggesting that RIKEN1 may also regulate myogenesis (data not shown). Moreover, our work verified the microarray data published (GDS4410/223440_at) about infantile-onset Pompe patients. We found higher protein levels of RIKEN1 in Pompe leukocites compared with the control. These results cannot ensure that RIKEN1 plays a significant role in the disease because it could also be a compensatory mechanism to enhance autophagic flux and to

degrade the accumulation of glycogen. However, this is an example of autophagosome-lysosome disease that has clinical manifestations in the muscle and thus we find relevant to do more research in order to reveal the role of RIKEN1 in this disease.

Furthermore, even though autophagy was thought to be a non-selective bulk degradation pathway, it is now widely accepted that there are two types of autophagy: non-selective and selective. In response to nutrient deprivation, non-selective autophagy is activated to provide cells with essential amino-acids and nutrients for their survival. On the other hand, selective autophagy occurs to specifically remove damaged or excessive organelles or protein aggregates even under nutrient-rich conditions[99]. Future studies need to investigate whether RIKEN1 may have a role in the selective- autophagic pathway such as mitophagy or if RIKEN1 is specific for non-selective autophagy. Preliminary data with KEIMA analysis did not show a reduced mitophagic flux and thus we hypothesized that RIKEN1 is required for general autophagy but not mitophagy.

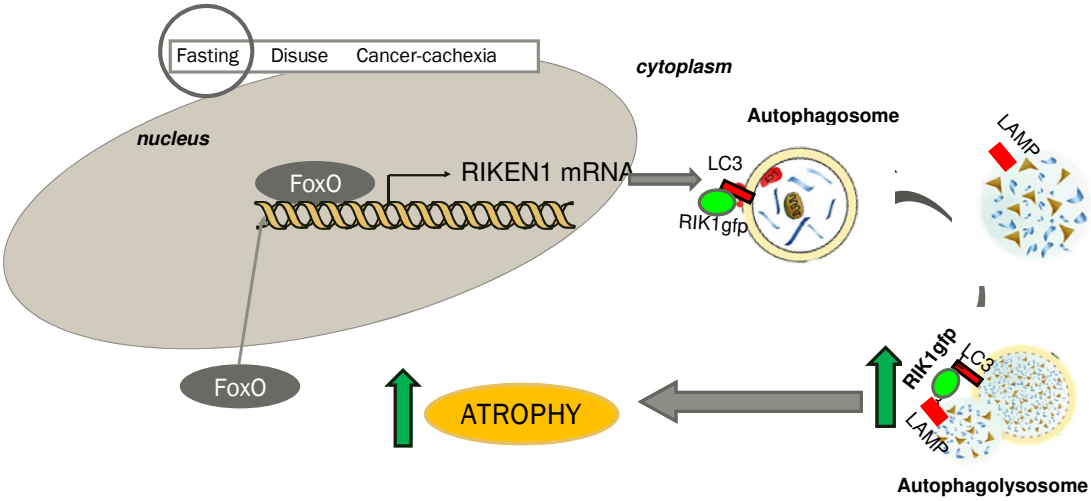

FIGURE 35. SUMMARY DIAGRAM. RIKEN1 is a novel atrophy-related gene under FoxO control that is involved in the regulation of autophagic system and may have an important role in inducing muscle atrophy. In catabolic conditions such as fasting, disuse or cancer-cachexia there is an increased RIKEN1 induction by FoxO and this leads to an elevated autophagic flux that degrades excessive amount of proteins and organelles leading to atrophy.

Taken together our study suggest for the first time that RIKEN1 is a novel atrophy-related gene under FoxO control that is involved in the regulation of autophagic system and that have an important role in inducing muscle atrophy. Our hypothesis is that the increased RIKEN1 induction by FoxO in catabolic conditions leads to an elevated autophagic flux that degrades excessive amount of proteins and organelles leading to atrophy (Figure 35). Inhibiting RIKEN1 we have a reduced autophagic flux and a reduced muscle loss in fasted and tumour-bearing animals. In conclusion, this study supports the idea that RIKEN1 may be a novel potential therapeutic target for preventing muscle wasting.

8. ABBREVIATIONS

AKT	Protein Kinase B
4EBP1	4E-Binding Protein 1
ALS	Autophagy-Lysosomal System
AMPK	AMP-Activated Protein Kinase
ATG proteins	Autophagy-Related (ATG) Proteins
ATP	Adenosine Triphosphate
Atrogin1 / Mafbx	Muscle Atrophy F-Box Protein
BMP	Bone Morphogenetic Proteins
BNIP3	Bcl2 Interacting Protein 3
CMA	Chaperone-Mediated Autophagy
CSA	Crossectional Area
DBD	DNA-Binding Domain
DFCP1	Double FYVE-Containing Protein 1
E1	Ubiquitin-Activating Enzyme E1
E2	Ubiquitin-conjugating enzyme E2
E3	Ubiquitin-protein Ligase E3
ECM	Extracellular Matrix
eif2B	Eukaryotic Translation Initiation Factor 2B
eiF4E	Eukaryotic Translation Initiation Factor 4E
ER	Endoplasmic Reticulum
FDB	Flexor Digitorum Brevis
FIP200	Focal Adhesion Kinase (FAK) Family Interacting Protein Of 200
FoxO	Forkhead-Box O
GABARAPL	Gaba Type A Receptor Associated Protein Like
GSK3	Glycogen Synthase Kinase 3 Beta
HSP70	Heat Shock Protein Family A
IGF	Insulin Like Growth Factor 1
JNK	C-Jun N-Terminal Kinase 1
LAMP	Lysosomal Associated Membrane Protein
LC3 /MAPLC3	Microtubule Associated Protein 1 Light Chain 3 Alpha
LIR	Lc3-Interacting Motifs
MAPK	Mitogen-Activated Protein Kinases
MDM2	Mdm2 Proto-Oncogene
MHC	Myosin-Heavy Chain
MLC	Myosin-Light Chain

MST1	Macrophage Stimulating 1
mTOR	Mechanistic Target Of Rapamycin Kinase
MUL1	Mitochondrial E3 Ubiquitin Protein Ligase 1
MurF1	Muscle RING-Finger Protein-1
MUSA /FboxO30	F-Box Protein 30
MYOG	Myogenin
NES	Nuclear Export Signal
NFKB	Nuclear Factor Kappa B Subunit 1
NLS	Nuclear Localization Signal
NMJ	Neuromuscular Junctions
PE	Phosphoryl Ethanolamine
Pi3P	Phosphatidylinositol-4,5-Bisphosphate 3-Kinase
PINK 1	Pten Induced Putative Kinase 1
Psma1	Proteasome Subunit Alpha 1
PSMA2	Proteasome Subunit Alpha 2
Psme4	Proteasome Activator Subunit 4
Rheb	Ras Homolog Mtorc1 Binding
C16orf70 /RIKEN1	Chromosome 16 Open Reading Frame 70
S6K	Ribosomal Protein S6 Kinase B1
SCF complex	Skp, Cullin, F-Box Containing Complex
SERPINB3	Serpin Family B Member 3
SMAD	SMAD Family Member
SMART	Specific Of Muscle Atrophy And Regulated By Transcription
SQTM1 / P62	Sequestosome 1
SR	Sarcoplasmic Reticulum
TA	Tibialis Anterior
TGFbeta	Transforming Growth Factor Beta 1
TNF	Tumor Necrosis Factor
TSC1/2	Tsc Complex Subunit 1/2
ULK1	Unc-51 Like Autophagy Activating Kinase 1
UPS	Ubiquitin-Proteasome System
UVRAG	UV Radiation Resistance Associated
VPS34	Phosphatidylinositol 3-Kinase VPS34
WIPI2	WD Repeat Domain, Phosphoinositide Interacting

9. BIBLIOGRAPHY

1. Bonaldo, P. & Sandri, M. Cellular and molecular mechanisms of muscle atrophy. *Dis. Model. Mech.* **6,** 25–39 (2013).
2. DeFronzo, R. A., Ferrannini, E., Sato, Y., Felig, P. & Wahren, J. Synergistic interaction between exercise and insulin on peripheral glucose uptake. *J. Clin. Invest.* **68,** 1468–1474 (1981).
3. DeFronzo, R. A. *et al.* The effect of insulin on the disposal of intravenous glucose. Results from indirect calorimetry and hepatic and femoral venous catheterization. *Diabetes* **30,** 1000–1007 (1981).
4. Schiaffino, S. & Reggiani, C. Molecular diversity of myofibrillar proteins: gene regulation and functional significance. *Physiol. Rev.* **76,** 371–423 (1996).
5. Schiaffino, S. & Reggiani, C. Fiber types in mammalian skeletal muscles. *Physiol. Rev.* **91,** 1447–1531 (2011).
6. Murgia, M. *et al.* Ras is involved in nerve-activity-dependent regulation of muscle genes. *Nat. Cell Biol.* **2,** 142–147 (2000).
7. Mounier, R., Théret, M., Lantier, L., Foretz, M. & Viollet, B. Expanding roles for AMPK in skeletal muscle plasticity. *Trends Endocrinol. Metab. TEM* **26,** 275–286 (2015).
8. McCarthy, J. J. & Esser, K. A. MicroRNA-1 and microRNA-133a expression are decreased during skeletal muscle hypertrophy. *J. Appl. Physiol. Bethesda Md 1985* **102,** 306–313 (2007).
9. Velloso, C. P. Regulation of muscle mass by growth hormone and IGF-I. *Br. J. Pharmacol.* **154,** 557–568 (2008).
10. Goldberg, A. L. Protein turnover in skeletal muscle. I. Protein catabolism during work-induced hypertrophy and growth induced with growth hormone. *J. Biol. Chem.* **244,** 3217–3222 (1969).

11. Schiaffino, S. & Mammucari, C. Regulation of skeletal muscle growth by the IGF1-Akt/PKB pathway: insights from genetic models. *Skelet. Muscle* **1,** 4 (2011).

12. Glass, D. J. Skeletal muscle hypertrophy and atrophy signaling pathways. *Int. J. Biochem. Cell Biol.* **37,** 1974–1984 (2005).

13. Blaauw, B. *et al.* Inducible activation of Akt increases skeletal muscle mass and force without satellite cell activation. *FASEB J. Off. Publ. Fed. Am. Soc. Exp. Biol.* **23,** 3896–3905 (2009).

14. Goldberg, A. L. Protein turnover in skeletal muscle. II. Effects of denervation and cortisone on protein catabolism in skeletal muscle. *J. Biol. Chem.* **244,** 3223–3229 (1969).

15. Lecker, S. H., Goldberg, A. L. & Mitch, W. E. Protein degradation by the ubiquitin-proteasome pathway in normal and disease states. *J. Am. Soc. Nephrol. JASN* **17,** 1807–1819 (2006).

16. Milan, G. *et al.* Regulation of autophagy and the ubiquitin-proteasome system by the FoxO transcriptional network during muscle atrophy. *Nat. Commun.* **6,** 6670 (2015).

17. Gomes, M. D., Lecker, S. H., Jagoe, R. T., Navon, A. & Goldberg, A. L. Atrogin-1, a muscle-specific F-box protein highly expressed during muscle atrophy. *Proc. Natl. Acad. Sci. U. S. A.* **98,** 14440–14445 (2001).

18. Lecker, S. H. *et al.* Multiple types of skeletal muscle atrophy involve a common program of changes in gene expression. *FASEB J. Off. Publ. Fed. Am. Soc. Exp. Biol.* **18,** 39–51 (2004).

19. Lang, C. H., Huber, D. & Frost, R. A. Burn-induced increase in atrogin-1 and MuRF-1 in skeletal muscle is glucocorticoid independent but downregulated by IGF-I. *Am. J. Physiol. Regul. Integr. Comp. Physiol.* **292,** R328-336 (2007).

20. Sartori, R. *et al.* Smad2 and 3 transcription factors control muscle mass in adulthood. *Am. J. Physiol. Cell Physiol.* **296,** C1248-1257 (2009).

21. Sartori, R. *et al.* BMP signaling controls muscle mass. *Nat. Genet.* **45,** 1309–1318

(2013).

22. Amirouche, A. *et al.* Down-regulation of Akt/mammalian target of rapamycin signaling pathway in response to myostatin overexpression in skeletal muscle. *Endocrinology* **150,** 286–294 (2009).

23. Sandri, M. Protein breakdown in cancer cachexia. *Semin. Cell Dev. Biol.* **54,** 11–19 (2016).

24. Lilienbaum, A. Relationship between the proteasomal system and autophagy. *Int. J. Biochem. Mol. Biol.* **4,** 1–26 (2013).

25. Mizushima, N. & Levine, B. Autophagy in mammalian development and differentiation. *Nat. Cell Biol.* **12,** 823–830 (2010).

26. Schiaffino, S., Dyar, K. A., Ciciliot, S., Blaauw, B. & Sandri, M. Mechanisms regulating skeletal muscle growth and atrophy. *FEBS J.* **280,** 4294–4314 (2013).

27. Hershko, A. & Ciechanover, A. The ubiquitin system. *Annu. Rev. Biochem.* **67,** 425–479 (1998).

28. Tenno, T. *et al.* Structural basis for distinct roles of Lys63- and Lys48-linked polyubiquitin chains. *Genes Cells Devoted Mol. Cell. Mech.* **9,** 865–875 (2004).

29. Bodine, S. C. *et al.* Identification of ubiquitin ligases required for skeletal muscle atrophy. *Science* **294,** 1704–1708 (2001).

30. Borden, K. L. & Freemont, P. S. The RING finger domain: a recent example of a sequence-structure family. *Curr. Opin. Struct. Biol.* **6,** 395–401 (1996).

31. Kamura, T. *et al.* Rbx1, a component of the VHL tumor suppressor complex and SCF ubiquitin ligase. *Science* **284,** 657–661 (1999).

32. Pryor, P. R. & Luzio, J. P. Delivery of endocytosed membrane proteins to the lysosome. *Biochim. Biophys. Acta* **1793,** 615–624 (2009).

33. van Meel, E. & Klumperman, J. Imaging and imagination: understanding the endo-lysosomal system. *Histochem. Cell Biol.* **129,** 253–266 (2008).

34. Mijaljica, D., Prescott, M. & Devenish, R. J. Microautophagy in mammalian cells:

revisiting a 40-year-old conundrum. *Autophagy* **7,** 673–682 (2011).

35. Takikita, S. *et al.* Fiber type conversion by PGC-1α activates lysosomal and autophagosomal biogenesis in both unaffected and Pompe skeletal muscle. *PloS One* **5,** e15239 (2010).

36. Bejarano, E. & Cuervo, A. M. Chaperone-mediated autophagy. *Proc. Am. Thorac. Soc.* **7,** 29–39 (2010).

37. Kon, M. & Cuervo, A. M. Chaperone-mediated autophagy in health and disease. *FEBS Lett.* **584,** 1399–1404 (2010).

38. Inoue, Y. & Klionsky, D. J. Regulation of macroautophagy in Saccharomyces cerevisiae. *Semin. Cell Dev. Biol.* **21,** 664–670 (2010).

39. Abounit, K., Scarabelli, T. M. & McCauley, R. B. Autophagy in mammalian cells. *World J. Biol. Chem.* **3,** 1–6 (2012).

40. Tooze, S. A. & Yoshimori, T. The origin of the autophagosomal membrane. *Nat. Cell Biol.* **12,** 831–835 (2010).

41. Hosokawa, N. *et al.* Atg101, a novel mammalian autophagy protein interacting with Atg13. *Autophagy* **5,** 973–979 (2009).

42. Kim, J. *et al.* Differential regulation of distinct Vps34 complexes by AMPK in nutrient stress and autophagy. *Cell* **152,** 290–303 (2013).

43. Axe, E. L. *et al.* Autophagosome formation from membrane compartments enriched in phosphatidylinositol 3-phosphate and dynamically connected to the endoplasmic reticulum. *J. Cell Biol.* **182,** 685–701 (2008).

44. Proikas-Cezanne, T. *et al.* WIPI-1alpha (WIPI49), a member of the novel 7-bladed WIPI protein family, is aberrantly expressed in human cancer and is linked to starvation-induced autophagy. *Oncogene* **23,** 9314–9325 (2004).

45. Dooley, H. C. *et al.* WIPI2 links LC3 conjugation with PI3P, autophagosome formation, and pathogen clearance by recruiting Atg12-5-16L1. *Mol. Cell* **55,** 238–252 (2014).

46. Bakula, D. *et al.* WIPI3 and WIPI4 β-propellers are scaffolds for LKB1-AMPK-TSC signalling circuits in the control of autophagy. *Nat. Commun.* **8,** 15637 (2017).

47. Rubinsztein, D. C., Mariño, G. & Kroemer, G. Autophagy and aging. *Cell* **146,** 682–695 (2011).

48. Komatsu, M. & Ichimura, Y. Selective autophagy regulates various cellular functions. *Genes Cells Devoted Mol. Cell. Mech.* **15,** 923–933 (2010).

49. Ichimura, Y. & Komatsu, M. Selective degradation of p62 by autophagy. *Semin. Immunopathol.* **32,** 431–436 (2010).

50. Zheng, Q. *et al.* Hsp70 participates in PINK1-mediated mitophagy by regulating the stability of PINK1. *Neurosci. Lett.* **662,** 264–270 (2018).

51. Petrovski, G. & Das, D. K. Does autophagy take a front seat in lifespan extension? *J. Cell. Mol. Med.* **14,** 2543–2551 (2010).

52. Masiero, E. *et al.* Autophagy Is Required to Maintain Muscle Mass. *Cell Metab.* **10,** 507–515 (2009).

53. Bodine, S. C. & Baehr, L. M. Skeletal muscle atrophy and the E3 ubiquitin ligases MuRF1 and MAFbx/atrogin-1. *Am. J. Physiol. Endocrinol. Metab.* **307,** E469-484 (2014).

54. Brocca, L. *et al.* FoxO-dependent atrogenes vary among catabolic conditions and play a key role in muscle atrophy induced by hindlimb suspension. *J. Physiol.* **595,** 1143–1158 (2017).

55. Navon, A. & Goldberg, A. L. Proteins are unfolded on the surface of the ATPase ring before transport into the proteasome. *Mol. Cell* **8,** 1339–1349 (2001).

56. Sandri, M. *et al.* Foxo transcription factors induce the atrophy-related ubiquitin ligase atrogin-1 and cause skeletal muscle atrophy. *Cell* **117,** 399–412 (2004).

57. Mammucari, C. *et al.* FoxO3 controls autophagy in skeletal muscle in vivo. *Cell Metab.* **6,** 458–471 (2007).

58. Zhao, J. *et al.* FoxO3 coordinately activates protein degradation by the

autophagic/lysosomal and proteasomal pathways in atrophying muscle cells. *Cell Metab.* **6,** 472–483 (2007).

59. Kaestner, K. H., Knochel, W. & Martinez, D. E. Unified nomenclature for the winged helix/forkhead transcription factors. *Genes Dev.* **14,** 142–146 (2000).

60. Nakae, J. *et al.* The LXXLL motif of murine forkhead transcription factor FoxO1 mediates Sirt1-dependent transcriptional activity. *J. Clin. Invest.* **116,** 2473–2483 (2006).

61. Obsil, T. & Obsilova, V. Structure/function relationships underlying regulation of FOXO transcription factors. *Oncogene* **27,** 2263–2275 (2008).

62. Salih, D. A. M. *et al.* FoxO6 regulates memory consolidation and synaptic function. *Genes Dev.* **26,** 2780–2801 (2012).

63. Chung, S. Y. *et al.* FoxO6 and PGC-1α form a regulatory loop in myogenic cells. *Biosci. Rep.* **33,** (2013).

64. Brunet, A. *et al.* Akt promotes cell survival by phosphorylating and inhibiting a Forkhead transcription factor. *Cell* **96,** 857–868 (1999).

65. Jacobs, F. M. J. *et al.* FoxO6, a novel member of the FoxO class of transcription factors with distinct shuttling dynamics. *J. Biol. Chem.* **278,** 35959–35967 (2003).

66. Greer, E. L. *et al.* The energy sensor AMP-activated protein kinase directly regulates the mammalian FOXO3 transcription factor. *J. Biol. Chem.* **282,** 30107–30119 (2007).

67. Essers, M. A. G. *et al.* FOXO transcription factor activation by oxidative stress mediated by the small GTPase Ral and JNK. *EMBO J.* **23,** 4802–4812 (2004).

68. Lehtinen, M. K. *et al.* A conserved MST-FOXO signaling pathway mediates oxidative-stress responses and extends life span. *Cell* **125,** 987–1001 (2006).

69. Asada, S. *et al.* Mitogen-activated protein kinases, Erk and p38, phosphorylate and regulate Foxo1. *Cell. Signal.* **19,** 519–527 (2007).

70. Bertaggia, E., Coletto, L. & Sandri, M. Posttranslational modifications control FoxO3

activity during denervation. *Am. J. Physiol. Cell Physiol.* **302,** C587-596 (2012).

71. Huang, K.-S. & Vassilev, L. T. High-throughput screening for inhibitors of the Cks1-Skp2 interaction. *Methods Enzymol.* **399,** 717–728 (2005).

72. Fu, W. *et al.* MDM2 acts downstream of p53 as an E3 ligase to promote FOXO ubiquitination and degradation. *J. Biol. Chem.* **284,** 13987–14000 (2009).

73. Brenkman, A. B., de Keizer, P. L. J., van den Broek, N. J. F., Jochemsen, A. G. & Burgering, B. M. T. Mdm2 induces mono-ubiquitination of FOXO4. *PloS One* **3,** e2819 (2008).

74. Kamei, Y. *et al.* FOXO1 activates glutamine synthetase gene in mouse skeletal muscles through a region downstream of 3'-UTR: possible contribution to ammonia detoxification. *Am. J. Physiol. Endocrinol. Metab.* **307,** E485-493 (2014).

75. Allen, D. L. & Unterman, T. G. Regulation of myostatin expression and myoblast differentiation by FoxO and SMAD transcription factors. *Am. J. Physiol. Cell Physiol.* **292,** C188-199 (2007).

76. Southgate, R. J. *et al.* FOXO1 regulates the expression of 4E-BP1 and inhibits mTOR signaling in mammalian skeletal muscle. *J. Biol. Chem.* **282,** 21176–21186 (2007).

77. Tracy, K. & Macleod, K. F. Regulation of mitochondrial integrity, autophagy and cell survival by BNIP3. *Autophagy* **3,** 616–619 (2007).

78. Kim, S.-Y., Kim, H. J., Byeon, H. K., Kim, D. H. & Kim, C.-H. FOXO3 induces ubiquitylation of AKT through MUL1 regulation. *Oncotarget* **8,** 110474–110489 (2017).

79. Sanchez, A. M. J., Candau, R. & Bernardi, H. AMP-activated protein kinase stabilizes FOXO3 in primary myotubes. *Biochem. Biophys. Res. Commun.* **499,** 493–498 (2018).

80. Bothe, G. W., Haspel, J. A., Smith, C. L., Wiener, H. H. & Burden, S. J. Selective expression of Cre recombinase in skeletal muscle fibers. *Genes. N. Y. N 2000* **26,** 165–166 (2000).

81. Komatsu, M. *et al.* Impairment of starvation-induced and constitutive autophagy in Atg7-deficient mice. *J. Cell Biol.* **169,** 425–434 (2005).

82. Winbanks, C. E. *et al.* Smad7 gene delivery prevents muscle wasting associated with cancer cachexia in mice. *Sci. Transl. Med.* **8,** 348ra98 (2016).

83. Aulino, P. *et al.* Molecular, cellular and physiological characterization of the cancer cachexia-inducing C26 colon carcinoma in mouse. *BMC Cancer* **10,** 363 (2010).

84. Penna, F. *et al.* Autophagic degradation contributes to muscle wasting in cancer cachexia. *Am. J. Pathol.* **182,** 1367–1378 (2013).

85. Lizio, M. *et al.* Update of the FANTOM web resource: high resolution transcriptome of diverse cell types in mammals. *Nucleic Acids Res.* **45,** D737–D743 (2017).

86. Masuya, H. *et al.* The RIKEN integrated database of mammals. *Nucleic Acids Res.* **39,** D861-870 (2011).

87. Zhang, Y. I-TASSER server for protein 3D structure prediction. *BMC Bioinformatics* **9,** 40 (2008).

88. Terry, E. E. *et al.* Transcriptional profiling reveals extraordinary diversity among skeletal muscle tissues. *eLife* **7,** (2018).

89. Carnio, S. *et al.* Autophagy impairment in muscle induces neuromuscular junction degeneration and precocious aging. *Cell Rep.* **8,** 1509–1521 (2014).

90. Raben, N., Roberts, A. & Plotz, P. H. Role of autophagy in the pathogenesis of Pompe disease. *Acta Myol. Myopathies Cardiomyopathies Off. J. Mediterr. Soc. Myol.* **26,** 45–48 (2007).

91. Wu, H. *et al.* Crosstalk Between Macroautophagy and Chaperone-Mediated Autophagy: Implications for the Treatment of Neurological Diseases. *Mol. Neurobiol.* **52,** 1284–1296 (2015).

92. Zhang, G. *et al.* Tumor induces muscle wasting in mice through releasing extracellular Hsp70 and Hsp90. *Nat. Commun.* **8,** 589 (2017).

93. Guan, J.-L. *et al.* Autophagy in stem cells. *Autophagy* **9,** 830–849 (2013).

94. Schäffner, I. *et al.* FoxO Function Is Essential for Maintenance of Autophagic Flux and Neuronal Morphogenesis in Adult Neurogenesis. *Neuron* **99,** 1188-1203.e6 (2018).

95. Zecchini, S. *et al.* Autophagy controls neonatal myogenesis by regulating the GH-IGF1 system through a NFE2L2- and DDIT3-mediated mechanism. *Autophagy* 1–20 (2018). doi:10.1080/15548627.2018.1507439

96. Autophagy controls neonatal myogenesis by regulating the GH-IGF1 system through a NFE2L2- and DDIT3-mediated mechanism: Autophagy: Vol 0, No ja. Available at: https://www.tandfonline.com/doi/abs/10.1080/15548627.2018.1507439. (Accessed: 1st September 2018)

97. Sandri, M. FOXOphagy path to inducing stress resistance and cell survival. *Nat. Cell Biol.* **14,** 786–788 (2012).

98. Eijkelenboom, A. & Burgering, B. M. T. FOXOs: signalling integrators for homeostasis maintenance. *Nat. Rev. Mol. Cell Biol.* **14,** 83–97 (2013).

99. Ding, W.-X. & Yin, X.-M. Mitophagy: mechanisms, pathophysiological roles, and analysis. *Biol. Chem.* **393,** 547–564 (2012).